arXiv:2403.17906v1 [math-ph] 26 Mar 2024

WKB asymptotics of Stokes matrices, spectral curves and rhombus inequalities

Anton Alekseev, Andrew Neitzke, Xiaomeng Xu and Yan Zhou

Abstract

We consider an $n \times n$ system of ODEs on $\mathbb{P}^1$ with a simple pole A at $z = 0$ and a double pole $u = \mathrm{diag}(u_1, \ldots, u_n)$ at $z = \infty$. This is the simplest situation in which the monodromy data of the system are described by upper and lower triangular Stokes matrices $S_\pm$, and we impose reality conditions which imply $S_- = S_+^\dagger$. We study leading WKB exponents of Stokes matrices in parametrizations given by generalized minors and by spectral coordinates, and we show that for u on the caterpillar line (which corresponds to the limit $(u_{j+1} - u_j)/(u_j - u_{j-1}) \to \infty$ for $j = 2, \cdots, n-1$), the real parts of these exponents are given by periods of certain cycles on the degenerate spectral curve $\Gamma(u_{\mathrm{cat}}(t), A)$.

These cycles admit unique deformations for u near the caterpillar line. Using the spectral network theory, we give for $n = 2$, and $n = 3$ exact WKB predictions for asymptotics of generalized minors in terms of periods of these cycles. Boalch's theorem from Poisson geometry implies that real parts of leading WKB exponents satisfy the rhombus (or interlacing) inequalities. We show that these inequalities are in correspondence with finite webs of the canonical foliation on the root curve $\Gamma^r(u, A)$, and that they follow from the positivity of the corresponding periods. We conjecture that a similar mechanism applies for $n > 3$.

We also outline the relation of the spectral coordinates with the cluster structures considered by Goncharov-Shen, and with $\mathcal{N} = 2$ supersymmetric quantum field theories in dimension four associated to some simple quivers.

Contents

1 Introduction

1.1 Meromorphic ODEs, Stokes matrices, and WKB expansion

In this section we briefly introduce the background material of our study: Stokes matrices for meromorphic ODEs, their WKB asymptotics, and their relation to Poisson geometry and spectral curves.

1.1.1 Meromorphic ODEs

The main object of study in this paper is the following system of ODEs on $\mathbb{P}^1 \backslash \{0, \infty\}$:

$$\varepsilon \frac{dF}{dz} = \left(\mathrm{i}u - \frac{1}{2\pi\mathrm{i}} \frac{A}{z} \right) F \,. \tag{1.1.1}$$

Here ε is a parameter, $u \in \mathfrak{h}_{\mathrm{reg}}(\mathbb{C})$ is an $n \times n$ diagonal matrix with distinct diagonal entries and $A \in \mathfrak{gl}_n(\mathbb{C})$ is an $n \times n$ matrix. Alternatively, we can view (1.1.1) as coming from the meromorphic flat connection

$$\nabla_{(u,A,\varepsilon)} = d - \frac{1}{\varepsilon} \left(\mathrm{i}u - \frac{1}{2\pi\mathrm{i}} \frac{A}{z} \right) dz$$

on the trivial rank n vector bundle over $\mathbb{P}^1$. This class of Poincaré rank 1 ODEs naturally appears in various contexts in geometry and representation theory, *e.g.* the study of Frobenius manifolds [18] and in particular the quantum cohomology of Fano manifolds [24], linearization in Poisson geometry [11], quantum Weyl group actions on Poisson groups [12], stability conditions [14, 15], Yang-Baxter equations [50] *etc.* These ODEs also provide simple local models for the wild non-abelian Hodge correspondence on curves [10].

In most of the paper, we impose the following *reality conditions*:

$$\varepsilon \in \mathbb{R}_+, \quad u \in \mathfrak{h}_{\mathrm{reg}}(\mathbb{R}), \quad A \in \mathrm{Herm}(n), \tag{1.1.2}$$

where $\mathrm{Herm}(n)$ is the space of $n \times n$ Hermitian matrices. We will see that these conditions are natural from the point of view of tropicalization of dual Poisson-Lie groups [2, 3].

1.1.2 Stokes matrices and WKB

The ODE (1.1.1) has a first-order pole at $z = 0$ and a second-order pole at $z = \infty$. Hence, its monodromy data is encoded in *Stokes matrices*. Under reality conditions (1.1.2), there are two Stokes supersectors with canonical solutions $F_\pm(z, \varepsilon)$ specified by a prescribed asymptotic behavior at $z \to \infty$. The Stokes matrices $S_\pm(u, A, \varepsilon)$ are transition matrices between these two canonical solutions. Up to permutations of indices, S_+ and S_- are upper and lower triangular matrices, respectively. The reality conditions imply that they are Hermitian conjugates of each other:

$$S_-(u, A, \varepsilon) = S_+(u, A, \varepsilon)^\dagger. \tag{1.1.3}$$

We will be interested in the asymptotic behavior of $S_\pm$ in the limit of $\varepsilon \to 0$. In order to describe these asymptotics, we use several parametrizations of Stokes matrices. One such parametrization is given by the *generalized minors* (see e.g. [2, 3]): for $1 \le i \le k \le n$, define $\Delta_i^{(k)}(S_+)$ to be the determinant of the $i \times i$ submatrix formed by taking the first i rows and $(k - i + 1)^{th}$ to k^{th} columns of the upper-triangular matrix S_+. Other possible parametrizations include matrix entries $(S_+)_{i,j}$ and spectral coordinates X_γ to be defined later. For any of these parametrizations, if (u, A) are generic, one expects an asymptotic expansion as $\varepsilon \to 0$:

$$\log X(u, A, \varepsilon) \sim \varepsilon^{-1} x(u, A) + x_0(u, A) + \varepsilon x_1(u, A) + \cdots \tag{1.1.4}$$

Here $X(u, A, \varepsilon)$ is one of the parameters (a generalized minor, a spectral coordinate, etc), $x(u, A)$ is the leading WKB exponent, and $x_i(u, A)$ are higher-order coefficients in the WKB expansion.

In this paper, we will be mostly concerned with the leading WKB exponents, so we often truncate (1.1.4) to the leading term

$$\log X(u, A, \varepsilon) \sim \varepsilon^{-1} x(u, A)\,.$$

In the case of a generalized minor $X = \Delta_i^{(k)}$ we denote the leading WKB exponent by $\delta_i^{(k)}$, and its real part by

$$l_i^{(k)} = \mathrm{Re}\, \delta_i^{(k)}\,. \tag{1.1.5}$$

1.1.3 Poisson structures and inequalities

Next let us discuss some constraints on WKB asymptotics, which arise from Poisson geometry.

Equip the set of data (u, A) with the linear Kirillov-Kostant-Souriau (KKS) Poisson structure on A and the vanishing Poisson structure on u. Then, by a theorem of Boalch [11], the Stokes matrices $S_\pm(u, A, \varepsilon)$ satisfy the Poisson brackets of the dual Poisson-Lie group $U(n)^*$, rescaled by ε^{-1}. These brackets are polynomial in the matrix entries, and Laurent polynomial in the generalized minors.

These facts alone already imply an interesting corollary for WKB asymptotics, as follows. Suppose we have two parameters X_1, X_2, either matrix entries or generalized minors, which have the WKB behavior $\log X_1 \sim \varepsilon^{-1} x_1$, $\log X_2 \sim \varepsilon^{-1} x_2$. Then, we have

$$e^{\frac{1}{\varepsilon}(x_1+x_2)+\cdots} \left(\frac{1}{\varepsilon^2} \{x_1, x_2\} + \cdots \right) = \{e^{\frac{1}{\varepsilon}x_1+\cdots}, e^{\frac{1}{\varepsilon}x_2+\cdots}\} = \{X_1, X_2\} = \frac{1}{\varepsilon} \sum_a e^{\frac{1}{\varepsilon}x_a+\cdots}, \tag{1.1.6}$$

where the x_a are the leading WKB exponents of the terms X_a appearing in $\{X_1, X_2\}$. In (1.1.6), the right-hand side stands for the Laurent polynomial expression for the Poisson bracket $\{X_1, X_2\}$, and the left-hand side stands for the

KKS bracket of the WKB expansions of X_1 and X_2. We observe that the left and right sides of (1.1.6) can match only if

$$\mathrm{Re}\,(x_1 + x_2) \geq \mathrm{Re}\, x_a \quad \text{for all} \quad a. \tag{1.1.7}$$

The inequalities (1.1.7) play an important role in this paper. For the generalized minors, they read (see [1] for details)

$$l_i^{(k+1)} + l_{i-1}^{(k)} \geq l_{i+1}^{(k+1)} + l_i^{(k)}, \quad l_i^{(k+1)} + l_i^{(k)} \geq l_{i+1}^{(k+1)} + l_{i-1}^{(k)}, \tag{1.1.8}$$

and we refer to them as *rhombus inequalities*.

It is sometimes convenient to introduce a linear change of variables, defining $\lambda_j^{(k)}$ for $1 \leq j \leq k \leq n$ by $\lambda_j^{(k)} = l_{k-j+1}^{(k)} - l_{k-j}^{(k)}$ (where we let $l_0^{(k)} = 0$). Then $l_i^{(k)} = \sum_{j=k-i+1}^{k} \lambda_j^{(k)}$. After this change of variables, the rhombus inequalities become the *interlacing inequalities*:

$$\lambda_j^{(k+1)} \leq \lambda_j^{(k)} \leq \lambda_{j+1}^{(k+1)}. \tag{1.1.9}$$

1.1.4 Spectral curves

The general philosophy of the WKB method predicts that the asymptotic series (1.1.4) should be determined by computations on the *spectral curve*.

Definition 1.1. The spectral curve $\Gamma(u, A)$ is given by the characteristic polynomial

$$\det \left[\mu \cdot I_n - \left(\mathrm{i}u - \frac{1}{2\pi \mathrm{i}} \frac{A}{z} \right) \right] = 0. \tag{1.1.10}$$

The spectral curve $\Gamma(u, A)$ is an n-to-1 cover of $\mathbb{P}^1 \setminus \{0, \infty\}$ with punctures over 0 and ∞. The *period* of the canonical 1-form $\omega = \mu(z)\, dz$ on a 1-cycle γ is

$$Z(\gamma) = \oint_\gamma \omega\,. \tag{1.1.11}$$

1.2 The main conjecture

The leading-order WKB prediction takes the following form:

Conjecture 1.2. For generic u and A, there exist cycles $\left\{ L_i^{(k)} \right\}_{1 \leq i \leq k \leq n}$ on $\Gamma(u, A)$ such that the asymptotic expansion (1.1.4) holds, with leading coefficient

$$l_i^{(k)} = -\frac{1}{2} Z\left(L_i^{(k)} \right). \tag{1.2.1}$$

Moreover, the quantities $-\frac{1}{2} Z\left(L_i^{(k)} \right)$ satisfy the rhombus inequalities (1.1.8).

In (1.2.1), the minus sign is a consequence of our conventions, with no essential significance. The factor $\frac{1}{2}$ arises because we consider $l_i^{(k)} = \frac{1}{2}\left(\delta_i^{(k)} + \overline{\delta}_i^{(k)} \right)$ instead of $\delta_i^{(k)}$.

To address Conjecture 1.2, we need a method of identifying the cycles $L_i^{(k)}$. We approach this by looking at a region in parameter space where we have a detailed understanding of the spectral curves $\Gamma(u, A)$. Namely, we consider the following limit in the space of parameters u:

$$u_2 - u_1 = t \in \mathbb{R}_+, \quad \frac{u_{j+1} - u_j}{u_j - u_{j-1}} \to +\infty \text{ for } j = 2, \ldots, n-1. \tag{1.2.2}$$

This limit makes sense in the *De Concini-Procesi space* [16] $\widehat{\mathfrak{h}_{\mathrm{reg}}}(\mathbb{R})$. We refer to configurations (1.2.2) as lying on the *caterpillar line* and denote them $u_{\mathrm{cat}}(t)$.[1] We refer readers to Appendix A for a more detailed description of the De Concini-Procesi space and the stratifications of its boundary.

[1]This terminology is inspired by the term *caterpillar point* in the existing literature (e.g. [30, 44]) which refers to the point $t = 0$; when we refer to $u_{\mathrm{cat}}(t)$ in this paper, though, we always mean $t > 0$.

1.3 The proof on the caterpillar line

We first investigate the WKB behavior of Stokes matrices on the caterpillar line. Fortunately, we have simple explicit formulas for the behavior of $S_+(u, A, \varepsilon)$ as $u \to u_{\mathrm{cat}}(t)$ (see Subsection 2.4 and Appendix B for more details). These formulas imply in particular (see Theorem 2.14 for the precise statement):

Theorem 1.3. The real parts of WKB exponents of minor coordinates, $l_i^{(k)}(u, A)$, have a limit as $u \to u_{\mathrm{cat}}(t)$, given by

$$l_i^{(k)}(u_{\mathrm{cat}}(t), A) = \sum_{j=k-i+1}^{k} \lambda_j^{(k)} \tag{1.3.1}$$

where $\lambda_j^{(k)}$ are the eigenvalues of the $k \times k$ upper left corner submatrix $A^{(k)}$ of A, ordered by $\lambda_1^{(k)} < \lambda_2^{(k)} < \cdots < \lambda_k^{(k)}$.

We remark that in this limit the interlacing inequalities (1.1.9) become familiar: they are the Cauchy interlacing inequalities obeyed by the eigenvalues of submatrices of the Hermitian matrix A. From this point of view, the interlacing inequalities obeyed by the WKB exponents at general u are some interesting deformation of the usual Cauchy interlacing inequalities.

Moreover, the spectral curve degenerates in this limit:

Theorem 1.4. (Theorem 3.12, Corollary 3.14) The family of curves $\Gamma(u, A)$ can be extended to include a curve $\Gamma(u_{\mathrm{cat}}(t), A)$ over $u_{\mathrm{cat}}(t)$, which is reducible, with components $\Gamma^{(2)}, \ldots, \Gamma^{(n)}$. For A in the generic locus as in Definition 3.8, each component $\Gamma^{(k)}$ is isomorphic to $\mathbb{P}^1$ with $2k$ punctures. In this case, there are loops $V_j^{(k)}(u_{\mathrm{cat}}(t), A)$ $(1 \le j \le k \le n)$ around punctures of $\Gamma(u_{\mathrm{cat}}(t), A)$ such that

$$Z\left(V_j^{(k)}(u_{\mathrm{cat}}(t), A)\right) = -\lambda_j^{(k)}\,. \tag{1.3.2}$$

Equation (1.3.2) motivates the following: define the *distinguished cycles* by

$$C_i^{(k)}(u_{\mathrm{cat}}(t), A) = \sum_{j=k-i+1}^{k} V_j^{(k)}(u_{\mathrm{cat}}(t), A)\,. \tag{1.3.3}$$

Then combining Theorem 1.3 and Theorem 1.4 we obtain a proof of Conjecture 1.2 at $u = u_{\mathrm{cat}}(t)$, with the cycles given by $L_i^{(k)} = C_i^{(k)}$.

1.4 Exact WKB and spectral networks

Next, we investigate Conjecture 1.2 near the caterpillar line. Then, the spectral curve admits the following description:

Theorem 1.5. (Corollary 3.14) Let U_{id} be the connected component of $\mathfrak{h}_{\mathrm{reg}}(\mathbb{R})$ labeled by the identity element in the symmetric group S_n as in (2.1.1). Fix A in the generic locus as in Definition 3.8. Then, there exists a punctured open neighborhood $B(u_{\mathrm{cat}}(t), A)$ of $u_{\mathrm{cat}}(t)$ in U_{id} such that for $u \in B(u_{\mathrm{cat}}(t), A)$, $\Gamma(u, A)$ is smooth and there are vanishing cycles $V_j^{(k)}(u, A)$ $(1 \le j \le k \le n)$ on $\Gamma(u, A)$ that become $V_j^{(k)}(u_{\mathrm{cat}}(t), A)$ as $u \to u_{\mathrm{cat}}(t)$.

As before, we will denote

$$C_i^{(k)}(u, A) = \sum_{j=k-i+1}^{k} V_i^{(k)}(u, A). \tag{1.4.1}$$

We study Conjecture 1.2 using the *exact WKB* method. Generally, given a family of ODEs of the form

$$\varepsilon \partial_z \psi = a(\varepsilon)\psi, \quad a(\varepsilon) = a_0 + \varepsilon a_1 + \cdots\,, \tag{1.4.2}$$

exact WKB predicts that the $\varepsilon \to 0$ asymptotics of the monodromy/Stokes data will be determined by computations that take place on the spectral curve of a_0. In particular, there are distinguished *spectral coordinates* X_γ on the moduli space of monodromy/Stokes data, labeled by cycles and open paths γ on the spectral curve. Exact WKB predicts that each spectral coordinate X_γ has leading WKB exponent given by a corresponding period $Z(\gamma)$. The construction of the spectral coordinates which we employ uses the *spectral networks* $\mathcal{W}(u, A, \vartheta = 0)$ as described in [22, 31] and briefly reviewed in Appendix C.

The linear system (1.1.1) clearly fits into the framework of (1.4.2), with

$$a_0 = \mathrm{i}u - \frac{1}{2\pi\mathrm{i}} \frac{A}{z}$$

and the spectral curve $\Gamma(u, A)$. We prove the following:

Theorem 1.6. For $n = 2, 3$, and for u near the caterpillar line and A near diagonal, the exact WKB prediction implies Conjecture 1.2, with the cycles $L_i^{(k)}$ given by the $C_i^{(k)}$ of (1.4.1).

Our proof requires us to describe the spectral networks $\mathcal{W}(u, A, \vartheta = 0)$. For $n = 2$ we do this analytically, but our proof for $n = 3$ involves some computer assistance. The obstacle to dealing with $n > 3$ has to do with the combinatorics of the spectral networks: some correction terms interfere with the translation from spectral coordinates to minor coordinates, and one needs to show that these correction terms do not affect the leading asymptotics. The precise desired statement is formulated in Conjecture 4.24. Modulo this obstacle, the extension of Theorem 1.6 to arbitrary rank is given in Theorem 4.25.

We remark that the exact WKB prediction is stronger than Conjecture 1.2: it predicts the full leading WKB exponent for generalized minors, both real and imaginary parts. We verify this prediction directly in the case $n = 2$, while for $n > 2$ it is a conjecture.

The exact WKB picture also gives a new geometric way of understanding the rhombus inequalities. Indeed, given the spectral network $\mathcal{W}(u, A, \vartheta = 0)$ one has the notion of *finite web*: this is a certain network of trajectories in $\mathcal{W}(u, A, \vartheta = 0)$. Each finite web determines a 1-cycle γ on $\Gamma(u, A)$, the *charge* of the web. Whenever γ arises in this way, the corresponding period is negative $Z(\gamma) < 0$. We show:

Theorem 1.7. For $n = 2$ and $n = 3$, and for u near the caterpillar line and A near diagonal, each rhombus inequality obeyed by the WKB exponents corresponds to a finite web in $\mathcal{W}(u, A, \vartheta)$, with a charge γ; the rhombus inequality is the fact that $Z(\gamma(u, A)) < 0$.

The exact WKB story which we develop here connects the equation (1.1.1) to various other areas of mathematics and physics. For instance, there is a known connection between exact WKB and cluster algebras as described in e.g. [21, 34]: the spectral coordinates X_γ are often identified with cluster coordinates on the moduli space of monodromy/Stokes data. The spectral networks that appear most directly in our WKB analysis are of a degenerate kind (ultimately because of the reality condition we impose on u, A and ε), so they don't directly give cluster coordinates; but, by perturbing ε to be complex, we can reach more generic spectral networks, which do give cluster coordinates. In the case $n = 2$ we work out the details, and show that the cluster structure which arises is the one considered by Goncharov-Shen in [27].

In another direction, there is a relation [21, 22] between exact WKB analysis of ODEs and $\mathcal{N} = 2$ supersymmetric field theories in four dimensions. In the particular example of (1.1.1), the relevant supersymmetric field theory is relatively simple: it is a Lagrangian gauge theory given by a certain quiver as described in [23]. We explain this briefly in Subsection 4.4.

1.5 Future directions

- In our discussion of spectral networks we left one important problem unsolved: how to prove Conjecture 4.24, and thus extend Theorem 1.6 beyond the cases $n = 2$ and $n = 3$? It seems possible that this will require some new insight into the structure of spectral networks for higher rank.

- We explored the connection between WKB for complex ε and the Goncharov-Shen cluster structure in detail for $n = 2$, and briefly for $n = 3$. It would be interesting to develop that connection in more detail in the $n \geq 3$ case.

- The connection between the ODE (1.1.1) and supersymmetric quantum field theory, briefly discussed in Subsection 4.4, has various consequences which would be interesting to explore. For example, it implies that one should be able to give an explicit representation of a τ function governing the isomonodromy deformations of (1.1.1), building it out of Nekrasov's partition function for the gauge theory [39]. This would be an analogue of the celebrated "Kiev formula" [25, 32] for rank 2 systems with regular singularities.

- The data of periods and Donaldson-Thomas invariants which we describe in Section 4 determines a Riemann-Hilbert problem in the ε-plane as explained in [21, 20, 14]. The solution of this Riemann-Hilbert problem should give the exact Stokes matrices.

- In this paper we focus mainly on the situation where u is a real diagonal matrix and A is Hermitian. For fixed u, the map that takes A to its WKB exponents (or equivalently the real parts of periods) is an example of a real integrable system, whose base is the Gelfand-Zeitlin cone cut out by the rhombus inequalities. If we also fix the conjugacy class of A then we again have a real integrable system $\mathcal{M}$, now with total space the flag manifold of $SL(n)$, and base a (compact) Gelfand-Zeitlin polytope.

  If we instead allow A to be complex, then we obtain a complex integrable system $\mathcal{M}_{\mathbb{C}}$ containing $\mathcal{M}$. We expect that $\mathcal{M}_{\mathbb{C}}$ can be described as a moduli space of framed wild Higgs bundles over $\mathbb{P}^1$. Such moduli spaces are expected to admit hyperkähler metrics at least in some open subsets, though the only example which is well understood so far is the "Ooguri-Vafa manifold" [41, 21, 45]. We expect that $\mathcal{M}_{\mathbb{C}}$ carries a hyperkähler metric in an open neighborhood of $\mathcal{M}$, and this metric should be a deformation of Kronheimer's hyperkähler metric on the cotangent bundle to the flag manifold. This can be confirmed directly in the case $n = 2$, where the relevant metric is of Gibbons-Hawking type, rather similar to Ooguri-Vafa; it should be interesting to explore it for $n > 2$.

1.6 Outline of the paper

In Section 2, we state the relation between Poisson brackets and WKB asymptotics, and we show that Conjecture 1.2 holds on the caterpillar line. In Section 3, we study the structure of the spectral curve. In particular, we show that it degenerates on the caterpillar line, and we use this degeneration pattern to construct cycles $C_i^{(k)}$. In Section 4, we use the spectral network theory to show that its predictions imply Conjecture 1.2 for the case of $n = 2, 3$. We also outline the relation to cluster coordinates of Goncharov-Shen, and to supersymmetric quantum gauge theory. In Appendix A, we collect information on the De Concini-Procesi compactification needed in the definition of the caterpillar line. In Appendix B, we give a detailed calculation of WKB asymptotics of the Stokes matrices on the caterpillar line for $n = 3$. In Appendix C, we recall some basic facts and conjectures about spectral networks.

Acknowledgements

The authors would like to thank Alexander Goncharov, Nikita Nikolaev, Alexander Shapiro, and Valerio Toledano Laredo for interesting and productive discussions. The research of A.A. was supported in part by grants 208235 and 200400 and by the National Center for Competence in Research (NCCR) SwissMAP of the Swiss National Science Foundation, and by the award of the Simons Foundation to the Hamilton Mathematics Institute of the Trinity College Dublin under the program "Targeted Grants to Institutes". The research of A.N. was supported by the National Science Foundation grant 2005312 and by a Simons Fellowship in Mathematics. Xu is supported by the National Key Research and Development Program of China (No. 2021YFA1002000) and by the National Natural Science Foundation of China (No. 12171006).

2 Stokes matrices, Poisson brackets and WKB

In Subsection 2.1, we recall the definitions of Stokes matrices and canonical solutions in Stokes supersectors. In Subsection 2.2, we recall Poisson geometry properties of Stokes matrices. In Subsection 2.3, we conjecture that Stokes matrices admit a WKB expansion, and under this assumption, we prove rhombus inequalities on leading WKB exponents. In Subsection 2.4, we define regularized Stokes matrices on the caterpillar line, give their explicit formulas in terms of Γ-functions following [49], study their WKB asymptotics, and give an algebraic interpretation of the corresponding rhombus inequalities.

2.1 Canonical solutions and Stokes matrices

The system (1.1.1) has a second-order pole at ∞ and (if $A \neq 0$) a first-order pole at 0, and it admits a unique formal power series solution of the form

$$\hat{F}(z; u, \varepsilon) = (\mathrm{Id}_n + F_1 z^{-1} + F_2 z^{-2} + \cdots) e^{\frac{\mathrm{i}uz}{\varepsilon}} z^{\frac{[A]}{2\pi\mathrm{i}\varepsilon}},$$

where Id_n is the rank n identity matrix, and $[A]$ is the diagonal part of A. The formal power series $\mathrm{Id}_n + F_1 z^{-1} + F_2 z^{-2} + \cdots$ is in general divergent. Thus, $\hat{F}(z, u, \varepsilon)$ is only a formal solution. However, the Borel resummation method gives rise to actual solutions with prescribed asymptotics defined in *Stokes supersectors*. In our case, there are two Stokes supersectors of (1.1.1), and they are given by

$$\begin{aligned} \widehat{\mathrm{Sect}}_+ &= \{z \in \mathbb{C} \mid -\pi < \arg(z) < \pi\}, \\ \widehat{\mathrm{Sect}}_- &= \{z \in \mathbb{C} \mid -2\pi < \arg(z) < 0\}. \end{aligned}$$

Choose the branch of $\log(z)$ which is real on the positive real axis and which has a branch cut along the nonnegative imaginary axis $\mathrm{i}\mathbb{R}_{\geq 0}$. Then, $\log(z)$ has imaginary part $-\pi$ on the negative real axis in $\widehat{\mathrm{Sect}}_-$. The following result is standard (see e.g., [8, 37, 48, 49]):

Theorem 2.1. For any $u \in \mathfrak{h}_{\mathrm{reg}}(\mathbb{R})$, there are unique fundamental solutions $F_\pm : \widehat{\mathrm{Sect}}_\pm \to \mathrm{GL}_n(\mathbb{C})$ of (1.1.1) such that

$$\begin{aligned} F_+(z; u, \varepsilon) \cdot e^{-\frac{\mathrm{i}uz}{\varepsilon}} \cdot z^{\frac{[A]}{2\pi\mathrm{i}\varepsilon}} &\sim \mathrm{Id}_n, \ \text{ as } \ z \to 0 \ \text{ within } \ \widehat{\mathrm{Sect}}_+, \\ F_-(z; u, \varepsilon) \cdot e^{-\frac{\mathrm{i}uz}{\varepsilon}} \cdot z^{\frac{[A]}{2\pi\mathrm{i}\varepsilon}} &\sim \mathrm{Id}_n, \ \text{ as } \ z \to 0 \ \text{ within } \ \widehat{\mathrm{Sect}}_-. \end{aligned}$$

The solutions $F_\pm$ are called *canonical solutions* in $\mathrm{Sect}_\pm$.

The set $\mathfrak{h}_{\mathrm{reg}}(\mathbb{R})$ consists of connected components labeled by elements of the permutation group. In more detail,

$$\mathfrak{h}_{\mathrm{reg}}(\mathbb{R}) = \cup_{\sigma \in S_n} U_\sigma, \quad U_\sigma = \{(u_1, \ldots, u_n) \in \mathbb{R}^n; u_{\sigma(1)} < u_{\sigma(2)} < \cdots < u_{\sigma(n)}\}. \tag{2.1.1}$$

We denote by $P_\sigma \in \mathrm{GL}(n)$ the $n \times n$ matrix implementing the permutation $\sigma \in S_n$.

Definition 2.2. For any $u \in U_\sigma$, the *Stokes matrices* of the system (1.1.1) (with respect to $\widehat{\mathrm{Sect}}_+$ and the branch of $\log(z)$) are the elements $S_\pm(u, A, \varepsilon) \in \mathrm{GL}(n)$ determined by

$$F_+(z; u, \varepsilon) = F_-(z; u, \varepsilon) \cdot e^{-\frac{[A]}{2\varepsilon}} P_\sigma S_+(u, A, \varepsilon) P_\sigma^{-1}, \tag{2.1.2}$$

$$F_-(z e^{-2\pi\mathrm{i}}; u, \varepsilon) = F_+(z; u, \varepsilon) \cdot P_\sigma S_-(u, A, \varepsilon) P_\sigma^{-1} e^{\frac{[A]}{2\varepsilon}}, \tag{2.1.3}$$

where the first (resp. second) identity is understood to hold in Sect_- (resp. Sect_+) after F_+ (resp. F_-) has been analytically continued clockwise.

The prescribed asymptotics of $F_\pm(z; u, \varepsilon)$ at $z = \infty$ and the identities in Definition 2.2 ensure that the Stokes matrices $S_+(u, A, \varepsilon)$ and $S_-(u, A, \varepsilon)$ are upper and lower triangular, respectively (see e.g. [7, Chapter 9.1] or [11, Lemma 17]). The reality conditions (1.1.2) imply that if $F(z)$ is a solution of (1.1.1), then so is the inverse of the conjugate transpose $(F(\bar{z})^{-1})^\dagger$ (see [11]). Thus, we have the following:

Lemma 2.3. $S_-(u, A, \varepsilon) = S_+(u, A, \varepsilon)^\dagger$.

Lemma 2.3 implies that the product

$$S(u, A, \varepsilon) = S_-(u, A, \varepsilon) \cdot S_+(u, A, \varepsilon) \tag{2.1.4}$$

is a positive definite Hermitian matrix. Also, note that S uniquely determines S_+ and S_- (under the condition that their diagonal entries are positive reals).

2.2 Poisson structure of Stokes matrices

Poisson geometry turns out to be a very useful tool in the study of the Stokes phenomenon. In more detail, we equip the set of data $(u, A) \in \mathfrak{h}_{\rm reg}(\mathbb{R}) \times \mathrm{Herm}(n)$ with the product Poisson structure π, where π vanishes on $\mathfrak{h}_{\rm reg}(\mathbb{R})$, and coincides with the linear Kirillov-Kostant-Souriau (KKS) Poisson structure on $\mathrm{Herm}(n)$. In particular, we have

$$\{A_{ij}, A_{kl}\} = \delta_{jk}A_{il} - \delta_{il}A_{kj}. \tag{2.2.1}$$

Note that equation (2.2.1) implies

$$\{\varepsilon^{-1}A_{ij}, \varepsilon^{-1}A_{kl}\} = \varepsilon^{-1}\left(\delta_{jk}\varepsilon^{-1}A_{il} - \delta_{il}\varepsilon^{-1}A_{kj}\right).$$

In other words, $(\varepsilon^{-1}u, \varepsilon^{-1}A) \in \mathfrak{h}_{\rm reg}(\mathbb{R}) \times \mathrm{Herm}(n)$ carry the Poisson bracket $\varepsilon^{-1}\pi$.

The results of Guillemin-Sternberg [28] show that eigenvalues $\lambda_i^{(k)}(A) = \lambda_i(A^{(k)})$ of submatrices $A^{(k)}$ Poisson commute with each other:

$$\left\{\lambda_i^{(k)}, \lambda_j^{(l)}\right\} = 0.$$

Furthermore, they satisfy Cauchy's interlacing inequalities

$$\lambda_i^{(k)} \leq \lambda_i^{(k+1)} \leq \lambda_{i+1}^{(k)}, \tag{2.2.2}$$

and they serve as action variables of the *Gelfand-Tsetlin integrable system*. Their Hamiltonian flows generate an action of the *Thimm torus* on the set $\mathrm{Herm}_0(n)$ where all the inequalities (2.2.2) are strict. This action preserves the action variables $\lambda_i^{(k)}$.

It is natural to ask whether the Stokes matrices $S_\pm(u, A, \varepsilon)$ carry a compatible Poisson structure which would make the map $(u, A) \mapsto S_\pm(u, A, \varepsilon)$ into a Poisson map. To explain the answer to this question, recall that the set of upper triangular matrices with positive reals on the diagonal is a Poisson Lie group $U(n)^*$ (over $\mathbb{R}$) dual under Poisson-Lie duality to the compact Poisson-Lie group $U(n)$ with the standard Poisson structure (see [38, 43]). That is, $U(n)^*$ carries a canonical Poisson structure π^* such that the multiplication map is a Poisson map. In terms of minor coordinates $\Delta_i^{(k)}$, the Poisson structure π^* is Laurent polynomial (see *e.g.* [1]).

The Poisson-Lie group $U(n)^*$ carries the Flaschka-Ratiu completely integrable system (see [19]). Let $S_+ \in U(n)^*$ and denote $S_- = S_+^\dagger$. Then, the matrix $S = S_-S_+ \in \mathrm{Herm}(n)$ is positive definite, and so are all $S^{(k)} = S_-^{(k)}S_+^{(k)} \in \mathrm{Herm}(k)$. The action variables of the Flaschka-Ratiu system are $\log \lambda_i^{(k)}(S)$. They satisfy the interlacing inequalities, and they generate the Thimm torus action which preserves $\log \lambda_i^{(k)}(S)$.

Example 2.4. For $n = 2$, we have minor coordinates $\Delta_1^{(1)}, \Delta_2^{(2)} \in \mathbb{R}_+, \Delta_1^{(2)}, \overline{\Delta}_1^{(2)} \in \mathbb{C}$. For simplicity, we put $\Delta_2^{(2)} = 1$ (this corresponds to considering $SU(2)^*$ instead of $U(2)^*$). Then, the Poisson bracket π^* has the form

$$\left\{\Delta_1^{(1)}, \Delta_1^{(2)}\right\}^* = -\frac{\mathrm{i}}{2}\Delta_1^{(1)}\Delta_1^{(2)}, \quad \left\{\Delta_1^{(2)}, \overline{\Delta}_1^{(2)}\right\}^* = \mathrm{i}\left(\left(\Delta_1^{(1)}\right)^{-2} - \left(\Delta_1^{(1)}\right)^2\right).$$

The following statement is one of the main results in [11]:

Theorem 2.5. For each $u \in \mathfrak{h}_{\mathrm{reg}}(\mathbb{R})$ and $\varepsilon \in \mathbb{R}_+$ the map

$$(\mathrm{Herm}(n), \pi) \to (U(n)^*, \varepsilon^{-1}\pi^*), \quad A \mapsto S_+(u, A, \varepsilon)$$

is a Poisson map.

Proof. In more detail, Theorem 1 in [11] is the statement above for $\varepsilon = 1$. Since pairs $(\varepsilon^{-1}u, \varepsilon^{-1}A)$ carry the Poisson bracket $\varepsilon^{-1}\pi$, the Poisson bracket π^* also gets rescaled by ε^{-1}. ■

2.3 WKB behavior

It is a common belief that in the limit of $\varepsilon \to 0$ the Stokes matrices admit a WKB behavior. In more detail, we will assume the following:

Conjecture 2.6. For A generic, the minor coordinates $\Delta_i^{(k)}(S_+(u, A, \varepsilon))$ admit an asymptotic expansion

$$\log\ \Delta_i^{(k)}(S_+(u, A, \varepsilon)) \sim \varepsilon^{-1}\delta_i^{(k)}(u, A) + \left(\delta_i^{(k)}\right)_0 + \varepsilon \left(\delta_i^{(k)}\right)_1 + \dots \tag{2.3.1}$$

The corresponding expansion of the eigenvalues $\lambda_i^{(k)}(S(u, A, \varepsilon))$,

$$\log\ \lambda_i^{(k)}(S(u, A, \varepsilon)) \sim \varepsilon^{-1}\, \eta_i^{(k)}(u, A) + \dots\ , \tag{2.3.2}$$

is uniform as u approaches the caterpillar line, $u \to u_{\mathrm{cat}}(t)$.

We refer to the coefficients $\delta_i^{(k)}(u, A)$ in (2.3.1) as *leading WKB exponents*. It is convenient to introduce a special notation for their real parts:

$$l_i^{(k)}(u, A) = \mathrm{Re}\ \delta_i^{(k)}(u, A).$$

In contrast to $\Delta_i^{(k)}(S_+)$, the eigenvalues $\lambda_i^{(k)}(S)$ are real, and so are the leading exponents $\eta_i^{(k)}(u, A)$ in (2.3.2).

Theorem 2.5 and Conjecture 2.6 imply the following interesting result:

Theorem 2.7. Assuming Conjecture 2.6, the real parts of leading WKB exponents $l_i^{(k)}(u, A)$ verify the rhombus inequalities

$$l_i^{(k+1)} + l_{i-1}^{(k)} \geq l_{i+1}^{(k+1)} + l_i^{(k)}, \quad l_i^{(k+1)} + l_i^{(k)} \geq l_{i+1}^{(k+1)} + l_{i-1}^{(k)}, \tag{2.3.3}$$

where $l_0^{(k)} \equiv 0$. Furthermore, all Poisson brackets between $\delta_i^{(k)}, \overline{\delta}_i^{(k)}$ vanish:

$$\left\{\delta_i^{(k)}, \delta_j^{(l)}\right\} = 0, \quad \left\{\delta_i^{(k)}, \overline{\delta}_j^{(l)}\right\} = 0, \quad \left\{\overline{\delta}_i^{(k)}, \overline{\delta}_j^{(l)}\right\} = 0. \tag{2.3.4}$$

Proof. We first consider the case of $n = 2$. We compute,

$$\left\{\Delta_1^{(2)}, \overline{\Delta}_1^{(2)}\right\}^* = \varepsilon\ \left\{e^{\varepsilon^{-1}\delta_1^{(2)}+\dots}, e^{\varepsilon^{-1}\overline{\delta}_1^{(2)}+\dots}\right\} = e^{2\varepsilon^{-1}l_1^{(2)}}\left(\varepsilon^{-1}\{\delta_1^{(2)}, \overline{\delta}_1^{(2)}\} + \dots\right), \tag{2.3.5}$$

where in the first equality we used Theorem 2.5 to pass from π^* to π. Next, we compute

$$\left\{\Delta_1^{(2)}, \overline{\Delta}_1^{(2)}\right\}^* = \mathrm{i}\ \left(\left(\Delta_1^{(1)}\right)^{-2} - \left(\Delta_1^{(1)}\right)^2\right) = \mathrm{i}\ \left(e^{-2\varepsilon^{-1}l_1^{(1)}+\dots} - e^{2\varepsilon^{-1}l_1^{(1)}+\dots}\right), \tag{2.3.6}$$

where we have used the fact that $\Delta_1^{(1)} \in \mathbb{R}_+$ and $\delta_1^{(1)} = l_1^{(1)}$. We observe that the right hand sides of (2.3.5) and (2.3.6) can only match if

$$l_1^{(2)} \geq l_1^{(1)}, \quad l_1^{(2)} \geq -l_1^{(1)},$$

and that these are exactly the rhombus inequalities in the case of $n = 2$ (under the simplifying assumption of $l_2^{(2)} = 0$). The analysis for arbitrary n is done in Theorem 5 in [1]. Note that in that paper one assumes

$$\log\ \Delta_i^{(k)} = \varepsilon^{-1} l_i^{(k)} + \mathrm{i}\varphi_i^{(k)},$$

and the resulting Poisson bracket on $(l_i^{(k)}, \varphi_i^{(k)})$ depends on ε. However, the $n = 2$ argument above shows that only the real part of the leading WKB exponent is relevant for the proof of rhombus inequalities. Hence, the proof of [1] applies verbatim.

To establish the vanishing of Poisson brackets of the leading WKB exponents, we re-examine the equality of the right-hand sides of (2.3.5) and (2.3.6). We observe that even if the exponential factors match, one has an extra ε^{-1} factor in front of $\{\delta_1^{(2)}, \overline{\delta}_1^{(2)}\}$ in (2.3.5) which is absent in (2.3.6). Hence,

$$\{\delta_1^{(2)}, \overline{\delta}_1^{(2)}\} = 0.$$

The same argument applies to the Poisson bracket of any two minor coordinates which in turn implies (2.3.4). ■

For $S_\pm$ generic, there is a simple linear relation between the leading WKB exponents $l_i^{(k)}$ and $\eta_i^{(k)}$:

Proposition 2.8. Assume that $S_\pm$ admits a WKB expansion and that all the rhombus inequalities for $l_i^{(k)}$ are strict. Then, we have

$$l_i^{(k)} = \frac{1}{2} \sum_{j=k-i+1}^{k} \eta_j^{(k)}. \tag{2.3.7}$$

Proof. This fact follows from Proposition 2 in [4] (see also Proposition 5.1 in [3]). For the convenience of the reader, we illustrate the proof in the case of $n = 2$. Consider a matrix S_+ which admits a WKB behavior:

$$S_+ = \begin{pmatrix} e^{\frac{1}{\varepsilon}\alpha + \dots} & e^{\frac{1}{\varepsilon}\beta + \dots} \\ 0 & e^{-\frac{1}{\varepsilon}\alpha + \dots} \end{pmatrix}.$$

Then, $\Delta_1^{(2)}(S_+) = (S_+)_{12} = e^{\frac{1}{\varepsilon}\beta + \dots}$ and $\delta_1^{(2)} = \beta, l_1^{(2)} = \operatorname{Re}\beta$. We also have

$$\lambda_1^{(2)}(S) + \lambda_2^{(2)}(S) = \operatorname{Tr} S = \operatorname{Tr}(S_+^\dagger S_+) = e^{\frac{2}{\varepsilon}\operatorname{Re}\beta + \dots} + e^{\frac{2}{\varepsilon}\alpha + \dots} + e^{-\frac{2}{\varepsilon}\alpha + \dots}.$$

Hence,

$$\eta_2^{(2)} = 2\max(\operatorname{Re}\beta, \alpha, -\alpha) = 2\operatorname{Re}\beta = 2\, l_1^{(2)},$$

as required. Here we have used the strict rhombus inequalities $\operatorname{Re}\beta > \alpha, -\alpha$. ■

Remark 2.9. Under the linear change of variables $l_i^{(k)} = \frac{1}{2}\sum_{j=k-i+1}^{k} \eta_i^{(k)}$, the rhombus inequalities for parameters $l_i^{(k)}$ are equivalent to the interlacing inequalities for parameters $\eta_i^{(k)}$. In this paper, we will see several instances of such a change of variables.

2.4 Stokes matrices on the caterpillar line

Determining Stokes matrices for $n \geq 3$ is a formidable task. However, there is a limit in which explicit formulas are available. In more detail, one considers the situation for $u \in U_{\mathrm{id}}$ (here $\mathrm{id} \in S_n$ is the identity element) when

$$u_2 - u_1 = t, \quad \frac{u_{j+1} - u_j}{u_j - u_{j-1}} \to +\infty \ \text{ for } \ j = 2, \dots, n-1. \tag{2.4.1}$$

Such configurations no longer belong to $\mathfrak{h}_{\mathrm{reg}}(\mathbb{R})$, but they make sense in its *De Concini - Procesi* compactification (see [16] and Appendix A for details). We say that configurations (2.4.1) belong to the *caterpillar line* and denote them by $u_{\mathrm{cat}}(t)$. The De Concini-Procesi compactification of $\mathfrak{h}_{\mathrm{reg}}(\mathbb{R})$ can also be identified with the tautological line bundle $\widetilde{\mathcal{M}}_{0,n+1}(\mathbb{R}) \to \overline{\mathcal{M}}_{0,n+1}(\mathbb{R})$ over (the real locus of) the Deigne-Mumford compactification of the moduli space of rational curves with $n+1$ marked points.

The results described in this Section were established in [49] by the method of isomonodromy deformation. We will need the following notation: for a matrix $A \in \mathrm{Mat}_n(\mathbb{C})$, we denote

$$\delta_k(A)_{ij} = \begin{cases} A_{ij}, & \text{if } 1 \le i,j \le k \text{ or } i=j; \\ 0, & \text{otherwise.} \end{cases} \tag{2.4.2}$$

Note that if $A \in \mathrm{Herm}(n)$, then so is $\delta_k(A)$. For a matrix $B \in \mathrm{Mat}_n(\mathbb{C})$, we denote by $\Delta^I_J(B)$ its minor formed by the rows $I = \{i_1, \dots, i_k\}$ and by the columns $J = \{j_1, \dots, j_k\}$.

While the Stokes matrices $S_\pm(u, A, \varepsilon)$ don't have a limit when $u \to u_{\mathrm{cat}}(t)$, one can separate their divergent and convergent parts in the following way. Define the unitary matrix

$$V(u, A, \varepsilon) = \overrightarrow{\prod_{k=2,\dots,n-1}} \left(\frac{u_k - u_{k-1}}{u_{k+1} - u_k} \right)^{\frac{\log(\delta_k(S_-)\delta_k(S_+))}{2\pi i \varepsilon}},$$

and denote

$$S^{\mathrm{reg}}(u, A, \varepsilon) = V(u, A, \varepsilon) \cdot S(u, A, \varepsilon) \cdot V(u, A, \varepsilon)^{-1}, \tag{2.4.3}$$

where S is given by equation (2.1.4). This expression uniquely defines the lower and upper triangular matrices $S^{\mathrm{reg}}_- = (S^{\mathrm{reg}}_+)^\dagger$ with the property $S^{\mathrm{reg}} = S^{\mathrm{reg}}_- S^{\mathrm{reg}}_+$.

Proposition 2.10. The map $S_\pm \mapsto S^{\mathrm{reg}}_\pm$ is a Poisson map under the bracket $\varepsilon^{-1}\pi^*$. It preserves the eigenvalues $\lambda^{(k)}_i(S^{\mathrm{reg}}) = \lambda^{(k)}_i(S)$.

Proof. The transformation (2.4.3) is a particular instance of the Thimm torus action, and hence it preserves all Gelfand-Tsetlin functions $\lambda^{(k)}_i(S)$. Furthermore, the parameters of that Thimm action depend only on action variables, and hence it is a canonical transformation: it preserves action variables, and it shifts the conjugate angle variables by a function of action variables. ■

The following result will be of importance to us:

Theorem 2.11. [49, Theorem 1.5] For fixed $\varepsilon > 0$ and for any $A \in \mathrm{Herm}(n)$, the expressions $S^{\mathrm{reg}}_\pm(u, A, \varepsilon)$ have a well defined limit for $u \to u_{\mathrm{cat}}(t)$. Furthermore, at $u = u_{\mathrm{cat}}(t)$ one has

$$\begin{aligned}(S^{\mathrm{reg}}_+)_{k,k+1} =& 2\pi i \cdot \left(\frac{u_2 - u_1}{\varepsilon} \right)^{\frac{A_{k+1,k+1} - A_{kk}}{2\pi i \varepsilon}} e^{\frac{A_{kk} + A_{k+1,k+1}}{4\varepsilon}} \cdot \\ & \sum_{i=1}^{k} \frac{\prod_{l=1, l\neq i}^{k} \Gamma\left(1 + \frac{\lambda^{(k)}_l - \lambda^{(k)}_i}{2\pi i \varepsilon}\right)}{\prod_{l=1}^{k+1} \Gamma\left(1 + \frac{\lambda^{(k+1)}_l - \lambda^{(k)}_i}{2\pi i \varepsilon}\right)} \frac{\prod_{l=1, l\neq i}^{k} \Gamma\left(\frac{\lambda^{(k)}_l - \lambda^{(k)}_i}{2\pi i \varepsilon}\right)}{\prod_{l=1}^{k-1} \Gamma\left(1 + \frac{\lambda^{(k-1)}_l - \lambda^{(k)}_i}{2\pi i \varepsilon}\right)} \cdot \Delta^{1,\dots,k-1,k}_{1,\dots,k-1,k+1} \left(\frac{A - \lambda^{(k)}_i}{2\pi i \varepsilon} \right).\end{aligned}$$

Other entries of $S^{\mathrm{reg}}_\pm(u_{\mathrm{cat}}(t), A, \varepsilon)$ are also given by explicit formulas.

Remark 2.12. We can further consider the limit $t = u_2 - u_1 \to 0$. In more detail, one can put

$$S^{\mathrm{reg}}_\pm(u_{\mathrm{cat}}, A, \varepsilon) = t^{\frac{\delta_1(A)}{2\pi i \varepsilon}} \cdot S^{\mathrm{reg}}_\pm(u_{\mathrm{cat}}(t), A, \varepsilon) \cdot t^{\frac{-\delta_1(A)}{2\pi i \varepsilon}}, \tag{2.4.4}$$

where the right-hand side turns out to be independent of t.

Example 2.13. Consider the case of $n = 2$:

$$\varepsilon \frac{dF}{dz} = \left(\begin{pmatrix} \mathrm{i}u_1 & 0 \\ 0 & \mathrm{i}u_2 \end{pmatrix} - \frac{1}{2\pi \mathrm{i} z} \begin{pmatrix} t_1 & a \\ \bar{a} & t_2 \end{pmatrix} \right) \cdot F.$$

Following Proposition 8 in [8], the Stokes matrices (with respect to the chosen branch of $\log(z)$) are

$$S_-(u, A, \varepsilon) = \begin{pmatrix} e^{\frac{t_1}{2\varepsilon}} & 0 \\ \frac{\frac{\bar{a}}{\varepsilon} \cdot e^{\frac{t_2+t_1}{4\varepsilon}} \left(\frac{u_2-u_1}{\varepsilon}\right)^{\frac{t_1-t_2}{2\pi \mathrm{i}\varepsilon}}}{\Gamma\left(1-\frac{\lambda_1-t_1}{2\pi\mathrm{i}\varepsilon}\right)\Gamma\left(1-\frac{\lambda_2-t_1}{2\pi\mathrm{i}\varepsilon}\right)} & e^{\frac{t_2}{2\varepsilon}} \end{pmatrix}, \quad S_+(u, A, \varepsilon) = \begin{pmatrix} e^{\frac{t_1}{2\varepsilon}} & \frac{\frac{a}{\varepsilon} \cdot e^{\frac{t_2+t_1}{4\varepsilon}} \left(\frac{u_2-u_1}{\varepsilon}\right)^{\frac{t_2-t_1}{2\pi \mathrm{i}\varepsilon}}}{\Gamma\left(1+\frac{\lambda_1-t_1}{2\pi\mathrm{i}\varepsilon}\right)\Gamma\left(1+\frac{\lambda_2-t_1}{2\pi\mathrm{i}\varepsilon}\right)} \\ 0 & e^{\frac{t_2}{2\varepsilon}} \end{pmatrix}.$$

By definition, for $t = u_2 - u_1 > 0$ we have $S_\pm(u_{\mathrm{cat}}(t), A, \varepsilon) = S_\pm(u, A, \varepsilon)$. Furthermore, we have

$$t^{\frac{\delta_1(A)}{2\pi \mathrm{i}}} = \mathrm{diag}\left((u_2 - u_1)^{\frac{t_1}{2\pi\mathrm{i}\varepsilon}}, (u_2 - u_1)^{\frac{t_2}{2\pi\mathrm{i}\varepsilon}} \right),$$

and we obtain

$$S_-^{\mathrm{reg}}(u_{\mathrm{cat}}, A, \varepsilon)^\dagger = S_+^{\mathrm{reg}}(u_{\mathrm{cat}}, A, \varepsilon) = \begin{pmatrix} e^{\frac{t_1}{2\varepsilon}} & \frac{a}{\varepsilon} \cdot \frac{\frac{1}{\varepsilon}^{\frac{t_2-t_1}{2\pi\mathrm{i}\varepsilon}} e^{\frac{t_1+t_2}{4\varepsilon}}}{\Gamma\left(1+\frac{\lambda_1-t_1}{2\pi\mathrm{i}\varepsilon}\right)\Gamma\left(1+\frac{\lambda_2-t_1}{2\pi\mathrm{i}\varepsilon}\right)} \\ 0 & e^{\frac{t_2}{2\varepsilon}} \end{pmatrix}.$$

One can use Theorem 2.11 to obtain information on the WKB expansion of regularized Stokes matrices on the caterpillar line:

Theorem 2.14. For all $A \in \mathrm{Herm}_0(n)$, the regularized Stokes matrices $S_\pm^{\mathrm{reg}}(u_{\mathrm{cat}}(t), A, \varepsilon)$ verify Conjecture 2.6, and one has

$$l_i^{(k)}(u_{\mathrm{cat}}(t), A) = \frac{1}{2} \sum_{j=k-i+1}^{k} \lambda_j^{(k)}(A), \tag{2.4.5}$$

where $\lambda_j^{(k)}(A)$ are eigenvalues of the Hermitian matrices $A^{(k)}$ ordered from bottom to top.

Proof. Since elements of $S_\pm^{\mathrm{reg}}(u_{\mathrm{cat}}(t), A, \varepsilon)$ are given by explicit formulas, one can check the statements of the theorem by a direct (albeit tedious) computation. We illustrate this strategy for $n = 2$. Recall that $r \in \mathbb{R}$ we have the following asymptotic expansion of the Γ-function with repect to the parameter $\varepsilon \to 0$:

$$\log \Gamma\left(1 + \frac{r}{2\pi\mathrm{i}\varepsilon}\right) = -\frac{r}{2\pi\mathrm{i}\varepsilon} \log(\varepsilon) + \frac{r}{2\pi\mathrm{i}\varepsilon} \log\left(\frac{|r|}{2\pi}\right) - \frac{|r|}{4\varepsilon} - \frac{r}{2\pi\mathrm{i}\varepsilon} + \frac{1}{2}\log\left(\frac{r}{\mathrm{i}\varepsilon}\right) + O(\varepsilon). \tag{2.4.6}$$

Following Example 2.13 and equation (2.4.6), consider the $n = 2$ case with

$$A = \begin{pmatrix} t_1 & a \\ \bar{a} & t_2 \end{pmatrix}$$

and eigenvalues $\lambda_1 < \lambda_2$. Then, the asymptotics of the entry $S_\pm^{\mathrm{reg}}(u_{\mathrm{cat}}(t), A, \varepsilon)_{12} = S_+(u_{\mathrm{cat}}(t), A, \varepsilon)_{12}$ is given by

$$(S_+)_{12} = \frac{\frac{a}{\varepsilon} \cdot e^{\frac{t_2+t_1}{4\varepsilon}} \left(\frac{u_2-u_1}{\varepsilon}\right)^{\frac{t_2-t_1}{2\pi\mathrm{i}\varepsilon}}}{\Gamma\left(1 + \frac{\lambda_1-t_1}{2\pi\mathrm{i}\varepsilon}\right)\Gamma\left(1 + \frac{\lambda_2-t_1}{2\pi\mathrm{i}\varepsilon}\right)} \sim e^{\varepsilon^{-1}\left(\frac{\lambda_2}{2} + \mathrm{i}\varphi\right)} \left(\frac{a}{\sqrt{(\lambda_1 - t_1)(t_1 - \lambda_2)}} + O(\varepsilon) \right).$$

This matches (2.4.5) since in this case $\Delta_1^{(2)} = (S_+)_{12}$ and $l_1^{(2)} = \lambda_2/2$, as required. Observe that the coefficients in front of the terms $\varepsilon^{-1}\log(\varepsilon)$ an $\log(\varepsilon)$ vanish confirming the WKB behavior: the actual leading term is proportional to ε^{-1}. Also, observe that the condition of $A \in \mathrm{Herm}_0(n)$ is necessary: in our example, $a = 0$ implies $(S_+)_{12} = 0$

and the WKB expansion does not apply. For completeness, we give an explicit formula for the imaginary part φ of the leading WKB exponent:

$$\varphi = \frac{(t_1 - t_2)}{2\pi} \log(u_2 - u_1) + \frac{t_1 - t_2}{2\pi} + \frac{(\lambda_1 - t_1)}{2\pi} \log\left(\frac{t_1 - \lambda_1}{2\pi}\right) + \frac{(\lambda_2 - t_1)}{2\pi} \log\left(\frac{\lambda_2 - t_1}{2\pi}\right).$$

For $n = 3$, we collect detailed calculations in Appendix B. For $n > 3$, the calculations are similar but more tedious.

We prove equation (2.4.5) using a combination of the following two results. First, Proposition 4.1 in [49] shows that the map $A \mapsto S_+^{\mathrm{reg}}(u_{\mathrm{cat}}, A, \varepsilon)$ intertwines (up to the factor of ε^{-1}) the Gelfand-Tsetlin and the Flaschka-Ratiu integrable systems. That is, for any $t = u_2 - u_1 > 0$

$$\log \lambda_i^{(k)}(u_{\mathrm{cat}}(t), A, \varepsilon) = \varepsilon^{-1} \lambda_i^{(k)}(A). \tag{2.4.7}$$

Hence,

$$\eta_i^{(k)}(u_{\mathrm{cat}}(t), A) = \lambda_i^{(k)}(A).$$

And by Proposition 2.8 we have

$$l_i^{(k)}(u_{\mathrm{cat}}(t), A) = \frac{1}{2} \sum_{j=k-i+1}^{k} \nu_j^{(k)}(u_{\mathrm{cat}}(t), A) = \frac{1}{2} \sum_{j=k-1+i}^{k} \lambda_j^{(k)}(A),$$

as required. ■

We conclude this section with the following observation:

Proposition 2.15. Under Conjecture 2.6, the leading WKB exponents of $S_+(u, A, \varepsilon)$ admit a limit for $A \in \mathrm{Herm}_0(n)$ and $u \to u_{\mathrm{cat}}(t)$, and

$$l_i^{(k)}(u, A) \to_{u \to u_{\mathrm{cat}}(t)} l_i^{(k)}(u_{\mathrm{cat}}(t), A) = \frac{1}{2} \sum_{j=k-i+1}^{k} \lambda_j^{(k)}(A).$$

Proof. By Proposition 2.10, $\lambda_i^{(k)}(S^{\mathrm{reg}}) = \lambda_i^{(k)}(S)$. Hence, they have the same leading WKB exponents $\eta_i^{(k)}(u, A)$. Under Conjecture 2.6, the WKB expansion of $\lambda_i^{(k)}(S)$ is uniform for $u \to u_{\mathrm{cat}}(t)$. Therefore,

$$\lim_{u \to u_{\mathrm{cat}}(t)} \eta_i^{(k)}(u, A) = \eta_i^{(k)}(u_{\mathrm{cat}}(t), A).$$

By Proposition 2.8, the WKB exponent $l_i^{(k)}$'s are related to $\eta_i^{(k)}$ by a linear transformation if the rhombus inequalities are strict. By assumption, $A \in \mathrm{Herm}_0(n)$ and the rhombus inequalities are strict on the caterpillar line. By continuity, they are also strict on a small open neighborhood of the caterpillar line which implies the desired result. ■

One of the goals of this paper is to understand the rhombus inequalities away from the caterpillar line. To address this question, in the next sections, we use more powerful geometric tools of spectral curves and spectral networks.

3 Spectral curves

In this section, we study the degeneration of the spectral curves as u approaches a point on the caterpillar line. The main results are Theorem 3.12, Corollary 3.14, and Theorem 3.16. In Subsection 3.1, we consider generic values of parameters (u, A) and compute the genus of smooth spectral curves. In Subsection 3.2, we consider spectral curves for the case when $u = E_n$ (the elementary matrix with $(E_n)_{nn} = 1$). In Subsection 3.3, we consider spectral curves as u approaches a point on the caterpillar line and define vanishing cycles on these curves. In Subsection 3.4, we introduce distinguished cycles as linear combinations of vanishing cycles, and in Theorem 3.16 we show that

Conjecture 1.2 holds on the caterpillar line. Finally, in Subsection 3.5 we discuss the situation of A being close to a diagonal matrix which will be our main playground in the next section.

Even though in this paper we impose a reality condition on the u- and A-parameters, most proofs in this section are in the *complex setting* for more generality. The reality condition induces a $\mathbb{Z}_2$-symmetry as we discuss in Proposition 3.17.

3.1 Spectral curves: generic case

Let $\mathfrak{g} = \mathfrak{gl}_n(\mathbb{C})$, and $\mathfrak{h} \subset \mathfrak{g}$ the Cartan Lie subalgebra of diagonal matrices. We start by considering $u \in \mathfrak{h}_{\text{reg}}(\mathbb{C})$ and $A \in \mathfrak{g}^* = \mathfrak{gl}_n(\mathbb{C})^* \simeq \mathfrak{gl}_n(\mathbb{C})$.

We denote by $\Gamma(u, A)$ the *spectral curve* of the equation (1.1.1) living in $T^*_{\mathbb{P}^1}$ and defined by

$$\det\left[\left(\mathrm{i}u - \frac{A}{2\pi \mathrm{i}z}\right)dz - \omega I_n\right] = 0\,. \tag{3.1.1}$$

Here $\omega = \mu(z)dz$, and $\mu(z)$ is a meromorphic function on $\mathbb{P}^1$. The 1-form ω is the pull-back to the spectral curve $\Gamma(u, A)$ of the tautological 1-form of $T^*_{\mathbb{P}^1}$. For this reason, one refers to ω as to the *canonical 1-form*. Equation (3.1.1) shows that ω has poles at points lying over $z = 0$ and $z = \infty$. We call such points *punctures*. In conclusion, $\Gamma(u, A)$ is an open curve with punctures lying over $z = 0$ and $z = \infty$.

One can reformulate equation (3.1.1) as a polynomial equation for a meromorphic function $\mu(z)$:

$$P(\mu, z^{-1}) = \det\left(\mathrm{i}u - \frac{1}{2\pi\mathrm{i}}\frac{A}{z} - \mu I_n\right) = 0 \tag{3.1.2}$$

This equation provides an embedding of $\Gamma(u, A)$ into $\mathbb{C}^2$. For $i = 1, \dots, n$, we denote by u_i the i^{th} entry on the diagonal of u, and by $t_i = A_{ii}$ the i^{th} diagonal entry of A.

This subsection aims to show that for u and A generic the spectral curve $\Gamma(u, A)$ is smooth, and to compute its genus. First, we prove the following two lemmas.

Lemma 3.1. Let $g(y)$ be a polynomial of degree n with coefficients $b_0, \dots, b_{n-1}$:

$$g(y) = y^n + b_{n-1}y^{n-1} + \cdots + b_1 y + b_0.$$

Then, its discriminant can be represented in the form

$$\Delta = b_0 \cdot h_1(b_0, b_1, \cdots, b_{n-1}) + b_1^2 \cdot h_2(b_1, \cdots, b_{n-1}).$$

Proof. Recall that the discriminant $\Delta(b_0, \dots, b_{n-1})$ can be written as

$$\Delta(b_0, \cdots, b_n) = (-1)^{\frac{n(n-1)}{2}} \prod_{i \neq j} (r_i - r_j),$$

where r_i's are the roots of the polynomial $g(y)$. Set $b_0 = 0$ and let $r_n = 0$. Then, we have $b_1 = (-1)^{n-1}\prod_{i=1}^{n-1} r_i$ and

$$\Delta = (-1)^{\frac{n(n-1)}{2}} \prod_{i=1}^{n-1}(r_i - r_n) \prod_{i=1}^{n-1}(r_n - r_i) \prod_{\substack{i \neq j \\ i,j \leq n-1}} (r_i - r_j) \tag{3.1.3}$$

$$= (-1)^{\frac{n(n-1)}{2}}(-1)^{n-1} b_1^2 \prod_{\substack{i \neq j \\ i,j \leq n-1}} (r_i - r_j). \tag{3.1.4}$$

Then, the statement follows from the fact that $\prod_{\substack{i \neq j \\ i,j \leq n-1}} (r_i - r_j)$ is a polynomial in $b_1, \cdots, b_{n-1}$. ■

Lemma 3.2. Let C be a plane curve, and suppose that on an analytic neighborhood of $(0,0)$ it is defined by equation

$$g(y,z) = y^n + f_1(z)y^{n-1} + f_2(z)y^{n-2} + \cdots + f_{n-1}(z)y + f_n(z) = 0,$$

where $f_1(z), \cdots, f_n(z)$ are polynomials, and $f_{n-1}(z)$ and $f_n(z)$ vanish at $z=0$. Then, C is smooth at $(0,0)$ if the discriminant of $g(y,z)$ viewed as a polynomial in y has a simple zero at $z=0$.

Proof. Denote by $\Delta(z)$ the discriminant of $g(y,z)$ viewed as a polynomial in y. Note that vanishing of $f_{n-1}(z)$ at $z=0$ implies that $\Delta(z)$ also vanishes at $z=0$. By Lemma 3.1, we can write $\Delta(z)$ as

$$\Delta(z) = f_n(z)\cdot h_1(f_1,\cdots,f_{n-1},f_n) + f_{n-1}^2(z)\cdot h_2(f_1,\cdots,f_{n-1})\,.$$

If Δ has a simple zero at $z=0$, then

$$\Delta'(0) = f_n'(0)h_1(f_1(0),\ldots,f_n(0)) \neq 0.$$

Thus, we must have $f_n'(0)\neq 0$, and

$$\frac{\partial g}{\partial z}(0,0) = f_n'(0) \neq 0.$$

This implies that the curve C is smooth at $(0,0)$, as required. ■

The following proposition describes the structure of the spectral curve $\Gamma(u,A)$ for (u,A) generic.

Proposition 3.3. For $u\in\mathfrak{h}_{\mathrm{reg}}(\mathbb{C})$ and $A\in\mathfrak{gl}_n(\mathbb{C})$ satisfying the following genericity condition:

i) eigenvalues of A are distinct,

ii) the discriminant of the equation $P(\mu,z^{-1})$ viewed as a polynomial in μ, has only simple zeroes for $z\in\mathbb{C}\backslash\{0\}$,

the spectral curve $\Gamma(u,A)$ is isomorphic to a smooth curve of genus $\frac{(n-1)(n-2)}{2}$ with $2n$ punctures.

Proof. By condition ii), it follows from Lemma 3.2 that the spectral curve $\Gamma(u,A)$ is smooth.

Next, we consider the punctures of $\Gamma(u,A)$. Over $z=\infty$, there are n distinct punctures $(\mu=u_i, z=\infty)$ for $i=1,\ldots,n$. Near $z=0$, μ has n branches

$$\mu_i(z) = -\frac{\lambda_i^{(n)}}{2\pi\mathrm{i}}\frac{1}{z} + \cdots\,,\ \text{ for } i=1,\ldots,n, \tag{3.1.5}$$

where $\lambda_i^{(n)}$ are the eigenvalues of A. These branches are distinct since A has n distinct eigenvalues. Therefore, after blowing up $\mathbb{P}^1_\mu\times\mathbb{P}^1_z$ at $(\mu=\infty, z=0)$, the closure $\overline{\Gamma}(u,A)$ of $\Gamma(u,A)$ inside the blowup will be a smooth compactification of $\Gamma(u,A)$. Moreover, $\bar{\Gamma}(u,A)\to\mathbb{P}^1$ will be unramified at punctures over $z=\infty$ and $z=0$.

By the Riemann-Hurwitz formula, we have

$$2g(\overline{\Gamma}) - 2 = n\cdot(2g(\mathbb{P}^1)-2) + \sum_{p\in\overline{\Gamma}}(e_p-1)\,, \tag{3.1.6}$$

where e_p is the ramification index at $p\in\overline{\Gamma}$.

Since $\partial_\mu P(\mu,z^{-1})$ has only simple zeroes for $z\in\mathbb{C}\setminus\{0\}$ as dictated by condition ii) and $\bar{\Gamma}(u,A)\to\mathbb{P}^1$ are unramified at punctures over $z=0$ and $z=\infty$, all ramification points in $\overline{\Gamma}$ have ramification index 2, and the number of ramification points is the number of zeroes of $\partial_\mu P(\mu,z^{-1})$. Since $\partial_\mu P(\mu,z^{-1})$ is a meromorphic function on $\overline{\Gamma}$, the number of zeroes and poles (counted with multiplicity) are the same. Therefore, it suffices to compute the number of poles, which only occur over $z=0$. On the i^{th} branch (3.1.5), we have

$$\partial_\mu P(\mu,z^{-1})\mid_{\mu=\mu_i} = \prod_{j|j\neq i}(\mu_i-\mu_j) = \prod_{j|j\neq i}\left(-\frac{\lambda_i^{(n)}-\lambda_j^{(n)}}{2\pi\mathrm{i}}\frac{1}{z}+O(1)\right)$$

Therefore, $\partial_\mu P(\mu, z^{-1})$ has a pole of order $(n-1)$ on each branch over $z = 0$, and the total pole order of $\partial_\mu P(\mu, z^{-1})$ is $n(n-1)$. The, equation (3.1.6) yields

$$2g(\overline{\Gamma}) - 2 = n(-2) + n(n-1) \Rightarrow g(\overline{\Gamma}) = \frac{(n-1)(n-2)}{2},$$

as desired. ■

In the next proposition, we collect information on the residues of the canonical 1-form ω at punctures of $\Gamma(u, A)$ lying over $z = 0$ and $z = \infty$:

Proposition 3.4. For $u \in \mathfrak{h}_{\mathrm{reg}}(\mathbb{C})$ and $A \in \mathfrak{gl}_n(\mathbb{C})$ with distinct eigenvalues, the canonical 1-form ω has residues $-\frac{\lambda_i^{(n)}}{2\pi \mathrm{i}}(1 \le i \le n)$ at punctures lying over $z = 0$ and residues $\frac{t_i}{2\pi \mathrm{i}}(1 \le i \le n)$ at punctures lying over $z = \infty$.

Proof. For punctures lying over $z = 0$, equation (3.1.5) directly gives the values $-\frac{\lambda_i^{(n)}}{2\pi \mathrm{i}}$ of residues corresponding to n branches.

Near $z = \infty$, $\mu(z)$ also has n branches of the form

$$\mu_i(z) = \mathrm{i}\, u_i - \frac{1}{2\pi \mathrm{i}} \frac{t_i}{z} + O\left(\frac{1}{z^2}\right), \quad 1 \le i \le n, \tag{3.1.7}$$

where $t_i = A_{ii}$ is the i^{th} diagonal entry of A. Indeed, let $\mu(z) = \Sigma_{k=0}^{\infty} c_k z^{-k}$ and substitute this power series into the defining equation of $\Gamma(u, A)$ to obtain

$$\det\left(\mathrm{i}\, u - \frac{A}{2\pi \mathrm{i} z} - \mu I_n\right) = \prod_{i=1}^{n}\left(\mathrm{i}\, u_i - \frac{t_i}{2\pi \mathrm{i} z} - c_0 - \frac{c_1}{z}\right) + h(z^{-1}) = 0.$$

Here $h(z^{-1})$ is a power series in z^{-1} with the lowest degree ≥ 2. Thus, for the constant term in z^{-1} to vanish, c_0 has to be equal to $\mathrm{i}\, u_i$ for $i = 1, \ldots, n$. By putting $c_0 = \mathrm{i}\, u_i$ (for some i), comparison of coefficients in front of z^{-1} yields

$$c_1 = -\frac{t_i}{2\pi \mathrm{i}}$$

giving the value of the residue at i^{th} branch. ■

3.2 Degeneration: $u = E_n$

In this subsection, we study the spectral curve $\Gamma(u, A)$ in a degenerate case of $u = E_n (n \ge 3)$, where E_n is the diagonal matrix with $(E_n)_{nn} = 1$, and all other matrix entries equal to zero. It turns out that in this case $\Gamma(u, A)$ is a rational curve.

Proposition 3.5. For $u = E_n (n \ge 3)$ and $A \in \mathfrak{gl}_n(\mathbb{C})$ satisfying the two genericity conditions in Proposition 3.3 together with the third condition that all eigenvalues of $A^{(n-1)}$ are distinct, the spectral curve $\Gamma(u, A)$ is isomorphic to $\mathbb{P}^1$ with $2n$ punctures.

Proof. We continue to follow the notations used in the proof of Proposition 3.3. We have

$$P(\mu, z^{-1}) = \left(\mathrm{i} - \frac{1}{2\pi \mathrm{i}} \frac{t_n}{z} - \mu\right) \cdot \det\left(-\frac{1}{2\pi \mathrm{i}} \frac{A^{(n-1)}}{z} - \mu I_{n-1}\right) + h(\mu, z^{-1}) \tag{3.2.1}$$

where $h(\mu, z^{-1})$ has degree $\le n-2$ in the μ variable. And if $h(\mu, z^{-1}) \ne 0$, it is a homogeneous polynomial in μ and z^{-1} of degree n.

Note that for $n \geq 3$, $E_n \notin \mathfrak{h}_{\mathrm{reg}}(\mathbb{C})$. In this case, $\partial_\mu P(\mu, z^{-1})$ will have non-simple zeros at $z = \infty$. Let us fist compute the order of zero of $\partial_\mu P(\mu, z^{-1})$ at $z = \infty$. We claim that near $z = \infty$,

$$P(\mu, z^{-1}) = (-1)^n \cdot \prod_{i=1}^{n-1} \left(\mu + \frac{\lambda_i^{(n-1)}}{2\pi \mathrm{i} z} + O(z^{-2}) \right) \cdot \left(\mu - \mathrm{i} + \frac{t_n}{2\pi \mathrm{i} z} + O(z^{-2}) \right). \tag{3.2.2}$$

Indeed, let $\mu(z^{-1})$ be one of n branches of solutions of the equation

$$P\left(\mu(z^{-1}), z^{-1}\right) = 0 \tag{3.2.3}$$

in a neighborhood of $z = \infty$. Expand $\mu(z^{-1}) = \sum_{k=m}^{\infty} c_k z^{-k}$ with $c_m \neq 0\,(m \geq 0)$.

- If $\mu(z^{-1})$ does not vanish at $z = \infty$, using (3.2.1), the constant coefficient of $P\left(\mu(z^{-1}), z^{-1}\right)$ is equal to $\mathrm{i}(-1)^{n-1} c_0^{n-1} + (-1)^n c_0^n$. Requiring this expression to vanish yields $c_0 = \mathrm{i}$. Next, the coefficient of the z^{-1} term is equal to $(-\frac{t_n}{2\pi \mathrm{i}} - c_1)(-1)^{n-1} c_0^{n-1}$, and requiring it in turn to vanish gives $c_1 = -\frac{t_n}{2\pi \mathrm{i}}$.
- If $\mu(z^{-1})$ has a zero at $z = \infty$, then $c_0 = 0$. Using (3.2.1), the coefficient of $z^{-(n-1)}$in $P\left(\mu(z^{-1}), z^{-1}\right)$ is $\mathrm{i} \det\left(-\frac{1}{2\pi \mathrm{i}} A^{(n-1)} - c_1 I_{n-1}\right)$. Requiring it to vanish shows that c_1 is an eigenvalue of $A^{(n-1)}$ scaled by $-\frac{1}{2\pi \mathrm{i}}$.

This finishes the proof of the claim (3.2.2). Let $\mu_i(z^{-1})\,(1 \leq i \leq n-1)$ be the branch near $z = \infty$ such that $\mu_i(z^{-1}) = -\frac{\lambda_i^{(n-1)}}{2\pi \mathrm{i} z} + O(z^{-2})$. Let $\mu_n(z^{-1})$ be the branch near $z = \infty$ such that $\mu_n(z^{-1}) = \mathrm{i} - \frac{t_n}{2\pi \mathrm{i} z} + O(z^{-2})$. Then, for $1 \leq i \leq n-1$,

$$\begin{aligned} \partial_\mu P\left(\mu(z^{-1}), z^{-1}\right)|_{\mu=\mu_i} &= (-1)^n \prod_{j|j \neq i} \left(\mu_i(z^{-1}) - \mu_j(z^{-1})\right) \\ &= (-1)^n \prod_{j|j \neq i,n} \left(-\frac{\lambda_i^{(n-1)} - \lambda_j^{(n-1)}}{2\pi \mathrm{i} z} + O(z^{-2}) \right) \cdot \left(-\mathrm{i} + \frac{t_n - \lambda_i^{(n-1)}}{2\pi \mathrm{i} z} + O(z^{-2}) \right), \end{aligned}$$

and for $i = n$,

$$\begin{aligned} \partial_\mu P\left(\mu(z^{-1}), z^{-1}\right)|_{\mu=\mu_n} &= (-1)^n \prod_{j|j \neq n} \left(\mu_n(z^{-1}) - \mu_j(z^{-1})\right) \\ &= (-1)^n \prod_{j|j \neq i,n} \left(\mathrm{i} + \frac{\lambda_j^{(n-1)} - t_n}{2\pi \mathrm{i} z} + O(z^{-2}) \right) \end{aligned}$$

By our assumption that $A^{(n-1)}$ has distinct eigenvalues, we conclude that $\partial_\mu P\left(\mu, z^{-1}\right)$ has a zero of order $(n-1)(n-2)$ at $z = \infty$.

Now, it follows from computations we have already done in Proposition 3.3 that the number of zeros of $\partial_\mu P(\mu, z^{-1})$ for $z \in \mathbb{C} \setminus \{0\}$, is equal to the order of poles at $z = 0$ minus the order of zeros at $z = \infty$, i.e.,

$$n(n-1) - (n-1)(n-2) = 2(n-1).$$

All these zeros are simple by the genericity condition ii), so $\Gamma(u, A)$ is still smooth by Lemma 3.1. However, the compactification $\bar{\Gamma}(u, A)$ defined in the proof of Proposition 3.3 now has singularity at $(\mu = 0, z = \infty)$. To resolve the singularity at $(\mu = 0, z = \infty)$, we blow up the ambient $\mathbb{P}^1_\mu \times \mathbb{P}^1_z$ at $(\mu = 0, z = \infty)$.

Let $\tilde{\bar{\Gamma}}(u, A)$ be the closure of $\Gamma(u, A)$ after blowing up $\mathbb{P}^1_\mu \times \mathbb{P}^1_z$ at $(\mu = 0, z = \infty)$ and $(\mu = \infty, z = 0)$. In particular, $\tilde{\bar{\Gamma}}(u, A)$ is smooth and unramified over $z = 0$ and $z = \infty$. Moreover, the ramification points of $\tilde{\bar{\Gamma}}(u, A) \to \mathbb{P}^1$ are the same as those of $\Gamma(u, A) \to \mathbb{P}^1$. They are all of index 2 by the genericity condition ii) and their number is equal to the number of zeros of $\partial_\mu P(\mu, z^{-1})$ for $z \in \mathbb{C}\setminus\{0\}$. Now we can use the Riemann-Hurwitz formula again, giving

$$2g(\tilde{\tilde{\Gamma}}) - 2 = n(-2) + 2n - 2 \Rightarrow g(\tilde{\tilde{\Gamma}}) = 0,$$

i.e., $\tilde{\tilde{\Gamma}}$ is a rational curve. ■

The following proposition gives values of residues of ω at punctures of the spectral curve:

Proposition 3.6. For $u = E_n (n \geq 3)$ and A such that eigenvalues of $A^{(k)}$ are distinct for $k = n-1, n$, the canonical 1-form ω has residues

i) $\frac{\lambda_i^{(n-1)}}{2\pi\mathrm{i}}$ for $i = 1, \ldots, n-1$ for $(n-1)$ punctures lying over $z = \infty$;
ii) $\frac{t_n}{2\pi\mathrm{i}}$ at the n^{th} puncture lying over $z = \infty$;
iii) $-\frac{\lambda_i^{(n)}}{2\pi\mathrm{i}}$ for $i = 1, \ldots, n$ at punctures lying over $z = 0$.

Proof. For punctures lying over $z = \infty$, the statement follows from equations (3.2.2). For punctures lying over $z = 0$, the result and the proof follow verbatim the result and the proof of Proposition 3.4. ■

3.3 Degeneration: $u = u_{\mathrm{cat}}(t)$

For the rest of this Section, we assume that $n \geq 3$. Notice that we also have the translation symmetry on the level of spectral curves, not only on the level of Stokes matrices (c.f. Appendix A): $\Gamma(u, A)$ and $\Gamma(u - cI_n, A)$ are isomorphic for any $c \in \mathbb{C}$ and their periods are the same. So, throughout the rest of this section, we just fix u_1 to be 0, and only vary parameters $u_2, u_3, \cdots, u_n$, as a concrete way to parametrize the space $\mathfrak{h}_{\mathrm{reg}}(\mathbb{C})/\mathbb{C}$ or $\mathfrak{h}_{\mathrm{reg}}(\mathbb{R})/\mathbb{R}$. Under this parametrization, the caterpillar line limit $u \to u_{\mathrm{cat}}(t)$ acquires the form

$$u_2 = t, \quad \frac{u_{j+1}}{u_j} \to +\infty \text{ for } j = 2, \ldots, n-1,$$

where $t > 0$ is a fixed constant that determines the position on the caterpillar line.

Since most of our proofs work in the complex setting, it will be more convenient to consider the complex De Concini-Procesi space (c.f. Appendix A) $\widehat{\mathfrak{h}_{\mathrm{reg}}}(\mathbb{C})$ in this subsection. The real De Concini-Procesi space and the caterpillar line are just the restriction of $\widehat{\mathfrak{h}_{\mathrm{reg}}}(\mathbb{C})$ to the real locus.

Proposition 3.7. Consider the 1-parameter family of spectral curves $\Gamma(u, A)$ $(u \in \mathfrak{h}_{\mathrm{reg}}(\mathbb{C}))$ we get by fixing u_2, $\cdots, u_{n-1}$ and varying u_n. Then, for a generic fixed $A \in \mathfrak{gl}_n(\mathbb{C})$, at $u_n = \infty$, the spectral curve degenerates into two irreducible components Γ_{n-1} and $\Gamma^{(n)}$; Γ_{n-1} is a smooth curve of genus $\frac{(n-2)(n-3)}{2}$ with $2(n-1)$ punctures, and $\Gamma^{(n)}$ is isomorphic to $\mathbb{P}^1$ with $2n$ punctures.

Proof. By fixing $u_2, \ldots, u_{n-1}$ and allowing u_n to vary in $\mathbb{C}$, we view (3.1.2) as defining a 1-parameter family of spectral curves parametrized by $\mathbb{C}_{u_n}$ in $\mathbb{P}^1_\mu \times \mathbb{P}^1_z \times \mathbb{C}_{u_n}$. We denote this 1-parameter family by $\mathscr{X}$.

Next, let $\mu' = \frac{1}{\mu}$ and $u_n' = \frac{1}{u_n}$. Let $V = \mathbb{P}^1_\mu \times \mathbb{P}^1_z \times \mathbb{P}^1_{u_n'}$. Let $\tilde{V}$ be the blowup of V at $\mu = \infty, z = 0, u_n = \infty$. Then, $\tilde{V}$ is a closed subscheme of $V \times \mathbb{P}^2$. Let y_1, y_2, y_3 be homogeneous coordinates on $\mathbb{P}^2$ satisfying

$$\mu' y_3 = u_n' y_1, \quad z y_3 = u_n' y_2.$$

Set $y_3 = 1$ and let $w = \frac{\mu}{u_n} = \frac{u_n'}{\mu'} = \frac{1}{y_1}$ and $v = z u_n = y_2$.

Now, to take the limit $u_n \to \infty$, we need to consider the strict transform of $\mathscr{X}$ in $\tilde{V}$ and then take its closure $\bar{\mathscr{X}}$ in $\tilde{V}$ when $u_n = \infty$. Given $u_n \in \mathbb{C}$, on the $\mathbb{P}^2$ component of $V \times \mathbb{P}^2$, the spectral curve needs to satisfy the equation

$$\det\left(\frac{1}{u_n} \cdot \mathrm{i}u - \frac{A}{2\pi\mathrm{i}} \frac{1}{z u_n} - \frac{\mu}{u_n} \cdot I_n\right) = \det\left(\frac{1}{u_n} \cdot \mathrm{i}u - \frac{A}{2\pi\mathrm{i}v} - w I_n\right) = 0\,. \tag{3.3.1}$$

On the chart where $z^{-1}, \mu \in \mathbb{C}$, V and $\tilde{V}$ are isomorphic, (3.1.2) reads

$$\left(\mathrm{i}u_n - \frac{t_n}{2\pi\mathrm{i}z} - \mu\right) \cdot \det\left(\mathrm{i}u^{(n-1)} - \frac{A^{(n-1)}}{2\pi\mathrm{i}z} - \mu I_{n-1}\right) + f = 0\,,$$

where f is a polynomial in the variables z^{-1} and μ whose coefficients do not involve u_n. For $z^{-1}, \mu \in \mathbb{C}$ and $u_n \neq 0$, we divide both sides of the above equation by $\mathrm{i}u_n$ and get

$$\det\left(\mathrm{i}u^{(n-1)} - \frac{A^{(n-1)}}{2\pi\mathrm{i}z} - \mu I_{n-1}\right)\left[1 + \frac{1}{\mathrm{i}u_n}(-\frac{t_n}{2\pi\mathrm{i}z} - \mu)\right] + \frac{f}{\mathrm{i}u_n} = 0\,.$$

When $u_n = \infty$, the above equation goes to the limit

$$\det\left(\mathrm{i}u^{(n-1)} - \frac{A^{(n-1)}}{2\pi\mathrm{i}z} - \mu I_{n-1}\right) = 0\,. \tag{3.3.2}$$

By Proposition 3.3, for a generic $A \in \mathfrak{gl}_n(\mathbb{C})$, (3.3.2) defines a spectral curve Γ_{n-1} of genus $\frac{(n-2)(n-3)}{2}$ with $n-1$ punctures above $z = 0$ and $n-1$ punctures above $z = \infty$. We denote by s_i the puncture above $z = \infty$ on Γ_{n-1} where the canonical differential $\omega = \mu dz$ has residue $\frac{t_i}{2\pi\mathrm{i}}$, and by r_i the puncture above $z = 0$ where ω has residue $-\frac{\lambda_i^{(n-1)}}{2\pi\mathrm{i}}$.

If $z^{-1} = \mu = \infty$, then, when $u_n = \infty$, we get an extra component in $\bar{\mathscr{X}} \setminus \mathscr{X}$, given by the limit of (3.3.1), which is

$$P(w, v^{-1}) = \det\left(\mathrm{i}E_n - \frac{A}{2\pi\mathrm{i}v} - wI_n\right) = 0\,, \tag{3.3.3}$$

which defines a spectral curve $\Gamma^{(n)}$. Notice that on $\Gamma^{(n)}$ the canonical differential is

$$\omega = \mu dz = u_n w \cdot \frac{dv}{u_n} = w \cdot dv\,. \tag{3.3.4}$$

By Proposition 3.5, for a generic $A \in \mathfrak{gl}_n(\mathbb{C})$, $\Gamma^{(n)}$ is isomorphic to $\mathbb{P}^1$ with $2n$ punctures. There are n punctures above $v = \infty$. $(n-1)$ of them are the punctures r_i $(1 \leq i \leq n-1)$ that $\Gamma^{(n)}$ shares with Γ_{n-1}. We label the last puncture over $v = \infty$ by s_n. The canonical differential has residue $\frac{t_n}{2\pi\mathrm{i}}$ at s_n. There are n punctures on $\Gamma^{(n)}$ above $v = 0$. We label by q_i $(1 \leq i \leq n)$ the puncture above $v = 0$ where the canonical differential has residue $-\frac{\lambda_i^{(n)}}{2\pi\mathrm{i}}$. ■

For future use, we introduce the following notation. For $2 \leq k \leq n$, let $\Gamma^{(k)}$ be the spectral curve defined by (3.3.3) with E_n replaced with E_k and A with $A^{(k)}$, i.e., given by the equation

$$P_k(\mu, z^{-1}) = \det\left(\mathrm{i}E_k - \frac{A^{(k)}}{2\pi\mathrm{i}z} - \mu I_k\right) = 0\,. \tag{3.3.5}$$

We emphasize that we still view $\Gamma^{(k)}$ as a punctured curve with punctures over $z = 0$ and over $z = \infty$.

From now on, it will be convenient for us to restrict A to $\mathrm{Herm}_0(n)$. However, to consider algebraic families of spectral curves, we still want to allow the u-parameters to vary in $\widehat{\mathfrak{h}_{\mathrm{reg}}}(\mathbb{C})$.

Definition 3.8. Denote by $\mathcal{B} \subset \mathrm{Herm}_0(n)$ the locus where for each $3 \leq k \leq n$ the discriminant of the polynomial $P_k(\mu, z^{-1})$ has only simple zeroes as a polynomial in μ for $z \in \mathbb{C} \setminus \{0\}$. We call $\mathcal{B}$ the *generic locus* of $\mathrm{Herm}(n)$.

Remark 3.9. Here is the reason why we define $\mathcal{B}$ to be contained in $\mathrm{Herm}_0(n)$ in the first place. If the spectral curve defined by (3.3.5) is smooth for each k, A has to be in $\mathrm{Herm}_0(n)$. For otherwise, (3.3.5) will split for some k. Then, the corresponding spectral curve $\Gamma^{(k)}$ will be reducible.

Lemma 3.10. Fix a $A \in \mathcal{B}$. For any $u_1, u_2 \in \mathbb{C}$ such that $u_1 \neq u_2$, the spectral curve defined by

$$\det\left(\mathrm{i}u^{(2)} - \frac{A^{(2)}}{2\pi\mathrm{i}z} - \mu I_2\right) = 0$$

is isomorphic to $\Gamma^{(2)}(A)$. Here, $u^{(2)}$ is the diagonal matrix whose first diagonal entry is u_1 and the second one is u_2.

Proof. It suffices to consider the case where $u_1 = 0$. The map $z \mapsto z \cdot (u_2 - u_1)$, $\mu \mapsto \mu/(u_2 - u_1)$ gives the isomorphism to $\Gamma^{(2)}(A)$. ■

Lemma 3.11. For a fixed $A \in \mathcal{B}$, $\Gamma^{(k)}(A)$ is isomorphic to $\mathbb{P}^1$ with $2k$ punctures for $2 \leq k \leq n$.

Proof. For $3 \leq k \leq n$, since $A^{(k)}$ satisfies the genericity conditions in Proposition 3.5 for $A \in \mathcal{B}$, $\Gamma^{(k)}$ is isomorphic to $\mathbb{P}^1$ with $2k$ punctures for $3 \leq k \leq n$ by Proposition 3.5.

For $k = 2$, it is a straightforward computation that $P_2(\mu, z^{-1})$ has only simple zeroes as a polynomial in μ for $z \in \mathbb{C} \setminus \{0\}$ if $A_{12} \cdot A_{21} \neq 0$. But this condition is automatically satisfied for $A \in \mathcal{B}$. Then, the case of $k = 2$ follows from Proposition 3.3. ■

Now, we are ready to describe the degeneration of the spectral curves at a point on the caterpillar line:

Theorem 3.12. Fix $A \in \mathrm{Herm}(n)$ and vary $u \in \widehat{\mathfrak{h}_{\mathrm{reg}}}(\mathbb{C})$. Let $u_{\mathrm{cat}}(t)$ $(t > 0)$ be a point on the caterpillar line. The family of spectral curves can be extended over $u_{\mathrm{cat}}(t)$, and the fiber over $u_{\mathrm{cat}}(t)$ has $(n-1)$ components isomorphic to $\Gamma^{(k)}(A)(2 \leq k \leq n)$. Moreover, if $A \in \mathcal{B}$, the $(n-1)$ components in the fiber over $u_{\mathrm{cat}}(t)$ are irreducible and isomorphic to $\mathbb{P}^1$ with $2k$ punctures $(2 \leq k \leq n)$ and there exists an open neighborhood $U \subset \widehat{\mathfrak{h}_{\mathrm{reg}}}(\mathbb{C})$ around $u_{\mathrm{cat}}(t)$ such that for any $u \in U \cap \mathfrak{h}_{\mathrm{reg}}(\mathbb{C})$, the spectral curve $\Gamma(u, A)$ is smooth.

Proof. The limit $u \to u_{\mathrm{cat}}(t)$ can be achieved iteratively. First, we fix $u_2, \ldots, u_{n-1}$ and let $u_n \to +\infty$; then we fix $u_2, \ldots, u_{n-2}$ and let $u_{n-1} \to +\infty$; and so on until we reach the point $u_{\mathrm{cat}}(t)$ by letting $u_3 \to +\infty$ while fixing u_2. Thus, we are iterating the degeneration process in Proposition 3.7, and the spectral curve degenerates into $(n-1)$ components at $u_{\mathrm{cat}}(t)$. These components are isomorphic to $\Gamma^{(k)}(A)(2 \leq k \leq n)$ by Proposition 3.7 and Lemma 3.10. If $A \in \mathcal{B}$, it follows from Lemma 3.11 these components are smooth, irreducible, and isomorphic to $\mathbb{P}^1$ with $2k$ punctures.

Again, for $A \in \mathcal{B}$, for $u \in \mathfrak{h}_{\mathrm{reg}}(\mathbb{C})$ close enough to $u_{\mathrm{cat}}(t)$, (3.1.2) has only simple zeroes; thus, by Lemma 3.1 and Lemma 3.2, $\Gamma(u, A)$ is smooth. In particular, there exists a neighborhood $U \subset \widehat{\mathfrak{h}_{\mathrm{reg}}}(\mathbb{C})$ around $u_{\mathrm{cat}}(t)$ such that for any $u \in U \cap \mathfrak{h}_{\mathrm{reg}}$, the discriminant of (3.1.2) has only simple zeroes. The existence of such a U follows from the fact that $\mathrm{Herm}_0(n) \setminus \mathcal{B}$ is cut out by polynomial conditions. Then, by Lemma 3.1 and Lemma 3.2, the spectral curve $\Gamma(u, A)$ is smooth for any $u \in U \cap \mathfrak{h}_{\mathrm{reg}}(\mathbb{C})$.

We also give an alternative proof for the first claim of the proposition, so that readers can see all the degenerations in one step rather than iteratively. Fixing u_2, we view (3.1.2) as defining a family of spectral curves $\mathscr{X}$ in $V = \mathbb{P}^1_\mu \times \mathbb{P}^1_z \times \mathbb{P}^1_{u_3} \times \mathbb{P}^1_{d_4} \times \cdots \times \mathbb{P}^1_{d_n}$ where $d_i = \frac{u_i}{u_{i-1}}$ for $4 \leq i \leq n$.

After dividing both sides by $(\mathrm{i}u_3) \cdots (\mathrm{i}u_n)$, (3.1.2) reads

$$\det\left(\mathrm{i}u^{(2)} - \frac{A^{(2)}}{2\pi\mathrm{i}z} - \mu I_2\right)\left[1 + \frac{1}{\mathrm{i}u_3}\left(-\frac{t_3}{2\pi\mathrm{i}z} - \mu\right)\right] \cdots \left[1 + \frac{1}{\mathrm{i}u_n}\left(-\frac{t_n}{2\pi\mathrm{i}z} - \mu\right)\right] + h \tag{3.3.6}$$

where h is a polynomial in z^{-1} and μ, whose coefficients all contain some negative powers of $u_3, \ldots, u_n$. For $z^{-1} \in \mathbb{C}$, as we go to the limit $\frac{u_{j+1} - u_j}{u_j - u_{j-1}} \to \infty$, or equivalently $\frac{u_{j+1}}{u_j} \to \infty$, for all $j = 2, \ldots, n-1$, we have $u_3, \ldots, u_n \to \infty$. Then, (3.3.6) goes to the limit

$$\det\left(\mathrm{i}u^{(2)} - \frac{A^{(2)}}{2\pi\mathrm{i}z} - \mu I_2\right) = 0, \tag{3.3.7}$$

which defines a spectral curve $\Gamma^{(2)}$ isomorphic to 4-punctured $\mathbb{P}^1$ for generic A.

Let $\nu_k = zu_k$ and $w_k = \frac{\mu}{u_k}$ for $3 \le k \le n$. We do a sequence of blowups of V as follows. First, we blow up the subscheme of V defined by $z^{-1} = \mu = u_3 = \infty$ and get the scheme V_3. Inductively, we blow up the subscheme of V_i defined by $v_k^{-1} = w_k = d_{k+1} = \infty$ and get the scheme V_{k+1} for $3 \le k \le n-1$.

We claim that as $\frac{u_{j+1}-u_j}{u_j - u_{j-1}} \to \infty$ for all $j = 2, \ldots, n-1$, for each $3 \le k \le n$, we get a component $\Gamma^{(k)}$ of the closure of $\mathscr{X}$ inside V_n, given by

$$\det\left(\mathrm{i}E_k - \frac{A^{(k)}}{2\pi\mathrm{i}\nu_k} - w_k I_k\right) = 0 \quad (3 \le k \le n) = 0, \tag{3.3.8}$$

which defines a $(2k)$-punctured $\mathbb{P}^1$ for generic A. The proof of this claim uses analysis similar to what we did in the proof of Proposition 3.7. Consider the case $k = 3$. Let $d_4' = d_4$, $d_5' = d_4 d_5, \ldots, d_n' = d_4 d_5 \cdots d_n$. Now (3.1.2), after dividing both sides by $u_3^n(\mathrm{i}d_4')(\mathrm{i}d_5')\cdots(\mathrm{i}d_n')$, reads

$$\det\left(\mathrm{i}\frac{u^{(3)}}{u_3} - \frac{A^{(3)}}{2\pi\mathrm{i}\nu_3} - w_3 I_3\right)\prod_{i=4}^{n}\left[1 + \frac{1}{\mathrm{i}d_i'}\left(-\frac{t_i}{2\pi\mathrm{i}\nu_3} - w_3\right)\right] + h_3\,, \tag{3.3.9}$$

where h_3 is a polynomial in ν_3^{-1} and w_3 whose coefficients all contain some negative power of $d_4', d_5', \cdots d_n'$. In the limit $u_3, d_4, \cdots, d_n \to \infty$, for $\nu_3 \neq 0$, (3.3.9) becomes

$$\det\left(\mathrm{i}E_3 - \frac{A^{(3)}}{2\pi\mathrm{i}\nu_3} - w_3 I_3\right) = 0\,. \tag{3.3.10}$$

The proof for $4 \le k \le n$ is similar. ■

Definition 3.13. (*Spectral curves at points on the caterpillar line*) Fix a point $u_{\mathrm{cat}}(t)$ $(t > 0)$ on the caterpillar line. It follows from Theorem 3.12 that for any $A \in \mathrm{Herm}(n)$, taking the limit $u \to u_{\mathrm{cat}}(t)$, the family of spectral curves degenerates into $n-1$ (not necessarily irreducible or smooth) components, each of which is defined by (3.3.8) for $3 \le k \le n$ and by (3.3.7) for $k = 2$. We call the degeneration at $u_{\mathrm{cat}}(t)$ the *spectral curve at* $u_{\mathrm{cat}}(t)$ and denote it by $\Gamma(u_{\mathrm{cat}}(t), A)$.

Corollary 3.14. Fix $A \in \mathcal{B}$ and a point $u_{\mathrm{cat}}(t)$ $(t > 0)$ on the caterpillar line. There exists a punctured open neighborhood $B(u_{\mathrm{cat}}(t), A) \subset U_{\mathrm{id}}$ around $u_{\mathrm{cat}}(t)$ such that for all $u \in B(u_{\mathrm{cat}}(t), A)$, $\Gamma(u, A)$ is smooth. Moreover, for any $u \in B(u_{\mathrm{cat}}(t), A)$, there exists *vanishing cycles* $V_j^{(k)}(u, A)(1 \le j \le k \le n)$, such that $V_j^{(k)}(u, A)$ that becomes a small loop $V_j^{(k)}(u_{\mathrm{cat}}(t), A)$ on $\Gamma(u_{\mathrm{cat}}(t), A)$ as $u \to u_{\mathrm{cat}}(t)$. For $2 \le k \le n$, $V_j^{(k)}(u_{\mathrm{cat}}(t), A)$ $(1 \le j \le k)$ is on $\Gamma^{(k)}$, oriented clockwise around the puncture where the canonical 1-form ω has residue $-\frac{\lambda_j^{(k)}}{2\pi\mathrm{i}}$. For $k = 1$, $V_1^{(1)}(u_{\mathrm{cat}}(t), A)$ is on $\Gamma^{(2)}$, oriented counterclockwise around the puncture where ω has residue $\lambda_1^{(1)} = \frac{t_1}{2\pi i}$. Here, t_1 is the first diagonal entry of A.

Proof. Let U be a neighborhood of $u_{\mathrm{cat}}(t)$ in $\widehat{\mathfrak{h}_{\mathrm{reg}}}(\mathbb{C})$ as in Theorem 3.12. Let $B(u_{\mathrm{cat}}(t), A) = U \cap U_{\mathrm{id}}$. Then, the first statement of this corollary follows from Theorem 3.12.

It remains to prove statements about vanishing cycles. For $k = 1$ and $k = n$, these vanishing cycles are just cycles around corresponding punctures with the prescribed residue by Proposition 3.4 and Proposition 3.6. For $2 \le k \le n-1$, it follows from Proposition 3.6 that the punctures where ω has the residue $-\frac{\lambda_j^{(k)}}{2\pi\mathrm{i}}$ are the nodes of the (compactified) spectral curve $\Gamma(u_{\mathrm{cat}}(t), A)$. Let $\Delta \hookrightarrow U$ be an analytic disc such that $\Delta \setminus \{0\}$ is contained in $U \cap \mathfrak{h}_{\mathrm{reg}}(\mathbb{C})$ and 0 is mapped to $u_{\mathrm{cat}}(t)$. Let $\mathcal{C} \to \Delta$ be the family of (fiberwise compactified) spectral curves $\Gamma(u, A)(u \in \Delta)$. Since $\Gamma(u, A)$ is smooth for $u \in \Delta \setminus \{0\}$ and $\Gamma(u_{\mathrm{cat}}(t), A)$ has only nodal singularities, $\mathcal{C}$ is smooth and $\mathcal{C} \to \Delta$ is holomorphic Morse. Then, the existence of vanishing cycles follows from the standard holomorphic Morse theory, e.g., Chapter II of [46]. ■

Remark 3.15. The irregularity in the definition of vanishing cycles in the case of $k = 1$ came from the fact that in this paper we use the *caterpillar line* rather than going to the *caterpillar point* as in the existing literature [30, 44]). We made this choice because the formulas for Stokes matrices are already exact on the caterpillar line: from this point of view, there is no need to make the last degeneration to the caterpillar point.

3.4 Distinguished cycles on $\Gamma(u, A)$

Fix $A \in \mathcal{B}$ and a point $u_{\text{cat}}(t)$ ($t > 0$) on the caterpillar line. Let $B(u_{\text{cat}}(t), A) \subset U_{\text{id}}$ be an open neighborhood as in Corollary 3.14. For $u \in B(u_{\text{cat}}(t), A)$, we define *distinguished cycles* $C_i^{(k)}(u, A)$ on $\Gamma(u, A)$ as linear combinations of vanishing cycles

$$C_i^{(k)}(u, A) = \sum_{j=k-i+1}^{k} V_j^{(k)}(u, A). \tag{3.4.1}$$

For $u = u_{\text{cat}}(t)$, we define *distinguished cycles*

$$C_i^{(k)}\left(u_{\text{cat}}(t), A\right) = \sum_{j=k-i+1}^{k} V_j^{(k)}\left(u_{\text{cat}}(t), A\right) \tag{3.4.2}$$

on $\Gamma\left(u_{\text{cat}}(t), A\right)$ where $V_j^{(k)}\left(u_{\text{cat}}(t), A\right)$ are as in Corollary 3.14.

Theorem 3.16. For $u \in B(u_{\text{cat}}(t), A) \subset U_{\text{id}}$, we have

$$\frac{1}{2}\lim_{u\to u_{\text{cat}}(t)} Z\left(C_i^{(k)}(u, A)\right) = \frac{1}{2} Z\left(C_i^{(k)}(u_{\text{cat}}(t), A)\right) = -l_i^{(k)}(u_{\text{cat}}, A). \tag{3.4.3}$$

In particular, Conjecture 1.2 holds on the caterpillar line.

Proof. By Corollary 3.14,

$$\lim_{u\to u_{\text{cat}}(t)} Z\left(V_j^{(k)}(u, A)\right) = \int_{V_j^{(k)}(u_{\text{cat}}(t),A)} \omega = -\lambda_j^{(k)}.$$

Next, we compute

$$\frac{1}{2}\lim_{u\to u_{\text{cat}}(t)} Z\left(C_j^{(k)}(u, A)\right) = \frac{1}{2} Z\left(C_i^{(k)}(u_{\text{cat}}(t), A)\right) = -\frac{1}{2}\sum_{j=k-i+1}^{k} \lambda_j^{(k)} = -l_i^{(k)}(u_{\text{cat}}, A),$$

where in the last equality we have used Theorem 2.14. ■

Under Conjecture 2.6, Theorem 3.16 combined with Proposition 2.15 suggests that near the caterpillar line, the distinguished cycles $C_i^{(k)}$'s may be suitable for the WKB analysis of the asymptotic behavior of minor coordinates. We will further explore this via the theory of spectral networks in the next section.

Finally, we note that the periods of the canonical form over the vanishing cycles are real:

Proposition 3.17. Let $u \in B(u_{\text{cat}}(t), A)$ and $A \in \mathcal{B}$. Then, the periods of the canonical 1-form ω over vanishing cycles $V_j^{(k)}(u, A)$ are real:

$$Z\left(V_j^{(k)}\right) \in \mathbb{R}.$$

Proof. Under the reality conditions (1.1.2) on (u, A), the spectral curve $\Gamma(u, A)$ has an involution $\iota(z, \mu) = (\bar{z}, -\bar{\mu})$. Since $\omega = \mu\, dz$ we have $\iota^*\omega = -\bar{\omega}$. At $u = u_{\text{cat}}(t)$, the punctures are fixed under ι, which implies that $\iota_* V_i^{(k)} = -V_i^{(k)}$. Indeed, since ι reverses the orientation of $\Gamma(u, A)$, it exchanges positive and negative orientations of small loops around the punctures. By continuity, this is still true for $u \in B(u_{\text{cat}}(t), A)$. Thus, for any $V = V_j^{(k)}(u, A)$ we have

$$Z(V) = \int_V \omega = -\int_{\iota_* V} \iota^*\omega = \int_{-V} (-\bar{\omega}) = \int_V \bar{\omega} = \overline{\int_V \omega} = \overline{Z(V)}, \tag{3.4.4}$$

as desired. ■

3.5 Spectral curves for A nearly diagonal

In this section, we consider the special case when u is near the caterpillar line, and A is nearly diagonal (that is, close to a diagonal matrix). In that case, we can explicitly see the degeneration phenomena described in the previous sections. This is also a preparation for the spectral network analysis of the next section.

Throughout this section, we assume the reality conditions (1.1.2).

3.5.1 The diagonal case

Recall that we denote by $t_i = A_{ii}$ the diagonal entries of A. If A is diagonal, then the eigenvalues of the operator $\mathrm{i}\left(u + \frac{A}{2\pi z}\right)$ are

$$\mu_i(z) = \mathrm{i}\left(u_i + \frac{t_i}{2\pi z}\right) . \tag{3.5.1}$$

These are also the sheets of the spectral curve $\Gamma(u, A)$.

Note that $\mu_i(\overline{z}) = -\overline{\mu_i(z)}$, so in particular $\mu_i(z) \in \mathrm{i}\mathbb{R}$ for $z \in \mathbb{R}$. The eigenvalues $\mu_i(z)$ are all distinct as long as $z \notin \{z_{ij}\}$ where

$$z_{ij} = -\frac{t_i - t_j}{2\pi(u_i - u_j)} . \tag{3.5.2}$$

At $z = z_{ij}$, we have $\mu_i(z) = \mu_j(z)$. If all z_{ij} with $i > j$ are distinct and nonzero, then they are nodal singularities of $\Gamma(u, A)$, and $\Gamma(u, A)$ is smooth away from these $\frac{n(n-1)}{2}$ singular points.

We will generally be interested in the situation where all u_i are distinct; then we may as well assume

$$u_1 < \cdots < u_n, \tag{3.5.3}$$

and we do so from now on. We also often assume u is close to the caterpillar line, as in the next proposition.

Proposition 3.18. Let $\Lambda = \max_{j \neq k, j' \neq k'} \left| \frac{t_j - t_k}{t_{j'} - t_{k'}} \right|$. Suppose $\frac{u_{i+1} - u_i}{u_i - u_{i-1}} > \Lambda$ for all i. Then, if $j < j'$, $|z_{ij}| > |z_{ij'}|$.

Said otherwise, if we divide the set of branch points z_{ij} with $i < j$ into $n - 1$ subsets $\{z_{12}\}$, $\{z_{13}, z_{23}\}$, ..., $\{z_{1,n}, z_{2,n}, \ldots, z_{n-1,n}\}$, these subsets are arranged in order of decreasing distance from the origin. Within each subset, the ordering of the z_{ij} matches the ordering of the t_i.

We often further assume $t_1 < \cdots < t_n$; this assumption is not essential, but it will simplify the exposition and the pictures below. Then all $z_{ij} < 0$, and Proposition 3.18 says

$$z_{12} < z_{13} < z_{23} < \cdots < z_{1,n} < z_{2,n} < \cdots < z_{n-1,n} . \tag{3.5.4}$$

See Figure 1 for the $n = 4$ case.

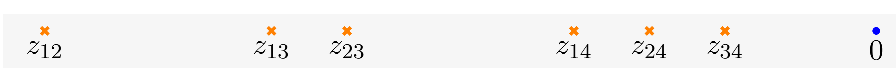

Figure 1: The schematic arrangement of the points $z_{ij} \in \mathbb{C}$ in case $n = 4$, with A diagonal, when $t_1 < t_2 < t_3 < t_4$ and u is sufficiently close to the caterpillar line.

3.5.2 The near-diagonal case

For u close to the caterpillar line, the effect of the off-diagonal entries of A is to broaden the singular points of $\Gamma(u, A)$ into vertical branch cuts, as described in the next proposition.

Here and below, we will be considering some open subset of $\mathfrak{h}_{\mathrm{reg}}(\mathbb{R}) \times \mathrm{Herm}(n)$, whose closure contains the locus where u is on the caterpillar line and A is diagonal. When (u, A) belongs to this open subset we say "u is sufficiently close to the caterpillar line and A is sufficiently close to diagonal."

Proposition 3.19. For u sufficiently close to the caterpillar line, and A sufficiently close to diagonal, with all off-diagonal entries of A nonzero, and $t_1 < \cdots < t_n$:

1. For large $|z|$, the operator $\mathrm{i}\left(u + \frac{A}{2\pi z}\right)$ has eigenvalues $\mu_i(z)$ obeying $\lim_{z\to\infty} \mu_i(z) = \mathrm{i}u_i$. Each μ_i can be continued to an analytic function on $\mathbb{C} \setminus \cup_{j\neq i} B_{ij}$, where each B_{ij} is a vertical segment $B_{ij} = [z_{ij}^+, z_{ij}^-] \subset \mathbb{C}$, and the ordering of the $\mathrm{Re}\, z_{ij}^\pm$ is the same as the ordering of the z_{ij}.
2. Continuation across B_{ij} exchanges $\mu_i(z)$ with $\mu_j(z)$, while all other $\mu_k(z)$ extend holomorphically across B_{ij}.
3. The $n(n-1)$ endpoints $z_{ij}^\pm$ are simple ramification points of $\Gamma(u, A)$.
4. $\Gamma(u, A)$ is smooth.
5. Each μ_i obeys the reality condition
$$\mu_i(\overline{z}) = -\overline{\mu_i(z)}\,. \tag{3.5.5}$$

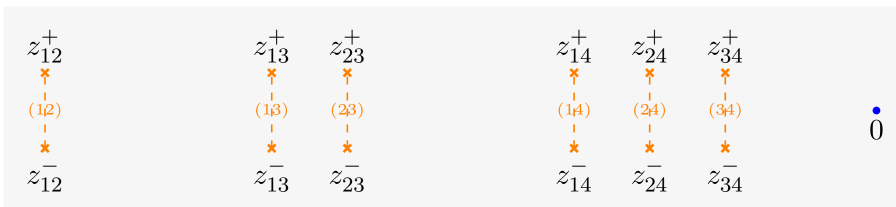

Figure 2: The arrangement of the branch points $z_{ij}^\pm$ and branch cuts B_{ij} in case $n = 4$, when the conditions of Proposition 3.19 are satisfied. Each branch cut is labeled with the induced transposition (ij) of the sheets.

See Figure 2 for a schematic picture of the cuts when $n = 4$.

Proof. Fix a pair (i, j) and choose any neighborhood U_{ij} which contains z_{ij} and excludes neighborhoods of all other z_{kl}. When A is diagonal, the eigenvalues $\mu_k(z)$ are given by (3.5.1), so they are all distinct in U_{ij}, except that $\mu_i(z_{ij}) = \mu_j(z_{ij})$. It follows that, when A is near diagonal, $M(z) = \mathrm{i}\left(u + \frac{A}{2\pi z}\right)$ has $n-2$ eigenvalues $\mu_k(z)$ ($k \notin \{i, j\}$) which vary analytically with z on U_{ij}; the other two eigenvalues $\mu_i(z)$, $\mu_j(z)$ vary analytically with z only on some U'_{ij} obtained by deleting a small disc around z_{ij}. Still, the local discriminant
$$\Delta_{ij}(z) = -(\mu_i(z) - \mu_j(z))^2 \tag{3.5.6}$$
extends analytically to the whole U_{ij}.

When A is diagonal, Δ_{ij} has a double zero at z_{ij} and vanishes nowhere else on U_{ij}. For A near diagonal, there are two possibilities: either the zero of Δ_{ij} remains double or it splits into a pair of simple zeroes. We have $\Delta_{ij}(\overline{z}) = \overline{\Delta_{ij}(z)}$, and moreover $\Delta_{ij}(z) \geq 0$ for $z \in \mathbb{R}$. It follows that $\Delta_{ij}(z)$ cannot have a simple zero on the real line, so if the double zero splits into a pair of simple zeroes, these two simple zeroes must be complex conjugate to one another.

Now fix a loop $c_{ij} \subset U'_{ij}$ which encircles z_{ij}. The period
$$p_{ij} = \oint_{c_{ij}} \sqrt{\Delta_{ij}(z)}\, dz = \mathrm{i} \oint_{c_{ij}} (\mu_i(z) - \mu_j(z))\, dz \tag{3.5.7}$$
can be nonvanishing only if $\Delta_{ij}(z)$ has two simple zeroes inside c_{ij} (as opposed to one double zero). The quantity p_{ij} varies smoothly with A, and we can compute it directly to quadratic order in the expansion around A^{diag}, as follows. Applying second-order perturbation theory for the eigenvalues of $M(z)$ [36] gives
$$\mu_i(z) = \mu_i^{\mathrm{diag}}(z) + \sum_{k\neq i} \frac{|A_{ik}|^2}{4\pi^2 z^2 (\mu_i^{\mathrm{diag}}(z) - \mu_k^{\mathrm{diag}}(z))} + O((A - A^{\mathrm{diag}})^3) \tag{3.5.8}$$

All terms on the right side are regular in U_{ij}, except for the $k=j$ term in the sum, which has a pole at $z=z_{ij}$. Thus we obtain residues

$$p_{ij} = \mathrm{i}\oint_{c_{ij}} (\mu_i(z) - \mu_j(z))\, dz = 2\mathrm{i}\oint_{c_{ij}} \frac{|A_{ij}|^2}{4\pi^2 z^2(\mu_i^{\mathrm{diag}}(z) - \mu_j^{\mathrm{diag}}(z))}\, dz + O((A - A^{\mathrm{diag}})^3) \tag{3.5.9}$$

$$= 2\mathrm{i}\frac{|A_{ij}|^2}{t_i - t_j} + O((A - A^{\mathrm{diag}})^3)\,. \tag{3.5.10}$$

For A close enough to diagonal, with all off-diagonal entries $A_{ij} \neq 0$, we conclude that all $p_{ij} \neq 0$. Thus all the double zeroes are split. Once we know this, the remaining assertions are straightforward. ∎

3.5.3 Distinguished cycles

We now discuss the vanishing cycles $V_j^{(k)}$ in the nearly diagonal case. We draw n concentric loops $V^{(k)}$, oriented counterclockwise, such that the annulus between $V^{(k)}$ and $V^{(k-1)}$ contains the branch cuts B_{jk} for $j = 1, \ldots, k$. The preimage of this annulus in $\Gamma(u, A)$ consists of one $2k$-holed sphere and $n-k$ cylinders. See Figure 3.

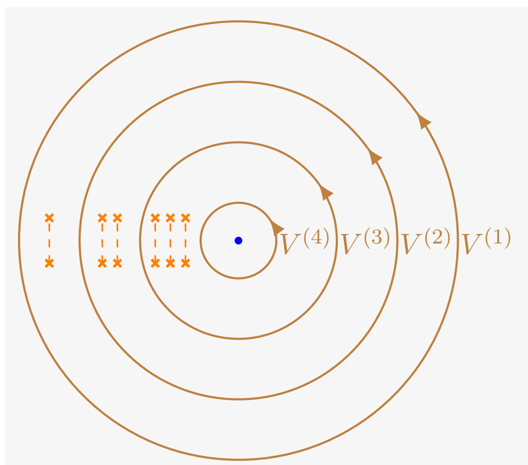

Figure 3: Dividing the base $\mathbb{C}$ into annuli, each containing one group of branch cuts. We show the example $n=4$.

Proposition 3.20. The vanishing cycle $V_j^{(k)}$ is the lift of $V^{(k)}$ to the j^{th} sheet of $\Gamma(u, A)$.

Proof. We consider the degeneration process from the previous sections, applied to the n-fold coverings described above. Taking $u_n \to \infty$ sends all of the $z_{in} \to 0$; said otherwise, in that limit, the group of branch cuts closest to $z=0$ disappears, and so $V^{(n-1)}$ can be contracted to a small loop around $z=0$. This continues to be true after blowing up as in Proposition 3.7: in the fiber over $u_n = \infty$, the lift of $V^{(n-1)}$ to sheet j can be contracted to the puncture over $z=0$ on that sheet. This matches the description of $V_j^{(n-1)}$ given above. Iterating the degeneration process we get the same statement for the other $V_j^{(k)}$. ∎

4 WKB predictions via spectral networks

In this section, we consider Conjecture 1.2 from another point of view, as an example of the general program of *exact WKB*. This program has a long history; see e.g. the pioneering works [47, 42, 17], and [9, 5, 6] which discuss the new features of the higher-order case ($n>2$ in our notation). Recently exact WKB has been reinterpreted in more geometric language, and also connected to various other areas of mathematics and physics, e.g. [22, 20, 40, 31, 33, 35, 26]. We quickly review here the features which will be important for us.

Suppose given a pencil of flat connections on a Riemann surface C, of the form

$$\nabla(\varepsilon) = \varepsilon^{-1}\varphi + D + \cdots \tag{4.0.1}$$

where φ is a Higgs field on C and D is a connection. Then the exact WKB program predicts the following picture. The monodromy and/or Stokes data of $\nabla(\varepsilon)$ can be expressed in terms of distinguished "spectral coordinates" X_γ on the moduli space of flat connections, and these distinguished coordinates have exponential asymptotics of the form

$$X_\gamma(\varepsilon) \sim \exp(Z(\gamma)/\varepsilon + \mathrm{i}\phi_\gamma)\,. \tag{4.0.2}$$

The leading coefficients $Z(\gamma)$ appearing in (4.0.2) are period integrals on cycles γ in the spectral curve determined by φ. The mapping between cycles γ and coordinate functions X_γ can be given by a general algorithm described in [22, 31], involving the technology of spectral networks.

The formula (4.0.2) evidently resembles Conjecture 1.2. In this section we make that resemblance precise, by applying the method of [22, 31] to the particular family of ODEs (1.1.1), when u is near the caterpillar point and the matrix A is close to diagonal. We find that the X_γ's are not exactly equal to the minor coordinates $\Delta_i^{(k)}$ which appear in Conjecture 1.2. Nevertheless, at least for $n = 2$ and $n = 3$, we show that (4.0.2) indeed leads to predicted asymptotics for $\left|\Delta_i^{(k)}\right|$ in the form of Conjecture 1.2, and gives a rule for determining the cycles $L_i^{(k)}$ appearing there. As expected, we find that $L_i^{(k)}$ matches with the cycle $C_i^{(k)}$ we defined in (3.4.1). (The obstacle to extending these statements to larger n has to do with the complexity of spectral networks in this case; see Conjecture 4.24 below.)

In fact, exact WKB leads to an extension of Conjecture 1.2: it predicts asymptotics for the full $\Delta_i^{(k)}$, including its phase. To get the full asymptotics, though, we need to consider periods along open paths as well as closed ones. We formulate these predictions for $n = 2$ and $n = 3$ below, and verify them directly in the case $n = 2$.

4.1 Periods and inequalities

Recall the definition of periods,

Definition 4.1. For $\gamma \in H_1(\Gamma(u, A))$, the period is

$$Z(\gamma) = \oint_\gamma \omega. \tag{4.1.1}$$

Definition 4.2. Let

$$\xi_i^{(j)} = -Z\left(V_i^{(j)}\right)\,. \tag{4.1.2}$$

The symmetry (3.5.5) implies that $\xi_i^{(j)} \in \mathbb{R}$. Also, $\xi_i^{(n)}$ and $\xi_i^{(1)}$ are residues of ω over $z = 0$ and $z = \infty$ respectively, which gives simple formulas:

$$\xi_i^{(n)} = \lambda_i^{(n)} = \lambda_i, \qquad \xi_i^{(1)} = t_i\,. \tag{4.1.3}$$

The intermediate $\xi_i^{(j)}$ for $j = 2, \ldots, n-1$ are not in general expressed in terms of eigenvalues, but as u approaches the caterpillar line, things are simpler:

Proposition 4.3. As u approaches the caterpillar line,

$$\xi_i^{(j)} \to \begin{cases} \lambda_i^{(j)} & \text{for } i \le j\,, \\ t_i & \text{for } i > j\,. \end{cases} \tag{4.1.4}$$

In particular, at the caterpillar line the $\xi_i^{(j)}$ for $i \le j$ obey the Cauchy interlacing inequalities. It follows by continuity that they also obey these inequalities sufficiently close to the caterpillar line. One spin-off of our description of the spectral networks is a direct geometric reproof of these inequalities, for $n = 2$ or $n = 3$. This involves the following homology classes:

Definition 4.4. Let

$$h_{ij} = V_i^{(j-1)} - V_i^{(j)}, \qquad \tilde{h}_{ij} = V_{i+1}^{(j)} - V_i^{(j-1)}. \tag{4.1.5}$$

The class $h_{ij} \in H_1(\Gamma(u, A))$ is represented by the 1-cycle which lies on sheet i and goes counterclockwise around the cut B_{ij}, $i < j$.

Again using the symmetry (3.5.5), we have $Z(h_{ij}), Z(\tilde{h}_{ij}) \in \mathbb{R}$. Below we will use spectral networks to prove the following:

Theorem 4.5. For $n = 2$ or $n = 3$, for all $1 \leq i < j \leq n$, $Z(h_{ij}) < 0$ and $Z(\tilde{h}_{ij}) < 0$.

Then we obtain as a consequence:

Corollary 4.6. For u sufficiently close to the caterpillar line, and A sufficiently close to diagonal, the $\xi_i^{(j)}$ for $i \leq j$ obey the (strict) interlacing inequalities.

See Figure 4 for the $n = 3$ example.

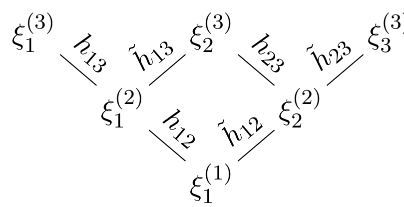

Figure 4: The coordinates $\xi_i^{(j)}$ which enter the interlacing inequalities in the case $n = 3$. The larger coordinates are to the right, e.g. $\xi_1^{(3)} < \xi_1^{(2)}$. For each pair of coordinates that are involved in an interlacing inequality, we indicate the corresponding h, e.g. $Z(h_{13}) = -\xi_1^{(2)} + \xi_1^{(3)}$.

4.2 Spectral networks for near-diagonal matrices and Stokes asymptotics

4.2.1 General setup

The conjectures of [21, 22] give a description of the $\varepsilon \to 0$ asymptotics of the Stokes matrices $(S_\pm)(u, A, \varepsilon)$ along any ray in the ε-plane. To write this description explicitly one needs a technical device, the *spectral network* $\mathcal{W}(u, A, \vartheta)$, where $\vartheta = \arg \varepsilon$. We briefly review the definition of $\mathcal{W}(u, A, \vartheta)$ in Appendix C.

We also need to introduce a relative homology group $H(u, A, \vartheta)$ defined as follows.

Definition 4.7. Consider the real oriented blow-up $\widehat{\Gamma}(u, A)$ of $\Gamma(u, A)$ at the n preimages of $z = \infty$. Then $\widehat{\Gamma}(u, A)$ has boundary consisting of n circles. On each of these n circles we mark two points ∞_i^+, ∞_i^-, lying over the two anti-Stokes rays at arguments ϑ, $\vartheta + \pi$. Let $L(\vartheta) = \{\infty_1^+, \infty_1^-, \infty_2^+, \infty_2^-, \ldots, \infty_n^+, \infty_n^-\}$, and define

$$H(u, A, \vartheta) = H_1(\widehat{\Gamma}(u, A); L(\vartheta)) \,. \tag{4.2.1}$$

$H(u, A, \vartheta)$ contains the subgroup $H_1(\Gamma(u, A))$ of closed paths, as a sublattice of index $2n - 1$.

There are some subtle minus signs in the spectral coordinates, which need to be incorporated into our bookkeeping. For this purpose, it is convenient to pass to a $\mathbb{Z}_2$ extension of $H(u, A, \vartheta)$, as follows. (These signs are probably best ignored at first; we emphasize that they are not related to the signs of periods or interlacing inequalities.)

Definition 4.8. Let $\widetilde{\Gamma}(u, A)$ be the surface obtained by puncturing $\widehat{\Gamma}(u, A)$ at each branch point. Then

$$\widetilde{H}(u, A, \vartheta) = (H_1(\widetilde{\Gamma}(u, A); L(\vartheta)) \times \mathbb{Z}_2)/I \,, \tag{4.2.2}$$

where I is the subgroup generated by elements $(\ell, 1)$ with ℓ a small loop around a branch point.

The projection $\widetilde{H}(u, A, \vartheta) \to H(u, A, \vartheta)$ given by $(\gamma, y) \mapsto \gamma$ is the $\mathbb{Z}_2$ extension.

Proposition 4.9.

1. The network $\mathcal{W}(u, A, \vartheta)$ determines *spectral coordinates* $X_\gamma^\vartheta(u, A, \varepsilon) \in \mathbb{C}^\times$, indexed by $\gamma \in \widetilde{H}(u, A, \vartheta)$. They are algebraic functions of the Stokes matrix entries $(S_\pm)_{ij}(u, A, \varepsilon)$, obeying the relations $X_\gamma^\vartheta X_{\gamma'}^\vartheta = X_{\gamma+\gamma'}^\vartheta$ (and thus $X_{(0,0)}^\vartheta = 1$), and $X_{(0,1)}^\vartheta = -1$.

2. Each Stokes matrix entry can be expressed as a linear combination of spectral coordinates, of the general form

$$(S_\pm)_{ij}(u, A, \varepsilon) = \sum_{\gamma \in \tilde{H}(u,A,\vartheta)} c_{\gamma,ij}^{\vartheta,\pm}(u, A) X_\gamma^\vartheta(u, A, \varepsilon) \tag{4.2.3}$$

   where the coefficients $c_{\gamma,ij}^{\vartheta,\pm}(u, A) \in \mathbb{Q}$, and the sum may be infinite.

The $c_{\gamma,ij}^{\vartheta,\pm}(u, A)$ are determined by the path-lifting rule, which we review in Appendix C. Now we recall the main conjecture about WKB asymptotics and spectral networks, specialized to our case (see Appendix C for a more general discussion):

Conjecture 4.10. As $\varepsilon \to 0$ with $\arg \varepsilon \in (\vartheta - \frac{\pi}{2}, \vartheta + \frac{\pi}{2})$, we have the asymptotics

$$X_\gamma^\vartheta(u, A, \varepsilon) \sim \exp(Z(\gamma)/\varepsilon + \mathrm{i}\phi_\gamma)\,, \tag{4.2.4}$$

where

$$Z(\gamma) = \int_\gamma^{\mathrm{reg}} \omega\,, \tag{4.2.5}$$

and ϕ_γ are some constants depending on (u, A).

If γ is closed, then the symbol $\int^{\mathrm{reg}}$ in (4.2.5) means the ordinary integral. If γ is open, then the ordinary integral would be divergent, and $\int^{\mathrm{reg}}$ instead means a regularized integral, as follows. Suppose γ is a path running from ∞_i^ε to $\infty_{i'}^{\varepsilon'}$. We can define a regularization γ_{reg} of γ, by perturbing the endpoints slightly off the boundary circle; call the perturbed initial and final points z_i, $z'_{i'}$ respectively. Then

$$Z(\gamma) = \lim_{z_i \to \infty_i^\varepsilon} \lim_{z'_{i'} \to \infty_{i'}^{\varepsilon'}} \left(-P(z'_{i'}) + P(z_i) + \int_{\gamma_{\mathrm{reg}}} \omega \right) \tag{4.2.6}$$

where we define the function P in a neighborhood of the boundary as follows: let z_i be the preimage of $z \in \mathbb{C}$ on sheet i; then

$$P(z_i) = \mathrm{i}u_i z - \frac{t_i}{2\pi\mathrm{i}} \left(\frac{1}{2}\log(z) + \frac{1}{2}\log(-z) + \mathrm{i}\pi \right)\,, \tag{4.2.7}$$

where $\log$ on the right side means the branch we fixed in Section 2, with its cut along the positive imaginary axis.

Loosely speaking, (4.2.4) says that the spectral coordinates X_γ^ϑ are especially well adapted for studying the asymptotics of the Stokes matrices as $\varepsilon \to 0$ with $\arg \varepsilon \in (\vartheta - \frac{\pi}{2}, \vartheta + \frac{\pi}{2})$. For instance, using (4.2.3) and (4.2.4) we can predict the leading asymptotics of $(S_\pm)_{ij}$. In the expansion (4.2.3), the dominant term will be the one with the largest value of $\mathrm{Re}\, Z(\gamma)/\varepsilon$ (assuming that there is a unique largest value), and then we predict

$$(S_\pm)_{ij}(u, A, \varepsilon) \sim c_{\gamma,ij}^{\vartheta,\pm} \exp(Z(\gamma)/\varepsilon + \mathrm{i}\phi_\gamma)\,. \tag{4.2.8}$$

4.2.2 The case $n = 2$

First, we discuss the case $n = 2$. This case is exceptional in that we can calculate the Stokes matrix exactly, so we can directly check that the predictions of exact WKB indeed hold.

Write

$$A = \begin{pmatrix} t_1 & a \\ \overline{a} & t_2 \end{pmatrix}\,. \tag{4.2.9}$$

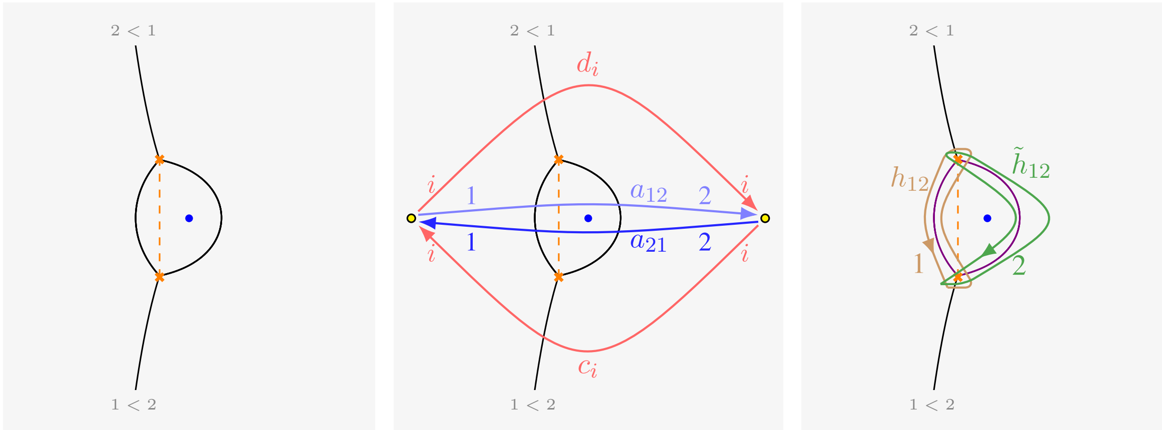

Figure 5: A spectral network $\mathcal{W}(u, A, \vartheta = 0)$ in the $n = 2$ case. Left: the bare spectral network. Middle: the spectral network with paths representing classes in $\tilde{H}(u, A, \vartheta)$. Numbers 1, 2 next to paths indicate the sheet on which the path travels. Right: the spectral network with the saddle connections highlighted in purple, and representatives of their charges in $\tilde{H}(u, A, \vartheta)$ marked.

The branch points of the spectral curve $\Gamma(u, A)$ are

$$z_{12}^{\pm} = \frac{t_1 - t_2 \pm 2\mathrm{i}\,|a|}{2\pi(u_2 - u_1)}\,. \tag{4.2.10}$$

From (4.2.10) we see directly that, when $t_1 < t_2$ and $a \neq 0$, the two branch points are simple. It follows that $\Gamma(u, A)$ is smooth of genus $g = 0$ with 4 punctures. The lattice $H(u, A, \vartheta)$ has rank 6, generated by the 6 open paths a_{12}, a_{21}, c_i, d_i $(i = 1, 2)$ shown in Figure 5. The sublattice $H_1(\Gamma(u, A))$ of closed paths has rank 3; it is spanned by $c_1 + d_1$, $c_2 + d_2$, and $a_{12} + a_{21}$. On this sublattice, all periods are real, and the intersection pairing is trivial.

Proposition 4.11. For $u_1 < u_2$, $t_1 < t_2$ and $a \neq 0$, the spectral network $\mathcal{W}(u, A, \vartheta = 0)$ has the topology shown in Figure 5.

Proof. $\mathcal{W}(u, A, \vartheta = 0)$ is the critical graph of the quadratic differential

$$\phi_2 = \frac{(t_1 - t_2 + 2\pi(u_1 - u_2)z)^2 + 4\,|a|^2}{16\pi^2 z^2}\, dz^2\,. \tag{4.2.11}$$

We can determine its topology with computer assistance, or more synthetically, using the following general constraints. Each branch point emits three trajectories, which must end up either at a Stokes ray or at the other branch point. Moreover, no two trajectories can cross, the picture has to be symmetric under reflection in the real axis, and no two trajectories can be homotopic to one another. This information is enough to determine the picture uniquely. ■

$\mathcal{W}(u, A, \vartheta = 0)$ is degenerate: there are two saddle connections connecting the two branch points. Their charges are the classes h_{12} and $\tilde{h}_{12}$ defined in Definition 4.4, and shown in the right of Figure 5. They can be written alternatively as

$$h_{12} = c_2 + d_2 - a_{12} - a_{21}, \quad \tilde{h}_{12} = c_1 + d_1 - a_{12} - a_{21}\,. \tag{4.2.12}$$

The fact that saddle connections with charges h_{12} and $\tilde{h}_{12}$ exist proves Theorem 4.5 in this case, using Proposition C.6.

Stokes matrix asymptotics

Now we discuss the $\varepsilon \to 0$ asymptotics of the Stokes matrix entries. Since $S_- = S_+^*$ for real ε, we will just discuss S_+. The first step is to expand the entries of S_+ in terms of spectral coordinates:

Proposition 4.12. The coordinate expansion (4.2.3) of S_+ has the form

$$(S_+)_{ii} = X^0_{c_i}, \tag{4.2.13}$$
$$(S_+)_{12} = X^0_{a_{21}} + \cdots \tag{4.2.14}$$

where $\cdots$ is a (infinite, convergent) sum of terms $c_\gamma X^0_\gamma$, with each $Z(\gamma) - Z(a_{21}) \in \mathbb{R}_-$.

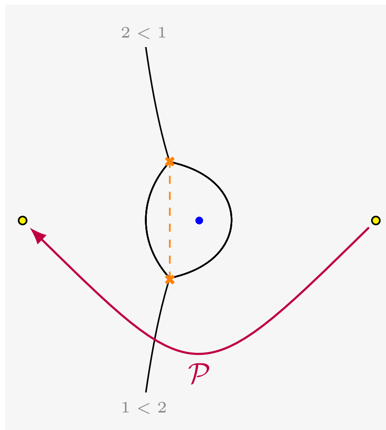

Figure 6: A spectral network $\mathcal{W}(u, A, \vartheta = 0)$ in the $n = 2$ case, with the path $\mathcal{P}$ marked.

Proof. Let $\mathcal{P}$ be the arc shown in Figure 6. Let Lift be the path-lifting functor induced by $\mathcal{W}(u, A, \vartheta = 0)$. The expansion of the entries of S_+ in spectral coordinates is given by $\mathrm{Lift}(\mathcal{P})$. According to Proposition C.12, we have

$$\mathrm{Lift}(\mathcal{P}) = c_1 + c_2 + a_{21} + \cdots \tag{4.2.15}$$

where all terms γ appearing in the $\cdots$ go from sheet 2 to sheet 1, and have $Z(\gamma) - Z(a_{21}) < 0$. The entry $(S_+)_{ij}$ is the sum of spectral coordinates for the terms that begin on sheet j and end on sheet i; this gives the desired results. ■

As $\varepsilon \to 0$ with $\arg \varepsilon \in (-\pi/2, \pi/2)$, the $\cdots$ terms in (4.2.14) are exponentially suppressed; thus the asymptotic we predict using (4.10) comes from the $X^0_{a_{21}}$ term, and is

$$(S_+)_{12} \sim \exp(Z(a_{21})/\varepsilon)\,. \tag{4.2.16}$$

For the diagonal entries we just have a single term in (4.2.13), and thus the asymptotic is

$$(S_+)_{ii} \sim \exp(Z(c_i)/\varepsilon)\,. \tag{4.2.17}$$

Thus we are predicting altogether

$$\varepsilon \log(S_+)_{ij} \to \begin{pmatrix} Z(c_1) & Z(a_{21}) \\ & Z(c_2) \end{pmatrix}. \tag{4.2.18}$$

To understand this prediction more explicitly, we need to study the regularized open periods $Z(\gamma)$, which we do next.

Real parts of periods

The real parts of the periods are relatively simple to obtain. Indeed, we have

$$\mathrm{Re}\, Z(\gamma) = \frac{1}{2} Z(\gamma - \iota(\gamma))\,, \tag{4.2.19}$$

and $\gamma - \iota(\gamma)$ is always a closed cycle, which we can identify directly. Moreover, since Γ has genus zero, the resulting closed periods are just sums of residues. We obtain:

$$\operatorname{Re} Z(a_{21}) = \frac{1}{2}(Z(a_{21}) + Z(a_{12})) = -\frac{1}{2} Z(V_2^{(2)}) = -\frac{1}{2}\xi_2^{(2)} = -\frac{1}{2}\lambda_2 \,, \tag{4.2.20}$$

$$\operatorname{Re} Z(c_i) = \frac{1}{2} Z(c_i + d_i) = -\frac{1}{2} Z(V_i^{(1)}) = \frac{1}{2}\xi_i^{(1)} = \frac{1}{2} t_i \,. \tag{4.2.21}$$

Thus we can summarize the predicted leading asymptotic magnitudes as

$$\varepsilon \log |(S_+)_{ij}| \to \frac{1}{2}\begin{pmatrix} t_1 & \lambda_2 \\ & t_2 \end{pmatrix} . \tag{4.2.22}$$

Moreover, this structure is in accordance with the general Conjecture 1.2. Indeed, the minor coordinates are $\Delta_1^{(1)} = (S_+)_{11}$, $\Delta_1^{(2)} = (S_+)_{12}$, $\Delta_2^{(2)} = (S_+)_{11}(S_+)_{22}$, and we have just seen that each entry $(S_+)_{ij}$ is controlled by a corresponding period; this matches Conjecture 1.2, with the cycles

$$L_1^{(1)} = V_1^{(1)}, \quad L_1^{(2)} = V_2^{(2)}, \quad L_2^{(2)} = V_1^{(1)} + V_2^{(1)} \,. \tag{4.2.23}$$

Comparing this with (3.4.1), we see that Conjecture 1.2 holds with $L_i^{(k)} = C_i^{(k)}$, as we expected.

Imaginary parts of periods

The imaginary parts of the periods are subtler than the real parts; they require us to use the detailed formula (4.2.6) defining the regularization of open paths.

The paths c_i can be isotoped into a small neighborhood of $z = \infty$ and computed explicitly from the series expansion of ω there, with the result:

Proposition 4.13. The regularized period on the path c_i is

$$Z(c_i) = \frac{1}{2} t_i \,. \tag{4.2.24}$$

For a_{21} the computation is more interesting, since this path cannot be isotoped to a small neighborhood of $z = \infty$. One can still compute the integral in (4.2.6) directly: indeed, since Γ has genus zero, the 1-form ω must have an elementary antiderivative, just involving square roots and logarithms. Using this antiderivative in (4.2.6) gives the following result:

Proposition 4.14. The regularized period on the path a_{21} is

$$Z(a_{21}) = \frac{\lambda_2}{2} - \frac{\mathrm{i}}{2\pi}\left((t_2 - t_1) \log \frac{2\pi \mathrm{e}(u_2 - u_1)}{|a|} + \frac{1}{2}(\lambda_2 - \lambda_1)\left(\log(t_1 - \lambda_1) - \log(\lambda_2 - t_1)\right)\right) . \tag{4.2.25}$$

A comparison

Now we can confront our asymptotic predictions with ground truth; indeed we know the exact form of S^+, given in Example 2.13. Comparing it to (4.2.24) and (4.2.25) gives:

Corollary 4.15. As $\varepsilon \to 0$ with $\arg \varepsilon \in (-\pi/2, \pi/2)$, we have $\varepsilon \log S_{12}^+ \to Z(a_{21})$ and $\varepsilon \log S_{ii}^+ = Z(c_i)$.

In particular, it follows that Conjecture 4.10 is indeed true in this case.

4.2.3 The case $n = 3$

Next, let us consider the case $n = 3$.

By Proposition 3.19, for u sufficiently close to the caterpillar line and A sufficiently close to diagonal, the spectral curve $\Gamma(u, A)$ is smooth, with genus $g = 1$ and $m = 6$ punctures. It follows that the lattice $H(u, A, \vartheta)$ has rank $2g + 2m - 2 = 12$, and the closed sublattice $H_1(\Gamma(u, A))$ has rank $2g + m - 1 = 7$. Inside the closed sublattice we can consider the kernel of the intersection pairing, $K(u, A) \subset H_1(\Gamma(u, A))$, of rank $m - 1 = 5$. On $K(u, A)$ all periods are sums of residues, and in particular, they are real.

We begin by describing the spectral networks:

Proposition 4.16. For $u_1 < u_2 < u_3$, $t_1 < t_2 < t_3$, u sufficiently close to the caterpillar line, and A sufficiently close to diagonal, $\mathcal{W}(u, A, \vartheta = 0)$ is equivalent to the spectral network shown in Figure 7.

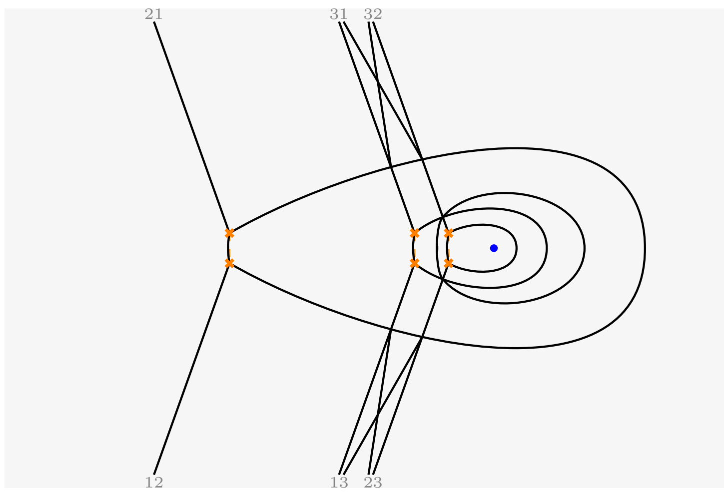

Figure 7: A spectral network $\mathcal{W}(u, A, \vartheta = 0)$ in the $n = 3$ case. We compress the notation for the wall labels by writing ij instead of $i < j$.

Proof. Using the code included with the arXiv version of this paper, we can check that, for one specific example of (u, A), the spectral network $\mathcal{W}(u, A, \vartheta = 0)$ is indeed of the form shown in Figure 7.[2]

Next, we consider what happens when we vary (u, A). It follows from Proposition C.22 that the lifting maps for the spectral network $\mathcal{W}(u, A, \vartheta = 0)$ vary by equivalences, except when (u, A) cross a locus where some $\gamma \notin K(u, A)$ has real period. Because $K(u, A)$ has index 2, the only way this can happen is if every period becomes real; in particular, $Z(\Delta)$ would have to be real, where Δ is shown in Figure 8.

[2]To be explicit, consider the case

$$u = \left(0, \frac{1}{4}, 1\right), \quad A = \begin{pmatrix} 0 & \frac{1}{6} & 1 \\ \frac{1}{6} & 3 & \frac{1}{3} \\ 1 & \frac{1}{3} & 4 \end{pmatrix}. \tag{4.2.26}$$

A computer-generated approximation of the resulting spectral network at $\vartheta = 0.0005$ is shown below.

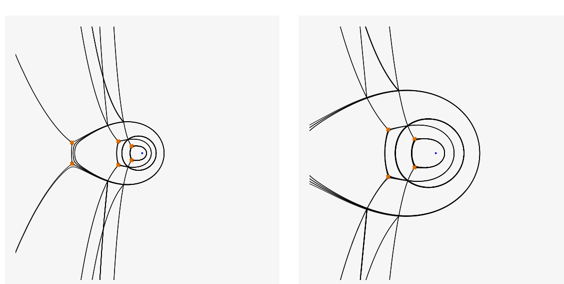

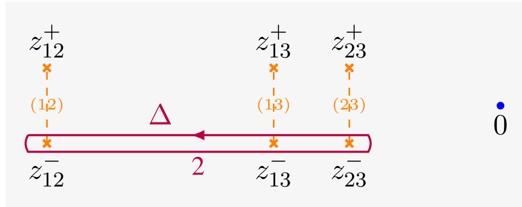

Figure 8: The cycle Δ on $\Gamma(u, A)$.

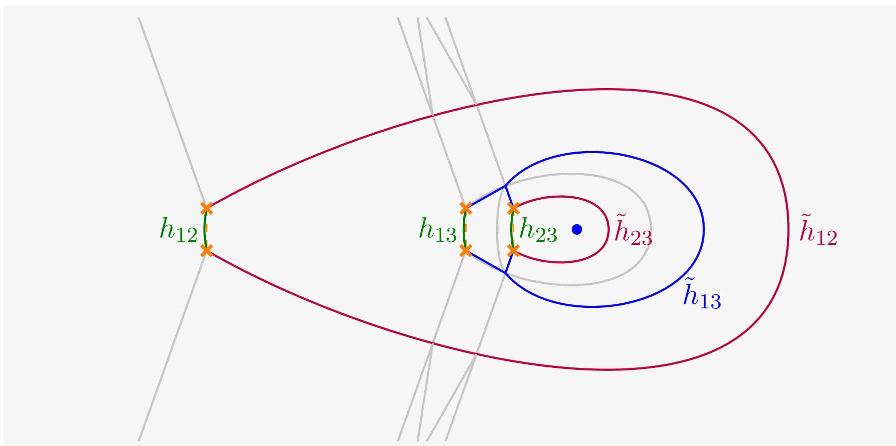

Figure 9: The 6 finite webs in the spectral network $\mathcal{W}(u, A, \vartheta = 0)$ responsible for the interlacing inequalities in the $n = 3$ case. 5 of them are saddle connections (3 green, 2 purple) and 1 is a 5-string tree (blue). Each finite web is labeled with its corresponding charge. Other walls of the network are shown in gray.

But we can compute $Z(\Delta)$ in the limit of diagonal A: using the explicit formulas (3.5.1), (3.5.2) we get

$$Z(\Delta) \to -\frac{\mathrm{i}}{2\pi}\left((t_2 - t_1)\log\frac{(t_3 - t_1)(u_2 - u_1)}{(t_2 - t_1)(u_3 - u_1)} + (t_3 - t_2)\log\frac{(t_3 - t_2)(u_3 - u_1)}{(t_3 - t_1)(u_3 - u_2)}\right) . \tag{4.2.27}$$

Near the caterpillar line $u_3 - u_2 \gg u_2 - u_1$, this becomes

$$Z(\Delta) \sim \frac{\mathrm{i}}{2\pi}(t_2 - t_1)\log\frac{u_3 - u_1}{u_2 - u_1} , \tag{4.2.28}$$

and thus the imaginary part does not vanish for u sufficiently close to the caterpillar line and A sufficiently close to diagonal. It follows that, as we vary (u, A) while maintaining this condition, $\mathcal{W}(u, A, \vartheta = 0)$ varies by equivalences. ∎

Let us discuss the spectral network in Figure 7. Looking first at the region near $z = \infty$, we see a structure which resembles the $n = 2$ case in Figure 5: two branch points, connected by two saddle connections, and emitting two walls to infinity, labeled $1 < 2$ and $2 < 1$. One of the two saddle connections looks like a large ring, almost encircling the singularity at $z = 0$.

Near $z = 0$ there is some more complicated fine structure, with two walls of types $1 < 3$ and $2 < 3$ emitted out to the large-z region. Along the way from small z to large z, these walls scatter off the ring, creating extra walls of type $1 < 3$ and $2 < 3$. Thus the Stokes matrix entries $(S_+)_{13}$ and $(S_+)_{23}$ ultimately involve a mixture between the structure of the small-z and large-z regions. In contrast, $(S_+)_{12}$ comes only from the large-z region.

Another important feature of $\mathcal{W}(u, A, \vartheta = 0)$ is that it contains finite webs. In Figure 9 we indicate 6 finite webs whose charges are the classes h_{ij} and $\tilde{h}_{ij}$. 5 of these 6 finite webs are saddle connections, similar to the ones that we had in the $n = 2$ case. The last one, with charge $\tilde{h}_{13}$, is a five-string tree. The existence of these finite webs proves Theorem 4.5 in case $n = 3$, using Proposition C.6.

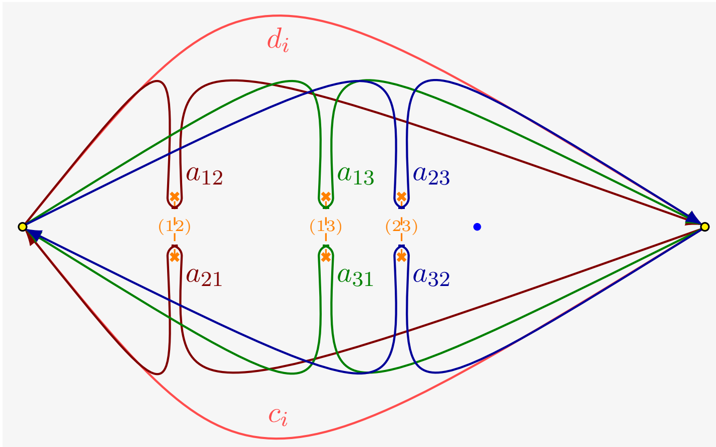

Figure 10: Open paths a_{ij} $(i \neq j)$, c_i, d_i, generating $H(u, A, \vartheta = 0)$. Each a_{ij} begins on sheet i and ends on sheet j; each c_i or d_i begins and ends on sheet i.

Stokes matrix entry asymptotics

Now suppose that we are interested in studying the $\varepsilon \to 0$ asymptotics of the Stokes matrix entries $(S_+)_{ij}$. In Figure 10 we show 12 open paths a_{ij} $(i \neq j)$, c_i, d_i, generating $H(u, A, \vartheta = 0)$. The Stokes matrix entries can be expanded in terms of spectral coordinates associated to these paths:

Proposition 4.17. The expansion (4.2.3) of Stokes matrix entries in spectral coordinates is:

$$(S_+)_{ii} = X^0_{c_i}, \tag{4.2.29}$$
$$(S_+)_{12} = X^0_{a_{21}} + \cdots, \tag{4.2.30}$$
$$(S_+)_{13} = X^0_{a_{32}-c_2+a_{21}} + \cdots, \tag{4.2.31}$$
$$(S_+)_{23} = X^0_{a_{32}} + X^0_{a_{31}-a_{21}+c_1} + \cdots, \tag{4.2.32}$$

where $\cdots$ represents a sum of terms X_γ with $\operatorname{Re} Z(\gamma)$ smaller than that for the leading term. In (4.2.32), the leading term can be either of the two terms shown.

Proof. All these formulas are obtained using Proposition C.12. (For the reader who is interested in reproducing them, we note one tricky point: the leading term indicated in $(S_+)_{13}$ arises from a term with two detours; there are two other terms in $(S_+)_{13}$ which naively appear to have larger $\operatorname{Re} Z(\gamma)$, but those two terms cancel one another.) ■

To get from these formulas to the $\varepsilon \to 0^+$ asymptotics for $|(S_+)_{ij}|$, we need to compute the real parts of the relevant periods. This can be done using the involution ι as we did in the $n = 2$ case. In particular, for the classes appearing in Proposition 4.17 we have

$$\operatorname{Re} Z(c_i) = -\frac{1}{2} Z(V_i^{(1)}) = \frac{1}{2} t_i\,, \tag{4.2.33}$$
$$\operatorname{Re} Z(a_{21}) = -\frac{1}{2} Z(V_2^{(2)}) = \frac{1}{2} \xi_2^{(2)}\,, \tag{4.2.34}$$
$$\operatorname{Re} Z(a_{32} - c_2 + a_{21}) = -\frac{1}{2} Z(V_3^{(3)}) = \frac{1}{2} \xi_3^{(3)}\,, \tag{4.2.35}$$
$$\operatorname{Re} Z(a_{32}) = -\frac{1}{2} Z(V_3^{(3)} - h_{12}) = \frac{1}{2} (\xi_3^{(3)} - \xi_1^{(1)} + \xi_1^{(2)})\,, \tag{4.2.36}$$
$$\operatorname{Re} Z(a_{31} - a_{21} + c_1) = -\frac{1}{2} Z(V_3^{(3)} - h_{23}) = \frac{1}{2} (\xi_3^{(3)} - \xi_2^{(2)} + \xi_2^{(3)})\,. \tag{4.2.37}$$

The resulting asymptotics are:

Proposition 4.18. For u sufficiently close to the caterpillar line and A near diagonal, if Conjecture 4.10 holds, the leading $\varepsilon \to 0^+$ asymptotics of the norms of entries of S_+ are

$$\varepsilon \log |(S_+)_{ij}| \sim \frac{1}{2} \begin{pmatrix} t_1 & \xi_2^{(2)} & \lambda_3 \\ & t_2 & \max(\lambda_3 - \xi_2^{(2)} + t_2, \lambda_3 - \xi_2^{(2)} + \lambda_2) \\ & & t_3 \end{pmatrix} . \tag{4.2.38}$$

Factorization coordinates

In (4.2.38) we see that the leading asymptotic of the Stokes matrix entry $(S_+)_{23}$ is controlled by a piecewise linear function of periods, rather than by a single period. This contrasts with the statement of Conjecture 1.2, which says that the minor coordinates of S_+ each should be controlled by a single period. How do we see from the point of view of the spectral network that the minor coordinates should behave better than the entry coordinates?

In this section, we will answer this question, by giving a spectral-network interpretation of the *factorization coordinates*: these are two related coordinate systems, defined on two double Bruhat cells $B^+ \cap B^- w_0 B^-$ associated to reduced words for the permutation $w_0 = (123)$. The factorization coordinates are related by a monomial transformation to the minor coordinates, so asymptotic formulas for one easily translate to asymptotic formulas for the other.

Let us briefly recall what the factorization coordinates are. We consider the reduced word $w_0 = (23)(12)(23)$, which corresponds to a coordinate system on the subset

$$U = \{Y \in B^+ \mid Y_{12} \neq 0 \text{ or } Y_{13} = 0\} \quad \subset \quad B^+ . \tag{4.2.39}$$

Namely, any $Y \in U$ admits a unique factorization

$$Y = \begin{pmatrix} \delta_1 & 0 & 0 \\ 0 & \delta_2 & 0 \\ 0 & 0 & \delta_3 \end{pmatrix} \begin{pmatrix} 1 & 0 & 0 \\ 0 & 1 & \alpha \\ 0 & 0 & 1 \end{pmatrix} \begin{pmatrix} 1 & \beta & 0 \\ 0 & 1 & 0 \\ 0 & 0 & 1 \end{pmatrix} \begin{pmatrix} 1 & 0 & 0 \\ 0 & 1 & \gamma \\ 0 & 0 & 1 \end{pmatrix} = \begin{pmatrix} \delta_1 & \delta_1\beta & \delta_1\beta\gamma \\ 0 & \delta_2 & \delta_2(\alpha+\gamma) \\ 0 & 0 & \delta_3 \end{pmatrix} , \tag{4.2.40}$$

and this factorization defines the coordinates $(\delta_1, \delta_2, \delta_3, \alpha, \beta, \gamma)$ of Y.

To study the asymptotics of the factorization coordinates of S_+, we apply an equivalence of spectral networks in the sense of [22], illustrated in Figure 11. Beginning from $\mathcal{W}(u, A, \vartheta = 0)$ we first slide the branch points $z_{12}^{\pm}$

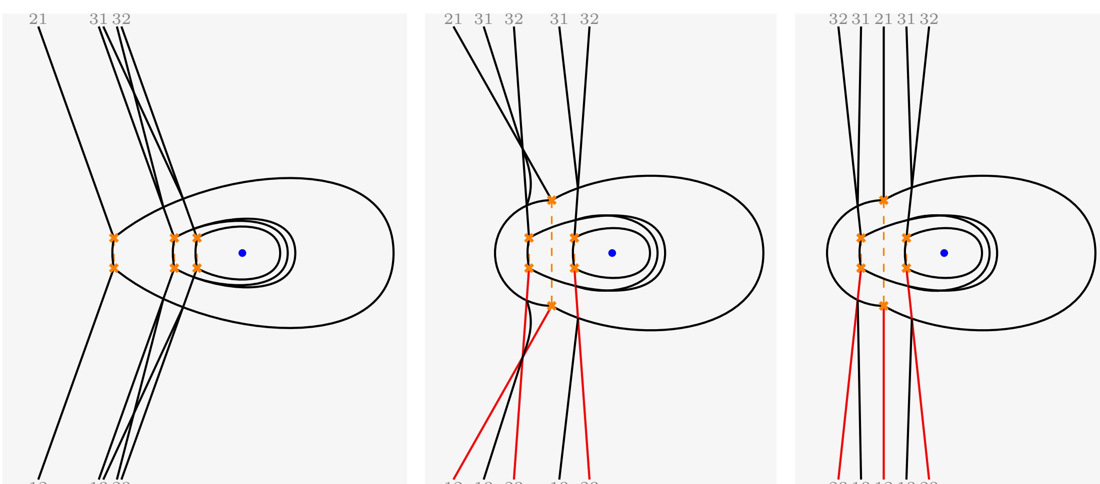

Figure 11: Spectral networks reached from $\mathcal{W}(u, A, \vartheta = 0)$ of Figure 7 by a sequence of equivalences. The figure should be read from left to right. The configuration on the right is the one we use for the study of the factorization coordinates of S_+. We highlight the relevant primary walls in red.

to a position near $z_{13}^{\pm}$ and $z_{23}^{\pm}$. In this process z_{12}^{-} crosses a line of type $1 < 3$, and the configuration of walls is transformed as indicated in [22] (section 10.6); this change does not affect the topology near infinity. Similarly z_{12}^{+}

crosses a line of type $3 < 1$. Next we move the branch cut B_{12} across the cut B_{13}; this has the effect of conjugating the transposition on B_{13}, changing it from (13) to (23). The resulting configuration is shown in the middle of Figure 11. Finally, we simplify the configuration by moving the primary wall of type $1 < 2$ across the primary wall of type $2 < 3$. The final configuration is indicated on the right of Figure 11.

Because this process is an equivalence, it does not change the spectral coordinates associated to closed paths. Moreover, because in this equivalence no walls cross the anti-Stokes rays, the equivalence also does not change the spectral coordinates or their relation to the Stokes matrix elements. Still, this equivalence makes manifest cancellations which would otherwise require computations to check, and makes the relation to the factorization coordinates easier to see.

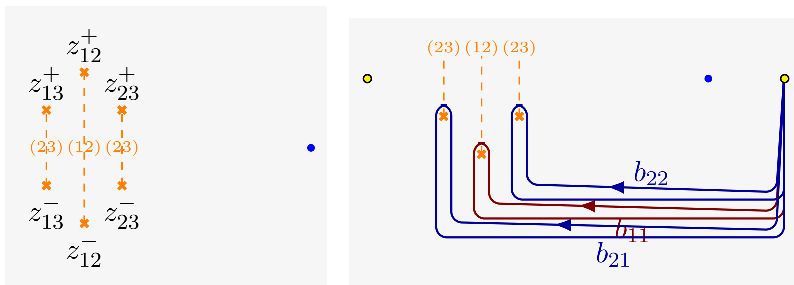

Figure 12: Left: the arrangement of the branch cuts after applying the equivalence of spectral networks described in the main text. Right: paths b_{ij} which correspond to the factorization coordinates.

Computing the Stokes matrix S_+ from this picture gives a factorization of the form

$$S_+ = D(\delta) M_{23}(\tilde{\alpha}) M_{13}(\eta_1) M_{12}(\tilde{\beta}) M_{13}(\eta_2) M_{23}(\tilde{\gamma}) \tag{4.2.41}$$

where $M_{ij}(x)$ is a unipotent matrix with ij entry x, and $D(\delta)$ is a diagonal matrix with ii entry δ_i. The five unipotent factors in (4.2.41) correspond to the five walls visible on the bottom of the right side of Figure 11, in order (left to right in (4.2.41) corresponds to left to right in the figure).

The coefficients $\tilde{\alpha}$, $\tilde{\beta}$, $\tilde{\gamma}$, η_1, η_2 are given by the path-lifting rule as linear combinations of spectral coordinates:

Proposition 4.19. For u sufficiently close to the caterpillar line and A near diagonal, we have

$$\delta_i = X^0_{c_i}, \qquad \tilde{\alpha} = X^0_{b_{21}} + \cdots, \qquad \tilde{\beta} = X^0_{b_{11}} + \cdots, \qquad \tilde{\gamma} = X^0_{b_{22}} + \cdots, \tag{4.2.42}$$

and

$$\eta_1 = X^0_{(b_{11}+b_{21})+h_{12}} + \cdots, \qquad \eta_2 = X^0_{(b_{22}+b_{11})+\tilde{h}_{12}} + \cdots, \tag{4.2.43}$$

where in each expression $\cdots$ means a sum of terms X^0_γ, with $\operatorname{Re} Z(\gamma)$ smaller than that of the leading term.

Because of the extra matrices $M_{13}(\eta_1)$ and $M_{13}(\eta_2)$ in the factorization (4.2.41), the factorization coordinates (α, β, γ) are not precisely equal to $(\tilde{\alpha}, \tilde{\beta}, \tilde{\gamma})$. Nevertheless, these extra matrices are negligible, in the sense that they do not affect the asymptotics of the factorization coordinates:

Proposition 4.20. For u sufficiently close to the caterpillar line and A near diagonal, the factorization coordinates of S_+ are

$$\delta_i = X^0_{c_i}, \quad (\alpha, \beta, \gamma) = (X^0_{b_{21}} + \cdots, X^0_{b_{11}} + \cdots, X^0_{b_{22}} + \cdots) \tag{4.2.44}$$

where in each expression $\cdots$ means a sum of terms X^0_γ, with $\operatorname{Re} Z(\gamma)$ smaller than that of the leading term.

Proof. Directly multiplying matrices gives the relations

$$\beta = \tilde{\beta}, \quad \alpha + \gamma = \tilde{\alpha} + \tilde{\gamma}, \quad \beta\gamma = \tilde{\beta}\tilde{\gamma} + \eta_1 + \eta_2 \,. \tag{4.2.45}$$

Moreover, from (4.2.42) and (4.2.43) it follows that both η_1 and η_2 are subleading compared to $\tilde{\beta}\tilde{\gamma}$, using the facts that $\operatorname{Re} Z(h_{12} + b_{21} - b_{22}) = \frac{1}{2}(Z(h_{12}) + Z(h_{23})) < 0$ (for η_1) and $Z(\tilde{h}_{12}) < 0$ (for η_2). Thus $\beta\gamma$ and $\tilde{\beta}\tilde{\gamma}$ differ only by subleading terms. From there, using (4.2.45) it is straightforward to show that α, γ, β have the same leading terms as $\tilde{\alpha}$, $\tilde{\gamma}$, $\tilde{\beta}$ respectively. The latter were given in (4.2.42). ■

Using the involution ι again, we compute the real parts of the periods:

$$\operatorname{Re} Z(b_{11}) = -\frac{1}{2} Z(\tilde{h}_{12}) = \frac{1}{2}(\xi_2^{(2)} - t_1), \tag{4.2.46}$$

$$\operatorname{Re} Z(b_{21}) = -\frac{1}{2} Z(\tilde{h}_{23} + h_{12} - h_{23}) = \frac{1}{2}(\lambda_3 - \xi_2^{(2)} + \lambda_2 - t_2), \tag{4.2.47}$$

$$\operatorname{Re} Z(b_{22}) = -\frac{1}{2} Z(\tilde{h}_{23}) = \frac{1}{2}(\lambda_3 - \xi_2^{(2)}). \tag{4.2.48}$$

Then we can make an explicit prediction for the asymptotics of the norms of factorization coordinates:

Proposition 4.21. For u sufficiently close to the caterpillar line and A near diagonal, if Conjecture 4.10 holds, the leading $\varepsilon \to 0^+$ asymptotics of the norms of the factorization coordinates of S_+ are

$$\varepsilon \log \delta_i = \frac{1}{2} t_i, \tag{4.2.49}$$

$$\varepsilon \log |\alpha| \sim \frac{1}{2}(\lambda_3 - \xi_2^{(2)} + \lambda_2 - t_2), \quad \varepsilon \log |\beta| \sim \frac{1}{2}(\xi_2^{(2)} - t_1), \quad \varepsilon \log |\gamma| \sim \frac{1}{2}(\lambda_3 - \xi_2^{(2)}) \,. \tag{4.2.50}$$

To compare this with Conjecture 1.2, we note that the minor coordinates are

$$\Delta_1^{(2)} = \beta \delta_1, \quad \Delta_1^{(3)} = \beta \gamma \delta_1, \quad \Delta_2^{(3)} = \beta \alpha \delta_1 \delta_2 \,. \tag{4.2.51}$$

This leads to:

Corollary 4.22. For u sufficiently close to the caterpillar line and A near diagonal, if Conjecture 4.10 holds, the leading $\varepsilon \to 0^+$ asymptotics of the norms of the minor coordinates of S_+ are

$$\varepsilon \log \left|\Delta_1^{(2)}\right| \sim \frac{1}{2} \xi_2^{(2)}, \quad \varepsilon \log \left|\Delta_1^{(3)}\right| \sim \frac{1}{2} \lambda_3, \quad \varepsilon \log \left|\Delta_2^{(3)}\right| \sim \frac{1}{2}(\lambda_2 + \lambda_3) \tag{4.2.52}$$

This matches with Conjecture 1.2, if we take $L_j^{(i)} = C_j^{(i)}$.

Dual factorization coordinates

Another system of factorization coordinates $(\delta_1, \delta_2, \delta_3, \alpha', \beta', \gamma')$ on $U' \subset B^+$, associated to the reduced word $w_0 = (12)(23)(12)$, is defined by

$$M = \begin{pmatrix} \delta_1 & 0 & 0 \\ 0 & \delta_2 & 0 \\ 0 & 0 & \delta_3 \end{pmatrix} \begin{pmatrix} 1 & \alpha' & 0 \\ 0 & 1 & 0 \\ 0 & 0 & 1 \end{pmatrix} \begin{pmatrix} 1 & 0 & 0 \\ 0 & 1 & \beta' \\ 0 & 0 & 1 \end{pmatrix} \begin{pmatrix} 1 & \gamma' & 0 \\ 0 & 1 & 0 \\ 0 & 0 & 1 \end{pmatrix} = \begin{pmatrix} \delta_1 & \delta_1(\alpha' + \gamma') & \delta_1 \alpha' \beta' \\ 0 & \delta_2 & \delta_2 \beta' \\ 0 & 0 & \delta_3 \end{pmatrix}. \tag{4.2.53}$$

This system also fits into our story, as follows. So far we have mainly considered the regime where $u_3 - u_2 \gg u_2 - u_1$. We could also consider the opposite situation, where $u_2 - u_1 \gg u_3 - u_2$ (still with $u_1 < u_2 < u_3$ and $t_1 < t_2 < t_3$.) In that case, all of our discussion goes through, with various sign flips and index reversals. In particular, we obtain spectral coordinate expansions indexed by the paths in Figure 13:

Proposition 4.23. For u sufficiently close to the dual caterpillar line, the dual factorization coordinates of S_+ are

$$\delta_i = X^0_{c_i}, \quad (\alpha', \beta', \gamma') = (X^0_{b'_{21}} + \cdots, X^0_{b'_{11}} + \cdots, X^0_{b'_{22}} + \cdots) \,. \tag{4.2.54}$$

where in each expression $\cdots$ means a sum of terms X^0_γ, with $\operatorname{Re} Z(\gamma)$ smaller than that of the leading term.

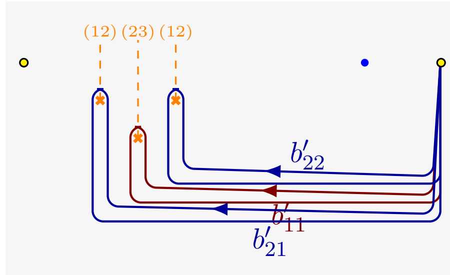

Figure 13: The analogues of the paths in Figure 12, arising near the dual caterpillar line, where $u_2 - u_1$ is much larger than $u_3 - u_2$.

4.2.4 The case of general n

Finally we discuss general n, with $u_1 < \cdots < u_n$ and $t_1 < \cdots < t_n$, and A near-diagonal. The spectral curve $\Gamma(u, A)$ has genus $g = \frac{(n-2)(n-1)}{2}$ and $2n$ punctures; the lattice $H(u, A, \vartheta)$ has rank $n^2 + n$.

We will not attempt a complete description of $\mathcal{W}(u, A, \vartheta = 0)$, but note some general features. The structure in the upper half-plane is the mirror-reflection of the structure in the lower half-plane, so we only describe the lower half-plane. The network is divided into $n - 1$ domains $A^{(k)}$, corresponding to the annuli in Figure 3:

- The domain $A^{(n-1)}$, bounded by $V^{(n)}$ and $V^{(n-1)}$, contains $n - 1$ branch cuts and emits $n - 1$ walls to the south, of types $i < n$.
- The domain $A^{(n-2)}$, bounded by $V^{(n-1)}$ and $V^{(n-2)}$, contains $n - 2$ branch cuts which emit walls of types $i < (n - 1)$. The walls of type $i < n$ emerging from $A^{(n-1)}$ also pass through $A^{(n-2)}$, and their intersections with walls of type $i' < i$ generate additional walls of type $i' < n$. Altogether, then, $A^{(n-2)}$ emits walls of type $i < (n - 1)$ and $i < n$ to the south.
- Continuing inductively, the domain $A^{(j-1)}$ emits walls of type $i < k$, for each (i, k) such that $i < k$ and $k \geq j$, to the south.

The spectral network $\mathcal{W}(u, A, \vartheta = 0)$ contains finite webs. There are short saddle connections with charges h_{ij} for all $i < j$. There are also saddle connections with charge $\tilde{h}_{ij}$ for $i = j - 1$, and five-string trees with charge $\tilde{h}_{ij}$ for $i < j - 1$.

By an equivalence we can adjust the spectral network in the lower half-plane to a configuration where the branch points are arranged in a triangle. (This equivalence involves moving each group of branch points to a row of the triangle, one row at a time, starting from the top.) The j-th row from the bottom consists of j branch points, each emitting a branch cut of type $(j, j + 1)$ due north, and a wall of type $j < j + 1$ due south (as well as two other walls). When $n > 3$ there are some branch points which are due north of others, so that the cuts overlap, and similarly the walls overlap; however, this overlap is harmless, since any two overlapping cuts always involve disjoint pairs ij, kl. For convenience, we sometimes displace the branch points slightly horizontally to eliminate these overlaps. See Figure 14 for the $n = 5$ case.

We number the branch points starting from the bottom: the bottom row is b_{11}, the second-bottom row b_{21}, b_{22}, and so on until the top row $b_{n-1,1}, \ldots, b_{n-1,n-1}$. Then for each branch point b_{ij} we define a corresponding path b_{ij}, which begins from ∞^+_{i+1}, follows the boundary arc clockwise on sheet $i + 1$ to the point directly south of b_{ij}, then follows the wall up to b_{ij}, then follows the wall back down to the boundary arc on sheet i, and returns along the boundary arc to ∞^+_i. In the case $n = 3$ these paths are homologous to the ones shown in Figure 12.

We expect that the asymptotics of the factorization coordinates are determined by the periods $Z(c_i) = \frac{t_i}{2}$ and $Z(b_{ij})$:

Conjecture 4.24. The factorization coordinates of S_+ are of the form

$$\alpha_{ij} = X_{b_{ij}} + \cdots \tag{4.2.55}$$

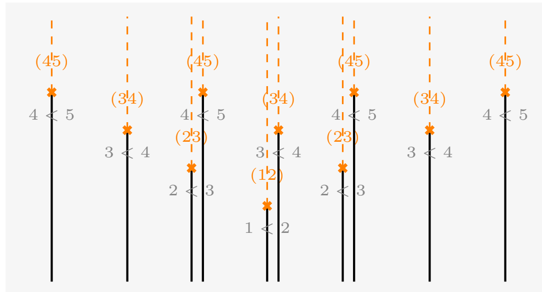

Figure 14: The configuration of branch points in the bottom half-plane, after applying an equivalence as described in the text, in the case $n = 5$. We also show the walls emanating south from each branch point. The full spectral network contains various additional walls, not shown here.

where $\cdots$ denotes a sum of terms X_γ with $\operatorname{Re} Z(\gamma) < \operatorname{Re} Z(b_{ij})$.

Conjecture 4.24 is a purely geometric/combinatorial statement about the shape of the spectral network. Note that if the lines shown in Figure 14 were the only lines of the spectral network, then we would have simply $\alpha_{ij} = X_{b_{ij}}$; thus Conjecture 4.24 amounts to the claim that all the other lines of the spectral network contribute to α_{ij} only through correction terms with smaller $\operatorname{Re} Z$. We saw explicitly above that Conjecture 4.24 is true in the $n = 2$ and $n = 3$ cases.

Now we want to work out the concrete asymptotics of the factorization coordinates; for this we need to know $\operatorname{Re} Z_{b_{ij}}$. By following the curves through the isotopy, we get

$$b_{ij} = a_{i+1,j} - a_{i,j} \tag{4.2.56}$$

where we extend the definition of $a_{i,j}$ to the case $i = j$ by setting $a_{j,j} = c_j$. Then using the real symmetry we can show that

$$\operatorname{Re} Z(b_{ij}) = -\frac{1}{2}\left(-t_{i+1} + t_i + \sum_{k=1}^{j}(\xi_k^{(i+1)} - \xi_k^{(i)}) + \sum_{k=1}^{j-1}(\xi_k^{(i-1)} - \xi_k^{(i)})\right) . \tag{4.2.57}$$

Finally, translating from factorization coordinates to minor coordinates, we obtain the desired asymptotics:

Theorem 4.25. For u near the caterpillar line and A near diagonal, Conjecture 1.2 follows from Conjecture 4.10 and Conjecture 4.24, with $L_j^{(i)} = C_j^{(i)}$ as defined in (3.4.1).

4.3 Spectral coordinates for nondegenerate networks

In this section we digress a bit, to explain how the usual connection between spectral networks, cluster algebras, and Donaldson-Thomas invariants (finite web counts) play out in this example.

4.3.1 The case $n = 2$

The spectral network $\mathcal{W}(u, A, \vartheta = 0)$ which we have discussed up to now is degenerate. These degenerate networks are often useful — in particular, here they preserve the natural symmetries of the problem at $\varepsilon \in \mathbb{R}$ — but they have the drawback that they obscure the connection to the cluster structure on moduli spaces of complex flat connections discussed in [28]. Thus in this section, we make a perturbation to reach the nondegenerate case, by varying the phase ϑ.

In the $n = 2$ example, the spectral networks for all $\vartheta \in (0, \pi)$ are isotopic, as are the spectral networks for $\vartheta \in (-\pi, 0)$. See Figure 15 for examples. At $\vartheta = 0$ we meet the degenerate network from Figure 5; this degeneration separates $\mathcal{W}(\vartheta_-)$ from $\mathcal{W}(\vartheta_+)$, so they are not necessarily isotopic, and indeed they are not isotopic.

Now we describe the spectral coordinate functions at $\vartheta_\pm$, following the recipe of [22, 31]. For convenience, we introduce a branch cut on the positive z-axis. Then we consider the 2-dimensional vector space Sol of solutions of

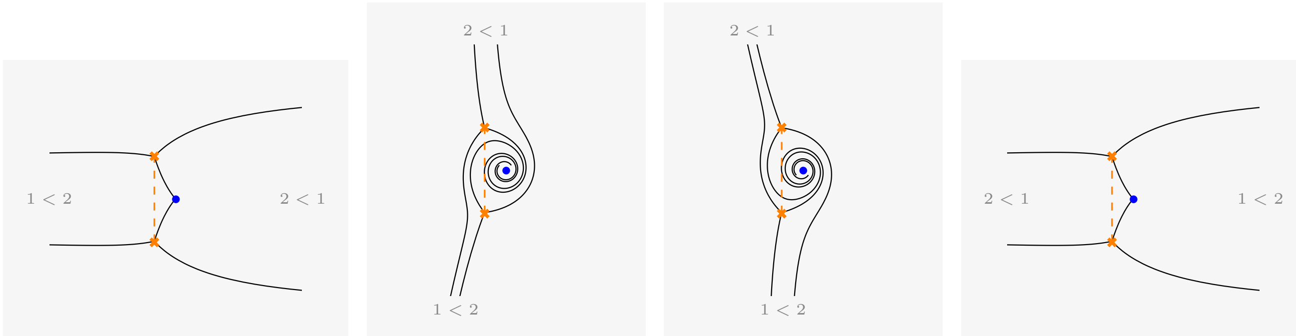

Figure 15: Spectral networks $\mathcal{W}(u, A, \vartheta)$ in the $n = 2$ case, with $\vartheta = -\frac{\pi}{2}, -\frac{1}{10}, +\frac{1}{10}, +\frac{\pi}{2}$. (The case $\vartheta = 0$ was shown in Figure 5 above.)

(1.1.1) in the cut plane. There is an endomorphism $M : \mathrm{Sol} \to \mathrm{Sol}$ given by counterclockwise monodromy around $z = 0$. In Sol we consider 5 distinguished vectors:

- Ψ_i^+ is the continuation of the i-th column of F_+ from the positive z-axis below the cut,
- Ψ_i^- is the continuation of the i-th column of $F_- \exp(-\frac{1}{2}[A])$ from the negative z-axis,
- Ψ^0 is an eigenvector of monodromy around $z = 0$, determined up to overall scale by the condition that $\Psi^0(z)$ decays as $z \to 0$.

Note that Ψ_1^- is a scalar multiple of Ψ_1^+ since both obey the same exponential decay condition in the half-plane containing the ray labeled $1 < 2$, and similarly, Ψ_2^- is a scalar multiple of $M\Psi_2^+$ since both obey the same exponential decay condition in the half-plane containing the ray labeled $2 < 1$. The definition of the Stokes matrix S_+ (Definition 2.2) gives

$$\Psi_2^+ = (S_+)_{12}\Psi_1^- + (S_+)_{22}\Psi_2^- \, . \tag{4.3.1}$$

Thus, if we let $(\cdot \wedge \cdot)$ denote any nondegenerate skew pairing on Sol,[3] we have

$$(S_+)_{12} = \frac{(\Psi_2^+ \wedge \Psi_2^-)}{(\Psi_1^- \wedge \Psi_2^-)} \, . \tag{4.3.2}$$

Now consider $\vartheta = \vartheta_- \in (-\pi, 0)$. The rules of [31] give formulas for the spectral coordinates in this case:

$$X_{c_1}^{\vartheta_-} = \frac{\Psi_1^+}{\Psi_1^-}, \quad X_{d_2}^{\vartheta_-} = \frac{\Psi_2^-}{M\Psi_2^+}, \quad X_{c_2}^{\vartheta_-} = \frac{(\Psi_2^+ \wedge \Psi_1^+)}{(\Psi_2^- \wedge \Psi_1^+)}, \quad X_{d_1}^{\vartheta_-} = \frac{(\Psi_1^- \wedge \Psi_2^-)}{(M\Psi_1^+ \wedge \Psi_2^-)} \, , \tag{4.3.3}$$

$$X_{a_{21}}^{\vartheta_-} = \frac{(\Psi_2^+ \wedge \Psi^0)}{(\Psi_1^- \wedge \Psi^0)}, \quad X_{a_{12}}^{\vartheta_-} = \frac{(\Psi_1^- \wedge \Psi^0)}{(M\Psi_2^+, \Psi^0)} \, . \tag{4.3.4}$$

Combining these formulas with (4.3.2) we find that the Stokes matrix entry is a sum of two spectral coordinates:

$$(S_+)_{12} = X_{a_{21}}^{\vartheta_-}(1 - X_{h_{12}}^{\vartheta_-}) \, . \tag{4.3.5}$$

We can make similar computations for $\vartheta = \vartheta_+ \in (0, \pi)$. There is one important subtlety: at $\vartheta = 0$ the behavior of the eigenvectors of monodromy as $z \to 0$ reverses. We use Ψ^0 to indicate the eigenvector which decays as $z \to 0$, irrespective of the value of ϑ; in consequence, Ψ^0 jumps discontinuously as ϑ crosses 0. At any rate, applying again the rules of [31] leads to

$$X_{c_1}^{\vartheta_+} = \frac{\Psi_1^+}{\Psi_1^-}, \quad X_{d_2}^{\vartheta_+} = \frac{\Psi_2^-}{M\Psi_2^+}, \quad X_{c_2}^{\vartheta_+} = \frac{(\Psi_2^+ \wedge \Psi_1^+)}{(\Psi_2^- \wedge \Psi_1^+)}, \quad X_{d_1}^{\vartheta_+} = \frac{(\Psi_1^- \wedge \Psi_2^-)}{(M\Psi_1^+ \wedge \Psi_2^-)} \, , \tag{4.3.6}$$

[3] For instance, we could fix some z and then take $(\psi \wedge \psi')$ to be the determinant of a matrix with columns $\psi(z)$, $\psi'(z)$. Changing the choice of z then changes $(\cdot \wedge \cdot)$ only by an overall factor, thanks to (1.1.1).

$$X_{a_{21}}^{\vartheta_+} = \frac{(\Psi_2^+ \wedge \Psi_1^+)(\Psi^0 \wedge \Psi_2^-)}{(\Psi^0 \wedge \Psi_1^+)(\Psi_1^- \wedge \Psi_2^-)}, \quad X_{a_{12}}^{\vartheta_+} = \frac{(\Psi_1^- \wedge \Psi_2^-)(\Psi^0 \wedge \Psi_1^+)}{(M\Psi^0 \wedge \Psi_2^-)(\Psi_2^+ \wedge \Psi_1^+)} \tag{4.3.7}$$

from which it follows that

$$(S_+)_{12} = X_{a_{21}}^{\vartheta_+}(1 - X_{\tilde{h}_{12}}^{\vartheta_+}) \,. \tag{4.3.8}$$

Now we have computed all of the $X_\gamma^{\vartheta_\pm}$, and in particular we can compare $X_\gamma^{\vartheta_+}$ to $X_\gamma^{\vartheta_-}$. When $\gamma = c_i$ or $\gamma = d_i$ we find simply that $X_\gamma^{\vartheta_+} = X_\gamma^{\vartheta_-}$. For $\gamma = a_{12}$ or $\gamma = a_{21}$ the relation is more nontrivial; for instance, comparing (4.3.8) to (4.3.5) we get[4]

$$X_{a_{21}}^{\vartheta_-}(1 - X_{h_{12}}) = X_{a_{21}}^{\vartheta_+}(1 - X_{\tilde{h}_{12}}) \,. \tag{4.3.9}$$

Altogether, the transformation relating $X_\gamma^{\vartheta_+}$ to $X_\gamma^{\vartheta_-}$ can be summarized as

$$X_\gamma^{\vartheta_+} = X_\gamma^{\vartheta_-} \cdot \left[(1 - X_{h_{12}})^{\langle \gamma, h_{12} \rangle} (1 - X_{\tilde{h}_{12}})^{\langle \gamma, \tilde{h}_{12} \rangle} \right] \tag{4.3.10}$$

As expected, this matches with the transformation law (C.0.13), in the case of two saddle connections with charges h_{12} and $\tilde{h}_{12}$.

4.3.2 Comparing to the Goncharov-Shen cluster structure on G^*

We are ready to compare the spectral coordinates to the cluster coordinates in [27]. Let $D(\vartheta)$ denote a punctured disc with two marked points on the boundary, at arguments ϑ and $\vartheta + \pi$. (These marked points will correspond to the anti-Stokes directions.) The marked points divide the boundary into two arcs.

Definition 4.26. A *framed* PGL_2*-local system with pinning* over $D(\vartheta)$ is:

1. A PGL_2-local system L over $D(\vartheta)$,
2. A flag in L (section of L/B) around the puncture and along each boundary arc,
3. A decoration of the flag (lift from L/B to L/U) along each boundary arc.

Let $\mathfrak{X}(\mathrm{PGL}_2, D(\vartheta))$ be the moduli space parameterizing framed PGL_2-local systems with pinning over $D(\vartheta)$.

Assume that $\vartheta \notin \{0, \pi\}$. Consider the flat GL_2-connection (1.1.1) determined by the data (u, A, ε), with $\arg \varepsilon = \vartheta$, and $u_2 > u_1$ as usual. The covariantly constant sections make up a GL_2-local system over $D(\vartheta)$, and reducing by the center gives a PGL_2-local system $L(u, A, \varepsilon)$. As $z \to \infty$ in a non-anti-Stokes direction, the line of exponentially decaying sections gives a flag in $L(u, A, \varepsilon)$ on each boundary arc.[5] Choosing moreover the particular exponentially decaying sections $\Psi^\pm$ determines a decoration of the flag. Finally, choosing the monodromy eigenline which decays as $z \to 0$ gives a flag in $L(u, A, \varepsilon)$ around the puncture. (This is what requires us to have $\vartheta \notin \{0, \pi\}$; under this condition there is one decaying eigenline and one growing one.) Thus we obtain a point of $\mathfrak{X}(\mathrm{PGL}_2, D(\vartheta))$.[6]

Now we can discuss cluster coordinates. Each spectral network $\mathcal{W}(u, A, \vartheta)$ with $\vartheta \notin \{0, \pi\}$ induces an ideal triangulation of $D(\vartheta)$, as follows. Each of the three walls emanating from each branch point ends up either at a Stokes ray or at $z = 0$; these three ends are the vertices of a triangle containing the branch point. See Figure 16 for the picture in one triangle. Now, for a given triangle and a choice of an edge, we consider the arc γ on Γ shown in

[4]Here we simplify the notation by dropping the superscript on $X_{h_{12}}$ and $X_{\tilde{h}_{12}}$, since those have $X_\gamma^{\vartheta_+} = X_\gamma^{\vartheta_-}$.

[5]This structure is sometimes called the "Stokes filtration", e.g. in the terminology of [13].

[6]The reader might be puzzled about the matching of dimensions: we might have expected that, for each fixed choice of u, the map from the space of matrices $A \in \mathfrak{pgl}_2 = \mathfrak{sl}_2$ to the cluster variety should be a local diffeomorphism. This is not quite true, since $\mathfrak{sl}_2$ has dimension 3, while the cluster variety has dimension 4. The resolution is that the points of the cluster variety which we obtain are special: they obey the "outer monodromy condition" of [27], explicitly $x_1^2 x_2 x_3 x_4^2 = 1$, which reduces the dimension by 1. This condition is an expression of our choice of the relative normalizations of $\Psi^\pm$ so that the Stokes matrices $S_\pm$ have the same diagonal entries. Explicitly, at $\vartheta = \vartheta_-$ it follows from the relation $x_1^2 x_2 x_3 x_4^2 = X_{-c_1+c_2+d_1-d_2}$ and the normalization conditions $X_{c_i} = X_{d_i}$, and similarly at $\vartheta = \vartheta_+$.

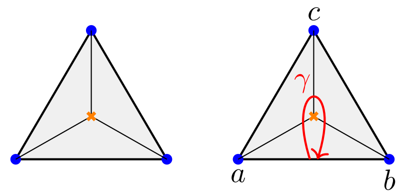

Figure 16: Left: the triangle containing one branch point of Γ. Right: an arc γ on Γ, determined by the choice of a triangle and an edge thereon. Recall that each vertex has a corresponding distinguished sheet of Γ; the arc γ begins on the sheet corresponding to vertex a, and ends on the sheet corresponding to vertex b.

Figure 16. The corresponding spectral coordinate is

$$X_\gamma^\vartheta = \frac{(\psi_a, \psi_c)}{(\psi_b, \psi_c)} \tag{4.3.11}$$

where ψ_a is a covariantly constant section over the triangle, associated with vertex a. (If a is a Stokes ray, then ψ_a is the corresponding normalized decaying solution at that ray; if a is the puncture, then ψ_a is the monodromy eigensection which decays going into the puncture.) On the other hand, [27] defines a coordinate system on $\mathfrak{X}(\mathrm{PGL}_2, D(\vartheta))$, with cluster coordinates $x_1, \dots, x_4$ associated to the four edges. For an edge on the boundary, the cluster coordinate is $X^\vartheta_{-\gamma}$; for an edge in the interior, the cluster coordinate is the product of $X^\vartheta_{-\gamma}$ over the two faces abutting this edge.

Now we apply this to the spectral networks in Figure 15. The corresponding triangulations of $D(\vartheta)$ are indicated in Figure 17 below. At $\vartheta = \vartheta_- \in (-\pi, 0)$ we obtain the following formula for the cluster coordinates x_i:

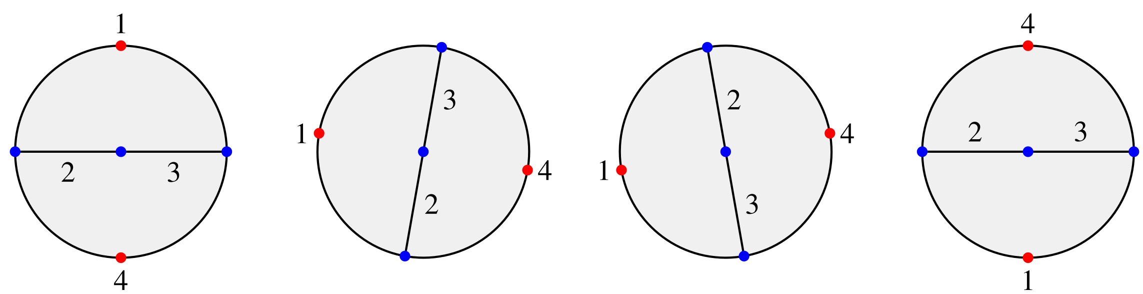

Figure 17: Triangulated discs $D(\vartheta)$ with $\vartheta = -\frac{\pi}{2}, -\frac{1}{10}, +\frac{1}{10}, +\frac{\pi}{2}$. The blue points are the vertices of the triangulation; the red points on the boundary are the marked points of $D(\vartheta)$ (corresponding to anti-Stokes lines). Each edge of the triangulation is labeled with an index $i = 1, \dots, 4$; each corresponds to a cluster coordinate x_i. Note that the labeling of the internal edges jumps as ϑ crosses 0. These four triangulated discs are induced by the four spectral networks in Figure 15.

$$x_1 = X^{\vartheta_-}_{a_{12}-d_2}, \quad x_2 = X^{\vartheta_-}_{h_{12}}, \quad x_3 = X^{\vartheta_-}_{\tilde{h}_{12}}, \quad x_4 = -X^{\vartheta_-}_{a_{21}-c_1}\,. \tag{4.3.12}$$

In short, the cluster coordinates are equal to the spectral coordinates.

At $\vartheta = \vartheta_+ \in (0, \pi)$, we get similar formulas for the cluster coordinates x'_i,

$$x'_1 = -X^{\vartheta_+}_{-a_{21}+c_2}, \quad x'_2 = X^{\vartheta_+}_{-h_{12}}, \quad x'_3 = X^{\vartheta_+}_{-\tilde{h}_{12}}, \quad x'_4 = X^{\vartheta_+}_{-a_{12}+d_1}\,, \tag{4.3.13}$$

so again the cluster coordinates are equal to the spectral coordinates.

Finally, the spectral transformation law (4.3.10) translates to the relations

$$x'_1 = x_1(1-x_3)(1-x_2^{-1})^{-1}, \quad x'_2 = x_2^{-1}, \quad x'_3 = x_3^{-1}, \quad x'_4 = x_4(1-x_2)(1-x_3^{-1})^{-1}\,. \tag{4.3.14}$$

The relations (4.3.14) can be described as the action of two cluster $\mathfrak{X}$-mutations, at the variables x_2 and x_3.

4.3.3 The case $n = 3$

In the $n = 2$ case above, we connected the spectral coordinates with the cluster structure of [27] on G^* by considering spectral networks for phases other than $\vartheta = 0$.

In the $n = 3$ case, we can try to do the same thing, but we will meet a much more intricate story, because the networks for different $\vartheta \in (-\pi, 0)$ are not all isotopic: there are closed cycles γ with $Z(\gamma) \notin \mathbb{R}$, and these cycles can be the charges of finite webs. The network $\mathcal{W}(u, A, \vartheta)$ jumps when ϑ crosses the phase of any finite web.

We can still make some predictions. For u near the caterpillar line, there may be countably many distinct finite webs whose phases approach 0 from either direction, so that $\mathcal{W}(u, A, \vartheta)$ jumps countably many times as $\vartheta \to 0^\pm$. Nevertheless, we expect that each spectral coordinate X_γ^ϑ has a limit as $\vartheta \to 0^\pm$; we call these limits $X_\gamma^{0^\pm}$. These two limits should differ by the usual transformation law (C.0.13). That transformation law depends on some BPS invariants $\Omega(\gamma)$; in principle they can be computed from the spectral network following the algorithm of [21], but here we guess them instead using the physical picture sketched in Subsection 4.4 below. That leads to the following prediction:

$$X_\gamma^{0_+} = X_\gamma^{0_-} \cdot \left(\prod_h (1 - X_h)^{\langle \gamma, h \rangle} \right) \cdot (1 + X_v)^{-2\langle \gamma, v \rangle} \tag{4.3.15}$$

Here $v = V_2^{(2)} - V_1^{(2)}$, and h runs over 8 values, the differences $V_i^{(2)} - V_j^{(3)}$, $V_i^{(1)} - V_j^{(2)}$ for $i \geq j$ and $V_j^{(3)} - V_i^{(2)}$, $V_j^{(2)} - V_i^{(1)}$ for $i < j$. This is the $n = 3$ analogue of the formula (4.3.10) which holds in the $n = 2$ case.

4.4 Relation to quantum field theory

The story we have been discussing is related to an $\mathcal{N} = 2$ supersymmetric quantum field theory in four dimensions, as recently discussed in [23].

On the one hand, we may think of it as a class S theory of type $\mathfrak{gl}_n$ built using a twice-punctured sphere, with a regular singularity at $z = 0$ and an irregular one at $z = \infty$. This theory has a $\mathrm{U}(n)$ flavor symmetry associated to the singularity at $z = 0$. In the pure class S theory there is also a $\mathrm{U}(1)^{n-1}$ flavor symmetry at the irregular puncture; the precise theory we want to consider is obtained by gauging that symmetry.

We can also describe the same theory concretely by a Lagrangian, determined by the quiver diagram shown in Figure 18.

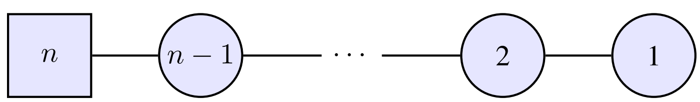

Figure 18: A linear quiver, describing the field content of a Lagrangian $\mathcal{N} = 2$ supersymmetric quantum field theory in four dimensions. The circular (gauge) nodes correspond to $\mathrm{U}(k)$ gauge groups with $1 \leq k \leq n - 1$. The leftmost node corresponds to a $\mathrm{U}(n)$ flavor symmetry. Each link corresponds to a bifundamental hypermultiplet.

The $\mathrm{SU}(n)$ parts of the gauge symmetry are conformal, but the $\mathrm{U}(1)$ parts are not conformal or asymptotically free. Nevertheless, we can consider this theory as an effective theory. For $n = 2$, it is a $\mathrm{U}(1)$ gauge theory coupled to 2 charged hypermultiplets; the fact that the gauge group is abelian is reflected in the fact that the Stokes matrices can be computed exactly in this case, as we already noted above. For $n > 2$, on the other hand, it is a nonabelian gauge theory.

The decomposition of the spectral curve shown in Figure 3 reflects the quiver description of the theory: the loop $V^{(k)}$ corresponds to the quiver node labeled k, and the annulus between $V^{(k)}$ and $V^{(k+1)}$ corresponds to a link in the quiver. Going to the caterpillar line $u_i - u_{i-1} \ll u_{i+1} - u_i$ corresponds to the weak-coupling limit in which the gauge couplings are sent to zero.

From this description of the theory we see that at weak coupling the BPS spectrum should include $k(k-1)$ hypermultiplets in the bifundamental of $\mathrm{U}(k) \times \mathrm{U}(k-1)$, for $k = 2, \ldots, n$, and W-bosons in the adjoint of $\mathfrak{su}(k)$ for $k = 2, \ldots, n-1$. This spectrum should then appear in the Stokes behavior of the $\varepsilon \to 0$ asymptotics at weak coupling. Concretely, this is reflected in the arguments of the gamma functions appearing in Appendix B: indeed the $\lambda_l^{(k)} - \lambda_i^{(k)}$ which appear with multiplicity -2 are the masses of the W-bosons, while the $\lambda_l^{(k+1)} - \lambda_i^{(k)}$ and $\lambda_l^{(k-1)} - \lambda_i^{(k)}$ which appear with multiplicity 1 are the masses of the hypermultiplets.

We saw part of the BPS spectrum explicitly above for $n = 2$ and $n = 3$. For $n = 2$ we just expect the bifundamental of $\mathrm{U}(2) \times \mathrm{U}(1)$, and indeed in Figure 5 we found 2 saddle connections with charges h_{12} and $\tilde{h}_{12}$. For $n = 3$ we expect bifundamentals of $\mathrm{U}(3) \times \mathrm{U}(2)$ and $\mathrm{U}(2) \times \mathrm{U}(1)$. Looking at Figure 9, we see that the saddle connections with charges h_{12} and $\tilde{h}_{12}$ give the expected bifundamental of $\mathrm{U}(2) \times \mathrm{U}(1)$, while the webs with charges $h_{13}, h_{23}, \tilde{h}_{13}, \tilde{h}_{23}$ give 4 of the 6 expected in the bifundamental of $\mathrm{U}(3) \times \mathrm{U}(2)$. The remaining two charges in the bifundamental are $h_{13} + \tilde{h}_{13} + h_{23}$ and $\tilde{h}_{13} + h_{23} + \tilde{h}_{23}$, which do not arise as indecomposable webs in Figure 9; rather they should be understood as composites.

A The De Concini-Procesi space

Recall that we denote by $\mathfrak{h}_{\mathrm{reg}}(\mathbb{R})$ the space of $n \times n$ diagonal matrices with distinct real eigenvalues, and in this paper we consider the meromorphic linear system

$$\frac{dF}{dz} = \left(\mathrm{i}u - \frac{1}{2\pi \mathrm{i}} \frac{A}{z}\right) \cdot F,$$

with $u \in \mathfrak{h}_{\mathrm{reg}}(\mathbb{R})$ and $A \in \mathrm{Herm}(n)$. By definition, the Stokes matrices $S_{\pm}(u, A)$ are invariant under the translation action of $\mathbb{R}$ on $\mathfrak{h}_{\mathrm{reg}}(\mathbb{R})$ given by $u \mapsto u + c \cdot \mathrm{Id}_n (c \in \mathbb{R})$. Then, for any fixed A, $S_{\pm}(u, A)$ are parameterized by $\mathfrak{t}_{\mathrm{reg}}(\mathbb{R}) \cong \mathfrak{h}_{\mathrm{reg}}(\mathbb{R})/\mathbb{R}$. Here, $\mathfrak{t}_{\mathrm{reg}}(\mathbb{R})$ is the space of $n \times n$ diagonal matrices $u = \mathrm{diag}(u_1, ..., u_n)$ with distinct real eigenvalues and such that $\sum_{k=1}^n u_k = 0$.

Before we introduce the De Concini-Procesi space $\widetilde{\mathfrak{t}_{\mathrm{reg}}(\mathbb{R})}$ of $\mathfrak{t}_{\mathrm{reg}}(\mathbb{R})$, we first work over the field of complex numbers and introduce $\widetilde{\mathfrak{t}_{\mathrm{reg}}(\mathbb{C})}$. Let $\mathfrak{g}$ be the simple Lie algebra $\mathfrak{sl}_n$, $\mathfrak{t} \subset \mathfrak{g}$ the Cartan subalgebra, $\Pi \subset \mathfrak{t}^*$ the set of roots, Π_+ the set of positive roots and $\{\alpha_i : i \in I\}$ the set of simple roots where I is the index set of vertices of the Dynkin diagram of $\mathfrak{g}$.

Denote by $\mathcal{G}$ the *minimal building set* associated with the set of roots. To define $\mathcal{G}$, let $\mathcal{G}'$ denote the set of all non-zero subspaces of $\mathfrak{t}^*$ which are spanned by a subset of Π. Let $V \in \mathcal{G}'$. We say that $V = V_1 \oplus \cdots \oplus V_k$ is a *decomposition* of V if $V_1, \ldots, V_k \in \mathcal{G}'$, and if whenever $\alpha \in \Pi$ and $\alpha \in V$, then $\alpha \in V_i$ for some i. From Section 2.1 of [16], every element of $\mathcal{G}'$ admits a unique decomposition. Then we define $\mathcal{G}$ to be the set of indecomposable elements of $\mathcal{G}'$. This set can be described as follows. There is an action of the Weyl group W on $\mathfrak{t}$. This action preserves Π. Thus, we get actions of W on $\mathcal{G}$ and $\mathcal{G}'$. If $J \subseteq I$ is a non-empty, connected subset of I, we can form $V_J = \mathrm{span}(\alpha_j : j \in J)$. Then $V_J \in \mathcal{G}$. Every $V \in \mathcal{G}$ is of the form $w(V_J)$ for some $w \in W$ and J as above.

Note that for any $V \in \mathcal{G}$, we have a map $\mathfrak{t}_{\mathrm{reg}} \to \mathbb{P}(\mathfrak{g}/V^{\perp})$.

Definition A.1. The De Concini-Procesi space $\widetilde{\mathfrak{t}_{\mathrm{reg}}} \subset \mathfrak{t} \times \prod_{V \in \mathcal{G}} \mathbb{P}(\mathfrak{t}/V^{\perp})$ is the closure of the image of the map $\mathfrak{t}_{\mathrm{reg}} \to \mathfrak{t} \times \prod_{V \in \mathcal{G}} \mathbb{P}(\mathfrak{t}/V^{\perp})$.

Let us consider its projective analog. Note that the multiplicative group $\mathbb{C}^{\times}$ acts on $\mathfrak{t}_{\mathrm{reg}}$, and the regular morphism $\mathfrak{t}_{\mathrm{reg}} \hookrightarrow \prod_{V \in \mathcal{G}} \mathbb{P}(\mathfrak{t}/V^{\perp})$ is constant on the $\mathbb{C}^{\times}$ orbits. Thus, we get a map $\mathfrak{t}_{\mathrm{reg}}/\mathbb{C}^{\times} \to \prod_{V \in \mathcal{G}} \mathbb{P}(\mathfrak{t}/V^{\perp})$.

Definition A.2. The De Concini-Procesi space $\overline{\mathfrak{t}_{\mathrm{reg}}} \subset \prod_{V \in \mathcal{G}} \mathbb{P}(\mathfrak{t}/V^{\perp})$ is the closure of the image of the map $\mathfrak{t}_{\mathrm{reg}}/\mathbb{C}^{\times} \to \prod_{V \in \mathcal{G}} \mathbb{P}(\mathfrak{t}/V^{\perp})$.

Thus a point of $\overline{\mathfrak{t}_{\mathrm{reg}}}$ consists of a collection $(L_V)_{V \in \mathcal{G}}$ where $L_V \in \mathfrak{t}/V^{\perp}$. We will think of L_V as a subspace of $\mathfrak{t}$ containing $V^{\perp}$ as a hyperplane. Note that if $\chi \in \mathfrak{t}_{\mathrm{reg}}$, then $\chi \notin V^{\perp}$ for all $V \in \mathcal{G}$ and the image of χ in $\overline{\mathfrak{t}_{\mathrm{reg}}}$ is the collection $L_V = V^{\perp} + \mathbb{C}\chi$.

By [16, Theorem 4.1], $\widetilde{\mathfrak{t}_{\mathrm{reg}}}$ is the total space of a tautological line bundle on $\overline{\mathfrak{t}_{\mathrm{reg}}}$. Furthermore, following [16, Theorem 3.1 and 3.2], the boundary D of $\mathfrak{t}_{\mathrm{reg}}$ in $\widetilde{\mathfrak{t}_{\mathrm{reg}}}$ is a divisor with normal crossings, and is the union of smooth irreducible divisors $D_{\omega(V_J)}$ indexed by the elements $\omega(V_J)$ in $\mathcal{G}$. Then, by [16, Theorem 4.1], $\overline{\mathfrak{t}_{\mathrm{reg}}}$ is isomorphic to the boundary divisor $D_{\omega(V_I)}$.

Since the root system Π is defined over $\mathbb{R}$, the variety $\widetilde{\mathfrak{t}_{\mathrm{reg}}}$ is defined over $\mathbb{R}$ and we get the De Concini-Procesi space $\widetilde{\mathfrak{t}_{\mathrm{reg}}(\mathbb{R})}$ of $\mathfrak{t}_{\mathrm{reg}}(\mathbb{R})$ by taking the set of real points.

A.1 The connection to moduli spaces of stable rational curves

The space $\overline{\mathfrak{t}_{\mathrm{reg}}}$ can be identified with the Deligne-Mumford space $\overline{\mathcal{M}_{0,n+1}}$ of stable rational curves with $n+1$ marked points. Here, a rational curve with $n+1$ marked points is a finite union Σ of projective lines $\Sigma_1, ..., \Sigma_m$ together with marked distinct points $z_1, ..., z_n \in \Sigma$ such that

- Each marked point belongs to a unique Σ_j;
- The intersection of projective lines $\Sigma_i \cap \Sigma_j$ is either empty or consists of one point, and in the latter case the intersection is transversal;
- The graph of components (whose vertices are the lines C_i and whose edges correspond to pairs of intersecting lines) is a tree;
- The total number of special points (i.e. marked points or intersection points) that belong to a given component Σ_i is at least 3.

A point of $\overline{\mathcal{M}_{0,n+1}}$ is then an isomorphism class of such stable curves. The space $\overline{\mathcal{M}_{0,n+1}}$ contains a dense open subset corresponding to curves with one component. This open subset is isomorphic to

$$\left(\left(\mathbb{P}^1\right)^{n+1} \setminus \Delta\right) / \mathrm{PSL}_2(\mathbb{C}$$

where Δ is the fat diagonal

$$\Delta = \{(u_1, ..., u_n) \in \mathbb{C}^n \mid u_i = u_j, \text{ for some } i \neq j\}$$

and $\mathrm{PSL}_2(\mathbb{C})$ is the automorphism group of $\mathbb{P}^1$. Since the group $\mathrm{PSL}_2(\mathbb{C})$ acts transitively on triples of distinct points, we can fix the $(n+1)$-th marked point to be $\infty \in \mathbb{P}^1$ and fix the sum of coordinates of other points to be zero. Then the space $\mathcal{M}_{0,n+1}$ gets identified with the quotient $\mathfrak{t}_{\mathrm{reg}}/\mathbb{C}^\times$. That is we have

$$\left(\left(\mathbb{P}^1\right)^{n+1} \setminus \Delta\right) / \mathrm{PSL}_2(\mathbb{C}) \cong (\mathbb{C}^n \setminus \Delta)/B \cong \mathfrak{h}_{\mathrm{reg}}/B \cong \mathfrak{t}_{\mathrm{reg}}/\mathbb{C}^\times$$

where $B \subset \mathrm{PSL}_2$ is the Borel subgroup, and $B \cong \mathbb{C}^\times \ltimes \mathbb{C}$ acting on $\mathbb{C}^n$ by scaling and translation. It follows from [16, Section 4.3] that the above isomorphism can be extended to an identification $\overline{\mathcal{M}_{0,n+1}} \cong \overline{\mathfrak{t}_{\mathrm{reg}}}$. On the other hand, the space $\overline{\mathcal{M}_{0,n+1}}$ comes with the tautological bundles L_i whose fiber is the line representing the point z_i. Then the total space $\widetilde{\mathcal{M}_{0,n+1}}$ of the tautological line bundle L_{n+1} is isomorphic to the total space of the tautological line bundle $\widetilde{\mathfrak{t}_{\mathrm{reg}}}$ on $\overline{\mathfrak{t}_{\mathrm{reg}}}$.

Taking the real points, we have

$$\widetilde{\mathcal{M}_{0,n+1}}(\mathbb{R}) \cong \widetilde{\mathfrak{t}_{\mathrm{reg}}}(\mathbb{R}).$$

A.2 Stratification indexed by planar rooted trees

We denote by $T(u)$ a planar rooted tree T with n leaves colored by the components $u_1, \ldots, u_n$ of u. We say that T is compatible with $\sigma \in S_n$ if all internal vertices of the tree are in the lower half plane, all leaves are on the horizontal line $y = 0$ and are colored by $u_{\sigma(1)}, \ldots, u_{\sigma(n)}$ from left to right.

To any planar binary rooted tree BT compatible with σ, one can assign a set of coordinates z_I, indexed by internal vertices I of BT, in an appropriate neighborhood U_{BT_σ} of the corresponding 0-dimensional stratum. The coordinate ring of the open chart $U_{BT_\sigma} \subset \widetilde{\mathfrak{t}_{\text{reg}}}(\mathbb{R})$ is generated by the following set of coordinate functions z_I on U_{BT_σ} indexed by inner vertices I of the tree BT,

$$z_I = \begin{cases} u_{r(I)} - u_{l(I)}, & \text{if } I \text{ is the root vertex,} \\ \frac{u_{r(I)} - u_{l(I)}}{u_{r(I')} - u_{l(I')}}, & \text{if } I \text{ is any other vertex,} \end{cases} \tag{A.2.1}$$

where I' is the preceding vertex of I in BT, i.e. $I' := \max\{J \in BT \mid J < I\}$ in the partial ordering $<$ of the vertices of BT_σ with the root being the minimal element, and for any vertex I, $l(I) \in [1, \ldots, n]$ is such that $\sigma(l(I))$ is the maximal index of the u_i's in the left branch at I, and analogously, $r(I) \in [1, \ldots, n]$ is such that $\sigma(r(I))$ the minimal index of the $u_i's$ in the right branch at I.

The space $\widetilde{\mathfrak{t}_{\text{reg}}}(\mathbb{R})$ has a stratification, with the strata indexed by rooted trees with n colored leaves. Let T be such a tree, then the corresponding stratum $\mathcal{M}_T$ is the product of $\mathcal{M}_{0,d(I)}$ over all internal vertices I of T with $d(I)$ the index of I. In particular, 0-dimensional strata correspond to binary rooted trees with n ordered leaves, while 1-dimensional strata correspond to almost binary trees (with exactly one 4-valent internal vertex). The stratum corresponding to a tree T lies in the closure of the one corresponding to another tree T' if and only if T' is obtained from T by contracting some edges. In the coordinate charts, the stratum $\mathcal{M}_T$ corresponding to a rooted tree T in the local coordinates determined by a binary rooted tree T' can be described as follows.

Proposition A.3. The stratum $\mathcal{M}_T$ has a nonempty intersection with the coordinate chart U_{BT_σ} if and only if T is obtained from BT by contracting some edges. In the latter case, $\mathcal{M}_T$ is a subset of U_{BT_σ} defined as follows: $z_I \neq 0$ if the (unique) edge of BT which ends at I is contracted in T, and $z_I = 0$ otherwise.

Let us take the following planar binary tree BT_σ with coloring

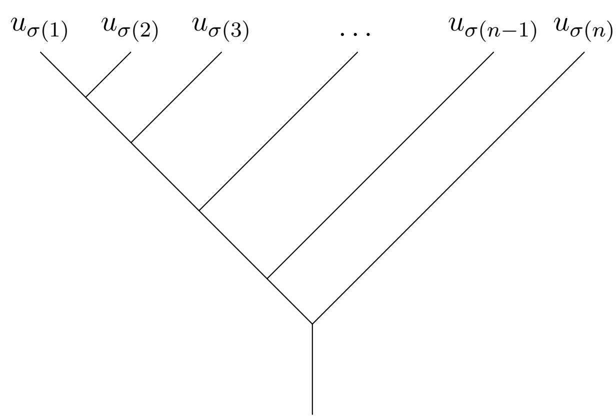

Figure 19: A planar rooted tree with coloring

Let us denote the vertices of BT_σ in the partial ordering by $I_1 > I_2 > \cdots > I_n$. And let $z_{I_1}, ..., z_{I_n}$ be the corresponding coordinates, then (following the definition in [44, Page 16])

Definition A.4. The point $u^\sigma_{\text{cat}} \in U_{BT_\sigma}$ with coordinates $z_{I_k} = 0$ for all $k = 1, ..., n$ is called a caterpillar point. And the line $l^\sigma_{\text{cat}} \in U_{BT_\sigma}$ consisting of the set of points in U_{BT_σ} with coordinates $z_{I_k} = 0$ for all $k = 1, ..., n-1$ is called a caterpillar line. For $\sigma = \text{id} \in S_n$, we simply denote $u^{\text{id}}_{\text{cat}}$ and $l^{\text{id}}_{\text{cat}}$ by u_{cat} and l_{cat} respectively.

Note that a caterpillar point u^σ_{cat} is in the 0-dimensional stratum of $\widehat{\mathfrak{h}_{\text{reg}}}(\mathbb{R})$, and l^σ_{cat} is the tautological line through u^σ_{cat}. In particular, the limit of elements $u = \text{diag}(u_1, ..., u_n)$ in U_{id} such that $u_2 - u_1$ is equal to a fixed real number $t > 0$ and $\frac{u_{j+1} - u_j}{u_j - u_{j-1}} \to +\infty$ for all $j = 2, ..., n-1$, is a point, denoted by $u_{\text{cat}}(t)$ in the caterpillar line l_{cat}.

B The WKB approximation of the 3×3 Stokes matrices on the caterpillar line

In this appendix, we show some explicit computation of the WKB approximation of the Stokes matrices on the caterpillar line based on the formula in Theorem 2.11. Recall that for $A = (A_{ij}) \in \mathrm{Herm}(n)$, we denote by $\lambda_1^{(k)} \leq \cdots \leq \lambda_k^{(k)}$ the ordered eigenvalues of its upper left $k \times k$ submatrix, and we use t_i for the diagonal entry A_{ii}.

Let us take the case $n = 3$. Then the explicit formula for the entries of the Stokes matrix $S_+^{\mathrm{reg}}(u_{\mathrm{cat}}(t), A)$ is

$$
\begin{aligned}
&(S_+^{\mathrm{reg}})_{11} = e^{\frac{t_1}{2\varepsilon}}, \quad (S_+^{\mathrm{reg}})_{22} = e^{\frac{t_2}{2\varepsilon}}, \quad (S_+^{\mathrm{reg}})_{33} = e^{\frac{t_3}{2\varepsilon}},\\
&(S_+^{\mathrm{reg}})_{12} = \frac{A_{12}}{\varepsilon} \cdot \frac{\left(\frac{u_2-u_1}{\varepsilon}\right)^{\frac{t_2-t_1}{2\pi \mathrm{i}\varepsilon}} e^{\frac{t_1+t_2}{4\varepsilon}}}{\Gamma\left(1+\frac{\lambda_1^{(2)}-t_1}{2\pi \mathrm{i}\varepsilon}\right)\Gamma\left(1+\frac{\lambda_2^{(2)}-t_1}{2\pi \mathrm{i}\varepsilon}\right)},\\
&(S_+^{\mathrm{reg}})_{23} = (S_+^{\mathrm{reg}})_{23}^1 + (S_+^{\mathrm{reg}})_{23}^2,\\
&(S_+^{\mathrm{reg}})_{13} = (S_+^{\mathrm{reg}})_{13}^1 + (S_+^{\mathrm{reg}})_{13}^2,
\end{aligned}
$$

where the components

$$
(S_+^{\mathrm{reg}})_{23}^1 = 2\pi \mathrm{i} \cdot \left(\frac{u_2-u_1}{\varepsilon}\right)^{\frac{t_3-t_2}{2\pi \mathrm{i}\varepsilon}} \cdot \frac{e^{\frac{t_2+t_3}{4\varepsilon}}\Gamma\left(1+\frac{\lambda_2^{(2)}-\lambda_1^{(2)}}{2\pi \mathrm{i}\varepsilon}\right)}{\prod_{j=1}^3\Gamma\left(1+\frac{\lambda_j^{(3)}-\lambda_1^{(2)}}{2\pi \mathrm{i}\varepsilon}\right)} \frac{\Gamma\left(\frac{\lambda_2^{(2)}-\lambda_1^{(2)}}{2\pi \mathrm{i}\varepsilon}\right)}{\Gamma\left(1+\frac{\lambda_1^{(1)}-\lambda_1^{(2)}}{2\pi \mathrm{i}\varepsilon}\right)} \cdot \Delta_{1,3}^{1,2}\left(\frac{A-\lambda_1^{(2)}}{2\pi \mathrm{i}\varepsilon}\right)
$$

$$
(S_+^{\mathrm{reg}})_{23}^2 = 2\pi \mathrm{i} \cdot \left(\frac{u_2-u_1}{\varepsilon}\right)^{\frac{t_3-t_2}{2\pi \mathrm{i}\varepsilon}} \cdot \frac{e^{\frac{t_2+t_3}{4\varepsilon}}\Gamma\left(1+\frac{\lambda_1^{(2)}-\lambda_2^{(2)}}{2\pi \mathrm{i}\varepsilon}\right)}{\prod_{j=1}^3\Gamma\left(1+\frac{\lambda_j^{(3)}-\lambda_2^{(2)}}{2\pi \mathrm{i}\varepsilon}\right)} \frac{\Gamma\left(\frac{\lambda_1^{(2)}-\lambda_2^{(2)}}{2\pi \mathrm{i}\varepsilon}\right)}{\Gamma\left(1+\frac{\lambda_1^{(1)}-\lambda_2^{(2)}}{2\pi \mathrm{i}\varepsilon}\right)} \cdot \Delta_{1,3}^{1,2}\left(\frac{A-\lambda_2^{(2)}}{2\pi \mathrm{i}\varepsilon}\right),
$$

and

$$
(S_+^{\mathrm{reg}})_{13}^1 = 2\pi \mathrm{i}\left(\frac{u_2-u_1}{\varepsilon}\right)^{\frac{t_3-t_1}{2\pi \mathrm{i}\varepsilon}} \frac{e^{\frac{-\lambda_1^{(1)}+2\lambda_1^{(2)}+t_3}{4\varepsilon}}\Gamma\left(1+\frac{\lambda_2^{(2)}-\lambda_1^{(2)}}{2\pi \mathrm{i}\varepsilon}\right)\Gamma\left(\frac{\lambda_2^{(2)}-\lambda_1^{(2)}}{2\pi \mathrm{i}\varepsilon}\right)}{\prod_{j=1}^3\Gamma\left(1+\frac{\lambda_j^{(3)}-\lambda_1^{(2)}}{2\pi \mathrm{i}\varepsilon}\right)\cdot\Gamma\left(1+\frac{\lambda_2^{(2)}-\lambda_1^{(1)}}{2\pi \mathrm{i}\varepsilon}\right)} \cdot \frac{A_{12}\Delta_{1,3}^{1,2}\left(\frac{A-\lambda_1^{(2)}}{2\pi \mathrm{i}\varepsilon}\right)}{(\lambda_1^{(1)}-\lambda_1^{(2)})}
$$

$$
(S_+^{\mathrm{reg}})_{13}^2 = 2\pi \mathrm{i}\left(\frac{u_2-u_1}{\varepsilon}\right)^{\frac{t_3-t_1}{2\pi \mathrm{i}\varepsilon}} \frac{e^{\frac{-\lambda_1^{(1)}+2\lambda_2^{(2)}+t_3}{4\varepsilon}}\Gamma\left(1+\frac{\lambda_1^{(2)}-\lambda_2^{(2)}}{2\pi \mathrm{i}\varepsilon}\right)\Gamma\left(\frac{\lambda_1^{(2)}-\lambda_2^{(2)}}{2\pi \mathrm{i}\varepsilon}\right)}{\prod_{j=1}^3\Gamma\left(1+\frac{\lambda_j^{(3)}-\lambda_2^{(2)}}{2\pi \mathrm{i}\varepsilon}\right)\cdot\Gamma\left(1+\frac{\lambda_1^{(2)}-\lambda_1^{(1)}}{2\pi \mathrm{i}\varepsilon}\right)} \cdot \frac{A_{12}\Delta_{1,3}^{1,2}\left(\frac{A-\lambda_2^{(2)}}{2\pi \mathrm{i}\varepsilon}\right)}{(\lambda_1^{(1)}-\lambda_2^{(2)})}
$$

It follows from a direct computation of asymptotics of the gamma functions that

Proposition B.1. The entries of the Stokes matrices at $u_{\mathrm{cat}}(t)$ have the following asymptotics as $\varepsilon \to 0^+$:

$$
\begin{aligned}
&(S_+^{\mathrm{reg}})_{11} = e^{\frac{t_1}{2\varepsilon}}, \quad (S_+^{\mathrm{reg}})_{22} = e^{\frac{t_2}{2\varepsilon}}, \quad (S_+^{\mathrm{reg}})_{33} = e^{\frac{t_3}{2\varepsilon}},\\
&(S_+^{\mathrm{reg}})_{12} \sim e^{\frac{\lambda_2^{(2)}+\mathrm{i}\theta_{12}(A)}{2\varepsilon}}(f_{12}(A)+O(\varepsilon))\\
&(S_+^{\mathrm{reg}})_{23} \sim e^{\frac{\lambda_2^{(3)}+\lambda_3^{(3)}-\lambda_2^{(2)}+\mathrm{i}\theta_{23}(A)}{2\varepsilon}}(f_{23}(A)+O(\varepsilon)) + e^{\frac{\lambda_2^{(3)}+\lambda_3^{(3)}-t_2+\mathrm{i}\psi_{23}(A)}{2\varepsilon}}(g_{23}(A)+O(\varepsilon)),\\
&(S_+^{\mathrm{reg}})_{13} \sim e^{\frac{\lambda_3^{(3)}+\mathrm{i}\theta_{13}(A)}{2\varepsilon}}(f_{13}(A)+O(\varepsilon)) + e^{\frac{\lambda_3^{(3)}-\lambda_1^{(1)}-\lambda_2^{(2)}+\lambda_1^{(2)}+\lambda_2^{(3)}+\mathrm{i}\psi_{13}(A)}{2\varepsilon}}(g_{13}(A)+O(\varepsilon)),
\end{aligned}
$$

for some real valued functions f_{ij}, g_{ij}, θ_{ij} and ψ_{ij} of A.

By the strict interlacing inequalities, we have $\lambda_1^{(2)} + \lambda_2^{(3)} < \lambda_1^{(1)} + \lambda_2^{(2)}$, so the first term in the asymptotics of $(S_+^{\mathrm{reg}})_{13}$ dominates. However, if some interlacing inequalities become non-strict, for example $\lambda_1^{(2)} + \lambda_2^{(3)} = \lambda_1^{(1)} + \lambda_2^{(2)}$, then, since in general $\theta_{13}(A) \neq \psi_{13}(A)$, the WKB asymptotics of $(S_+^{\mathrm{reg}})_{13}$ may not exist.

We also remark that the interlacing inequalities do not impose any relation between $\lambda_2^{(3)} + \lambda_3^{(3)} - \lambda_2^{(2)}$ and $\lambda_2^{(3)} + \lambda_3^{(3)} - t_2$. Thus depending on different choices of A, either term in the asymptotics of $(S_+^{\mathrm{reg}})_{23}$ may dominate.

Proposition B.2. Under the assumption that the interlacing inequalities are strict, the minors of the Stokes matrices at $u_{\mathrm{cat}}(t)$ have the following asymptotics as $\varepsilon \to 0^+$:

$$
\begin{aligned}
&\Delta_1^{(1)}(S_+^{\mathrm{reg}}) = e^{\frac{t_1}{2\varepsilon}}, \quad \Delta_2^{(2)}(S_+^{\mathrm{reg}})_{22} = e^{\frac{t_1+t_2}{2\varepsilon}}, \quad \Delta_3^{(3)}(S_+^{\mathrm{reg}})_{33} = e^{\frac{t_1+t_2+t_3}{2\varepsilon}},\\
&\Delta_1^{(2)}(S_+^{\mathrm{reg}}) \sim e^{\frac{\lambda_2^{(2)}+\mathrm{i}\theta_1^{(2)}(A)}{2\varepsilon}}(f_1^{(2)}(A) + O(\varepsilon))\\
&\Delta_1^{(3)}(S_+^{\mathrm{reg}}) \sim e^{\frac{\lambda_3^{(3)}+\mathrm{i}\theta_1^{(3)}(A)}{2\varepsilon}}(f_1^{(3)}(A) + O(\varepsilon)),\\
&\Delta_2^{(3)}(S_+^{\mathrm{reg}}) \sim e^{\frac{\lambda_2^{(3)}+\lambda_3^{(3)}+\mathrm{i}\theta_2^{(3)}(A)}{2\varepsilon}}(f_2^{(3)}(A) + O(\varepsilon)),
\end{aligned}
$$

for some real valued functions $f_i^{(k)}$ and $\theta_i^{(k)}$ of A.

Proof. The minors $\Delta_1^{(1)}$, $\Delta_1^{(2)}$, $\Delta_2^{(2)}$, $\Delta_1^{(3)}$ and $\Delta_3^{(3)}$ are either entries or monomials in entries. So we only need to compute $\Delta_2^{(3)} = (S_+^{\mathrm{reg}})_{12}(S_+^{\mathrm{reg}})_{23} - (S_+^{\mathrm{reg}})_{22}(S_+^{\mathrm{reg}})_{13}$. Let us compute $(S_+^{\mathrm{reg}})_{12}(S_+^{\mathrm{reg}})_{23}^1$ and $(S_+^{\mathrm{reg}})_{12}(S_+^{\mathrm{reg}})_{23}^2$ respectively. Along the way, we use the reflection formula of Γ-function to simplify the expressions. First, we have

$$
\begin{aligned}
&(S_+^{\mathrm{reg}})_{12}(S_+^{\mathrm{reg}})_{23}^1\\
&= \frac{A_{12}}{\varepsilon}2\pi\mathrm{i}\cdot\left(\frac{u_2-u_1}{\varepsilon}\right)^{\frac{t_3-t_2}{2\pi\mathrm{i}\varepsilon}}\left(\frac{u_2-u_1}{\varepsilon}\right)^{\frac{t_2-t_1}{2\pi\mathrm{i}\varepsilon}} e^{\frac{t_1+t_2}{4\varepsilon}}e^{\frac{t_2+t_3}{4\varepsilon}}\\
&\times \frac{\Gamma\left(1+\frac{\lambda_2^{(2)}-\lambda_1^{(2)}}{2\pi\mathrm{i}\varepsilon}\right)\Gamma\left(\frac{\lambda_2^{(2)}-\lambda_1^{(2)}}{2\pi\mathrm{i}\varepsilon}\right)}{\Gamma\left(1+\frac{\lambda_1^{(1)}-\lambda_1^{(2)}}{2\pi\mathrm{i}\varepsilon}\right)\Gamma\left(1+\frac{\lambda_1^{(2)}-\lambda_1^{(1)}}{2\pi\mathrm{i}\varepsilon}\right)\Gamma\left(1+\frac{\lambda_2^{(2)}-\lambda_1^{(1)}}{2\pi\mathrm{i}\varepsilon}\right)\prod_{j=1}^3\Gamma\left(1+\frac{\lambda_j^{(3)}-\lambda_1^{(2)}}{2\pi\mathrm{i}\varepsilon}\right)}\cdot\Delta_{1,3}^{1,2}\left(\frac{A-\lambda_1^{(2)}}{2\pi\mathrm{i}\varepsilon}\right)\\
&= 2\pi\mathrm{i}\cdot\left(\frac{u_2-u_1}{\varepsilon}\right)^{\frac{t_3-t_1}{2\pi\mathrm{i}\varepsilon}} e^{\frac{t_1+t_2}{4\varepsilon}}e^{\frac{t_2+t_3}{4\varepsilon}}\left(e^{\frac{\lambda_1^{(1)}-\lambda_1^{(2)}}{2\varepsilon}} - e^{-\frac{\lambda_1^{(1)}-\lambda_1^{(2)}}{2\varepsilon}}\right)\\
&\times \frac{\Gamma\left(1+\frac{\lambda_2^{(2)}-\lambda_1^{(2)}}{2\pi\mathrm{i}\varepsilon}\right)\Gamma\left(\frac{\lambda_2^{(2)}-\lambda_1^{(2)}}{2\pi\mathrm{i}\varepsilon}\right)}{\Gamma\left(1+\frac{\lambda_2^{(2)}-\lambda_1^{(1)}}{2\pi\mathrm{i}\varepsilon}\right)\prod_{j=1}^3\Gamma\left(1+\frac{\lambda_j^{(3)}-\lambda_1^{(2)}}{2\pi\mathrm{i}\varepsilon}\right)}\frac{A_{12}\Delta_{1,3}^{1,2}\left(\frac{A-\lambda_1^{(2)}}{2\pi\mathrm{i}\varepsilon}\right)}{\lambda_1^{(1)}-\lambda_1^{(2)}}\\
&= 2\pi\mathrm{i}\cdot\left(\frac{u_2-u_1}{\varepsilon}\right)^{\frac{t_3-t_1}{2\pi\mathrm{i}\varepsilon}} e^{\frac{3t_1+2t_2+t_3-2\lambda_1^{(2)}}{4\varepsilon}}\frac{\Gamma\left(1+\frac{\lambda_2^{(2)}-\lambda_1^{(2)}}{2\pi\mathrm{i}\varepsilon}\right)\Gamma\left(\frac{\lambda_2^{(2)}-\lambda_1^{(2)}}{2\pi\mathrm{i}\varepsilon}\right)}{\Gamma\left(1+\frac{\lambda_2^{(2)}-\lambda_1^{(1)}}{2\pi\mathrm{i}\varepsilon}\right)\prod_{j=1}^3\Gamma\left(1+\frac{\lambda_j^{(3)}-\lambda_1^{(2)}}{2\pi\mathrm{i}\varepsilon}\right)}\frac{A_{12}\Delta_{1,3}^{1,2}\left(\frac{A-\lambda_1^{(2)}}{2\pi\mathrm{i}\varepsilon}\right)}{\lambda_1^{(1)}-\lambda_1^{(2)}}\\
&+ 2\pi\mathrm{i}\cdot\left(\frac{u_2-u_1}{\varepsilon}\right)^{\frac{t_3-t_1}{2\pi\mathrm{i}\varepsilon}} e^{\frac{-t_1+2t_2+t_3+2\lambda_1^{(2)}}{4\varepsilon}}\frac{\Gamma\left(1+\frac{\lambda_2^{(2)}-\lambda_1^{(2)}}{2\pi\mathrm{i}\varepsilon}\right)\Gamma\left(\frac{\lambda_2^{(2)}-\lambda_1^{(2)}}{2\pi\mathrm{i}\varepsilon}\right)}{\Gamma\left(1+\frac{\lambda_2^{(2)}-\lambda_1^{(1)}}{2\pi\mathrm{i}\varepsilon}\right)\prod_{j=1}^3\Gamma\left(1+\frac{\lambda_j^{(3)}-\lambda_1^{(2)}}{2\pi\mathrm{i}\varepsilon}\right)}\frac{A_{12}\Delta_{1,3}^{1,2}\left(\frac{A-\lambda_1^{(2)}}{2\pi\mathrm{i}\varepsilon}\right)}{\lambda_1^{(1)}-\lambda_1^{(2)}}
\end{aligned}
$$

Here in the second identity, we use the reflection formula of the gamma function to reduce

$$\frac{1}{\Gamma\left(1+\frac{\lambda_1^{(1)}-\lambda_1^{(2)}}{2\pi\mathrm{i}\varepsilon}\right)\Gamma\left(1+\frac{\lambda_1^{(2)}-\lambda_1^{(1)}}{2\pi\mathrm{i}\varepsilon}\right)}=\frac{2\mathrm{i}\varepsilon\sin\left(\frac{\lambda_1^{(1)}-\lambda_1^{(2)}}{2\mathrm{i}\varepsilon}\right)}{\lambda_1^{(1)}-\lambda_1^{(2)}}=\varepsilon\cdot\frac{e^{\frac{\lambda_1^{(1)}-\lambda_1^{(2)}}{2\varepsilon}}-e^{-\frac{\lambda_1^{(1)}-\lambda_1^{(2)}}{2\varepsilon}}}{\lambda_1^{(1)}-\lambda_1^{(2)}}.$$

Similarly, we have

$$\begin{aligned}&(S_+^{\mathrm{reg}})_{12}(S_+^{\mathrm{reg}})_{23}^2\\&=2\pi\mathrm{i}\cdot\left(\frac{u_2-u_1}{\varepsilon}\right)^{\frac{t_3-t_1}{2\pi\mathrm{i}\varepsilon}}e^{\frac{3t_1+2t_2+t_3-2\lambda_2^{(2)}}{4\varepsilon}}\frac{\Gamma\left(1+\frac{\lambda_1^{(2)}-\lambda_2^{(2)}}{2\pi\mathrm{i}\varepsilon}\right)\Gamma\left(\frac{\lambda_1^{(2)}-\lambda_2^{(2)}}{2\pi\mathrm{i}\varepsilon}\right)}{\Gamma\left(1+\frac{\lambda_1^{(2)}-\lambda_1^{(1)}}{2\pi\mathrm{i}\varepsilon}\right)\prod_{j=1}^3\Gamma\left(1+\frac{\lambda_j^{(3)}-\lambda_2^{(2)}}{2\pi\mathrm{i}\varepsilon}\right)}\frac{A_{12}\Delta_{1,3}^{1,2}\left(\frac{A-\lambda_2^{(2)}}{2\pi\mathrm{i}\varepsilon}\right)}{\lambda_1^{(1)}-\lambda_2^{(2)}}\\&+2\pi\mathrm{i}\cdot\left(\frac{u_2-u_1}{\varepsilon}\right)^{\frac{t_3-t_1}{2\pi\mathrm{i}\varepsilon}}e^{\frac{-t_1+2t_2+t_3+2\lambda_2^{(2)}}{4\varepsilon}}\frac{\Gamma\left(1+\frac{\lambda_1^{(2)}-\lambda_2^{(2)}}{2\pi\mathrm{i}\varepsilon}\right)\Gamma\left(\frac{\lambda_1^{(2)}-\lambda_2^{(2)}}{2\pi\mathrm{i}\varepsilon}\right)}{\Gamma\left(1+\frac{\lambda_1^{(2)}-\lambda_1^{(1)}}{2\pi\mathrm{i}\varepsilon}\right)\prod_{j=1}^3\Gamma\left(1+\frac{\lambda_j^{(3)}-\lambda_2^{(2)}}{2\pi\mathrm{i}\varepsilon}\right)}\frac{A_{12}\Delta_{1,3}^{1,2}\left(\frac{A-\lambda_2^{(2)}}{2\pi\mathrm{i}\varepsilon}\right)}{\lambda_1^{(1)}-\lambda_2^{(2)}}.\end{aligned}$$

Therefore, from the explicit expressions of the entries we get

$$\begin{aligned}&(S_+^{\mathrm{reg}})_{12}(S_+^{\mathrm{reg}})_{23}-(S_+^{\mathrm{reg}})_{22}(S_+^{\mathrm{reg}})_{13}\\&=2\pi\mathrm{i}\cdot\left(\frac{u_2-u_1}{\varepsilon}\right)^{\frac{t_3-t_1}{2\pi\mathrm{i}\varepsilon}}e^{\frac{3t_1+2t_2+t_3-2\lambda_1^{(2)}}{4\varepsilon}}\frac{\Gamma\left(1+\frac{\lambda_2^{(2)}-\lambda_1^{(2)}}{2\pi\mathrm{i}\varepsilon}\right)\Gamma\left(\frac{\lambda_2^{(2)}-\lambda_1^{(2)}}{2\pi\mathrm{i}\varepsilon}\right)}{\Gamma\left(1+\frac{\lambda_2^{(2)}-\lambda_1^{(1)}}{2\pi\mathrm{i}\varepsilon}\right)\prod_{j=1}^3\Gamma\left(1+\frac{\lambda_j^{(3)}-\lambda_1^{(2)}}{2\pi\mathrm{i}\varepsilon}\right)}\frac{A_{12}\Delta_{1,3}^{1,2}\left(\frac{A-\lambda_1^{(2)}}{2\pi\mathrm{i}\varepsilon}\right)}{\lambda_1^{(1)}-\lambda_1^{(2)}}\\&+2\pi\mathrm{i}\cdot\left(\frac{u_2-u_1}{\varepsilon}\right)^{\frac{t_3-t_1}{2\pi\mathrm{i}\varepsilon}}e^{\frac{3t_1+2t_2+t_3-2\lambda_2^{(2)}}{4\varepsilon}}\frac{\Gamma\left(1+\frac{\lambda_1^{(2)}-\lambda_2^{(2)}}{2\pi\mathrm{i}\varepsilon}\right)\Gamma\left(\frac{\lambda_1^{(2)}-\lambda_2^{(2)}}{2\pi\mathrm{i}\varepsilon}\right)}{\Gamma\left(1+\frac{\lambda_1^{(2)}-\lambda_1^{(1)}}{2\pi\mathrm{i}\varepsilon}\right)\prod_{j=1}^3\Gamma\left(1+\frac{\lambda_j^{(3)}-\lambda_2^{(2)}}{2\pi\mathrm{i}\varepsilon}\right)}\frac{A_{12}\Delta_{1,3}^{1,2}\left(\frac{A-\lambda_2^{(2)}}{2\pi\mathrm{i}\varepsilon}\right)}{\lambda_1^{(1)}-\lambda_2^{(2)}}\end{aligned}$$

Using the ordering $\lambda_1^{(3)}<\lambda_2^{(3)}<\lambda_3^{(3)}$ and $\lambda_1^{(2)}<\lambda_2^{(2)}$, and the strict interlacing inequalities, we can compute the leading asymptotics of the two summands to get

$$\Delta_2^{(3)}\sim e^{\frac{\lambda_2^{(3)}+\lambda_3^{(3)}+\mathrm{i}\theta_2^{(3)}(A)}{2\varepsilon}}(f_2^{(3)}(A)+O(\varepsilon))+e^{\frac{\lambda_3^{(3)}+\lambda_1^{(1)}+\lambda_1^{(2)}-\lambda_2^{(2)}+\mathrm{i}\psi_2^{(3)}(A)}{2\varepsilon}}(g_2^{(3)}(A)+O(\varepsilon))$$

for some real-valued functions $\theta_2^{(3)}$, $f_2^{(3)}$ and $\psi_2^{(3)}$, $g_2^{(3)}$ of A.

By the strict interlacing inequalities, we have $\lambda_2^{(3)}+\lambda_3^{(3)}>\lambda_3^{(3)}+\lambda_1^{(1)}+\lambda_1^{(2)}-\lambda_2^{(2)}$. Therefore the first term dominates. This completes the proof. ■

Remark B.3. In the computation of the asymptotics of $(S_+^{\mathrm{reg}})_{12}(S_+^{\mathrm{reg}})_{23}-(S_+^{\mathrm{reg}})_{22}(S_+^{\mathrm{reg}})_{13}$, by using the reflection formula of the gamma function we decompose $(S_+^{\mathrm{reg}})_{12}(S_+^{\mathrm{reg}})_{23}$ into a summation of four terms. Two summands then cancel with $(S_+^{\mathrm{reg}})_{22}(S_+^{\mathrm{reg}})_{13}$. This cancellation exhibits the leading asymptotics of the minor as a linear combination of the $\lambda_i^{(k)}$.

C A quick review of spectral networks

Here we recall the main facts and conjectures about spectral networks which we use in the main text. Most of this material can be found in [22, 31].

Basic definitions

Definition C.1 (Oriented foliation for a holomorphic 1-form). For a Riemann surface S equipped with a nowhere vanishing holomorphic 1-form ρ, we have the distribution $\ker \operatorname{Im} \rho$, which integrates to give a foliation F_ρ of S. This foliation is oriented by $\operatorname{Re} \rho$. For example, if $S = \mathbb{C}$ and $\rho = dz$, then F_ρ is the foliation by horizontal lines oriented to the right. More generally, for $\vartheta \in \mathbb{R}/2\pi\mathbb{Z}$, we also define

$$F_\rho^\vartheta = F_{e^{\mathrm{i}\vartheta}\rho}\,.$$

If ρ has isolated zeroes, we make the same definitions, now getting a singular foliation F_ρ of S.

Fix a Riemann surface C and a complex curve $\Gamma \subset T^*C$, such that the projection $\pi : T^*C \to C$ makes Γ a degree n branched covering of C. In our application, we will take $C = \mathbb{C}^\times$ and $\Gamma = \Gamma(u, A)$.[7] We always assume that Γ has simple ramification, so in particular it is smooth.

Definition C.2 (Root curve). The *root curve* Γ^r is the closure of the fiber product with the diagonal removed,

$$\Gamma^r = \overline{\{(y, y') \in \Gamma \times \Gamma : \pi(y) = \pi(y'), y \neq y\}} \subset T^*C \times T^*C. \tag{C.0.1}$$

Γ^r is a smooth $n(n-1)$-sheeted branched covering of C. We often think of a point of Γ^r as a point $z \in C$ plus a choice of an ordered pair ij of distinct sheets of Γ over z. Γ^r carries a holomorphic 1-form

$$\rho = p_1^*\omega - p_2^*\omega \tag{C.0.2}$$

where ω is the Liouville 1-form and p_1, p_2 are the two projections $T^*C \times T^*C \to T^*C$; ρ vanishes only at the ramification points. Thus we have the foliations F_ρ^ϑ on Γ^r, with isolated singularities at the branch points.

If c is a 1-chain on Γ^r, let $p(c)$ be a 1-chain on Γ given by

$$p(c) = (p_1)_*c - (p_2)_*c\,. \tag{C.0.3}$$

(So if c lies on the sheet of Γ^r corresponding to the pair ij, then $p(c)$ consists of two components on Γ, one on sheet i and one on sheet j, with the second one oppositely oriented.) Note it has

$$\int_{p(c)} \omega = \int_c \rho. \tag{C.0.4}$$

Definition C.3 (Topological solitons). Fix $z \in C$ and $y, y' \in \pi^{-1}(z)$. A *topological soliton from y to y'* is a 1-chain c on Γ^r, such that $\partial(p(c)) = y' - y$.

The projection of a topological soliton from Γ^r to C looks like a graph (generically trivalent), with one leaf at z and all other leaves at branch points. Each edge of the graph carries a label ij keeping track of which sheet of Γ^r it came from. The labels are constrained: there is a balancing condition at each internal vertex, and also a condition at each branch point.

Definition C.4 (WKB solitons). Fix $z \in C$ and $y, y' \in \pi^{-1}(z) \subset \Gamma$. A *WKB soliton from y to y' with phase ϑ* is a topological soliton from y to y' made up of positively oriented paths lying in leaves of the foliation F_ρ^ϑ (permitting turns at the singularities).

Definition C.5 (Finite web). A *finite web on* Γ *with phase* ϑ is a 1-chain c on Γ^r, made up of positively oriented paths in leaves of the foliation F_ρ^ϑ (permitting turns at the singularities), with $\partial(p(c)) = 0$. The *charge* of the finite web c is the class $[p(c)] \in H_1(\Gamma)$.

Proposition C.6 (Phases of periods of finite webs). If γ is the charge of a finite web with phase ϑ, then $\arg(-Z(\gamma)) = \vartheta$.

[7] We note a notational clash: in the literature on spectral networks Γ is usually the name of the charge lattice, but in this paper, we use Γ to denote the spectral curve.

Definition C.7 (WKB spectral network). The *WKB spectral network* $\mathcal{W}(\Gamma, \vartheta)$ is the set of all $(y, y') \in \Gamma^r$ such that there exists a WKB soliton from y to y' with phase ϑ.

Each point of $\mathcal{W}(\Gamma, \vartheta)$ thus carries the additional data of the set of such WKB solitons. There is an algorithm for computing $\mathcal{W}(\Gamma, \vartheta)$ described in [22] and implemented in a Mathematica notebook included with the arXiv version of this paper. It realizes $\mathcal{W}(\Gamma, \vartheta)$ as a collection of walls in Γ^r. The projection of $\mathcal{W}(\Gamma, \vartheta)$ to C is a collection of walls as well, with each wall carrying a label ij keeping track of a sheet in Γ^r. We sometimes write this label as $i < j$. This notation keeps track of two facts: first, the arrow pointing from j to i reminds us that the WKB solitons are paths beginning on sheet j and ending on sheet i [13]; second, in the application of spectral networks to exact WKB, we have an ODE on the surface C, and a a basis of solutions $\psi^{(k)}$ indexed by the sheets; then along the wall we have $\psi^{(i)} \ll \psi^{(j)}$ as $\varepsilon \to 0$ with $\arg \varepsilon = \vartheta$.

Path lifting

Definition C.8 (Path categories). For $Y \subset X$:

- Let $\mathrm{Path}(X, Y)$ be the category of paths in X with endpoints in Y, enriched over abelian groups (so the objects are points $y \in Y$, and $\mathrm{Hom}(y, y')$ is the abelian group of formal $\mathbb{Q}$-linear combinations of paths from y to y' in X, with composition extended linearly).
- Given a map $\pi : Z \to X$, let $\mathrm{Path}^Z(X, Y)$ be the category of paths in Z with endpoints in $\pi^{-1}(Y)$ (so the objects are points $y \in Y$, and $\mathrm{Hom}(y, y')$ is the abelian group of formal $\mathbb{Q}$-linear combinations of paths from any $z \in \pi^{-1}(y)$ to any $z' \in \pi^{-1}(y')$ in Z, with composition extended linearly, and with the composition of paths that do not concatenate taken to be zero).

Definition C.9 (Path-lifting functors). For $\mathcal{W} \subset \Gamma^r$, a *path-lifting functor off* $\mathcal{W}$ is a map

$$\mathrm{Lift} : \mathrm{Path}(C, C \setminus \pi(\mathcal{W})) \to \mathrm{Path}^{\Gamma}(C, C \setminus \pi(\mathcal{W})) \tag{C.0.5}$$

which is almost-homotopy-invariant, i.e. if $\mathcal{P} \sim \mathcal{P}'$ then $\mathrm{Lift}(\mathcal{P}) \sim^{al} \mathrm{Lift}(\mathcal{P}')$, where $\sim^{al}$ means ordinary homotopy except that if we move a path across a branch point we multiply by -1.

Proposition C.10 (WKB path-lifting functor). There exists a path-lifting functor off $\mathcal{W}(\Gamma, \vartheta)$, $\mathrm{Lift}_{\mathcal{W}(\Gamma,\vartheta)}$, with the following property: all terms in $\mathrm{Lift}_{\mathcal{W}(\Gamma,\vartheta)}(\mathcal{P})$ are obtained by splicing paths $p(c)$, where c is a WKB soliton with phase ϑ, into lifts of $\mathcal{P}$.

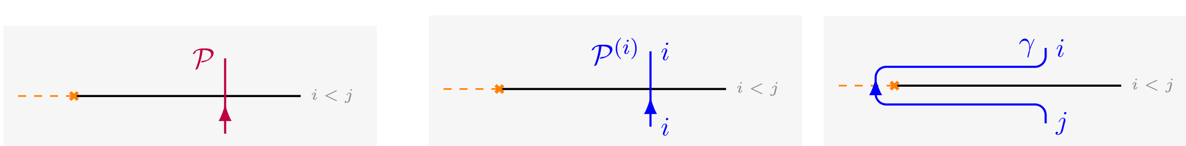

Figure 20: Left: a path $\mathcal{P}$ crossing one primary wall on C. Middle, right: paths on Γ which arise as terms in $\mathrm{Lift}(\mathcal{P})$, as indicated in Proposition C.11 and Proposition C.12.

Proposition C.11. Suppose that there are no finite webs on Γ with phase ϑ. Then the path-lifting functor $\mathrm{Lift}_{\mathcal{W}(\Gamma,\vartheta)}$ in Proposition C.10 is unique, and determined by an algorithm given in [21]. It has the following additional property. Call a wall of $\mathcal{W}(\Gamma, \vartheta)$ *primary* if it originates from a branch point. Suppose that $\mathcal{P}$ is a path crossing a single primary wall of $\mathcal{W}(\Gamma, \vartheta)$. Then

$$\mathrm{Lift}_{\mathcal{W}(\Gamma,\vartheta)}(\mathcal{P}) = \sum_{i=1}^{n} \mathcal{P}^{(i)} + \gamma \tag{C.0.6}$$

where $\mathcal{P}^{(i)}$ and γ are shown in Figure 20.

The extra term γ in $\mathrm{Lift}(\mathcal{P})$ is sometimes referred to as a "detour" path: it travels along $\mathcal{P}$ to the wall, then takes a detour along the wall to the branch point and back, then resumes along $\mathcal{P}$ again.

Proposition C.12. If there are finite webs on Γ with phase ϑ, then the path-lifting functor in Proposition C.10 is not unique, but there are two canonical choices $\mathrm{Lift}_{\mathcal{W}(\Gamma,\vartheta\pm)}$, again described in [21]. They have the following additional property. Call a wall of $\mathcal{W}(\Gamma,\vartheta)$ *primary one-way* if it originates from a branch point and ends at a singularity. Suppose that $\wp$ is a path crossing only one wall, and that wall is a primary one-way wall. Then

$$\mathrm{Lift}_{\mathcal{W}(\Gamma,\vartheta\pm)}(\wp) = \sum_{i=1}^{n} \mathcal{P}^{(i)} + \gamma + \cdots \tag{C.0.7}$$

where $\mathcal{P}^{(i)}$ and γ are shown in Figure 20, and all paths μ in the $\cdots$ terms have $\arg(Z(\gamma) - Z(\mu)) = \vartheta$.

In the situation of this paper, we will be particularly interested in the phase $\vartheta = 0$, where we do have finite webs, and we will use either of the path-lifting functors $\mathrm{Lift}_{\mathcal{W}(\Gamma,\vartheta\pm)}$ from Proposition C.12.[8] Because $\mathrm{Lift}_{\mathcal{W}(\Gamma,\vartheta\pm)}$ is compatible with composition of paths, we can use Proposition C.12 to compute $\mathrm{Lift}_{\mathcal{W}(\Gamma,\vartheta\pm)}(\mathcal{P})$ for any $\mathcal{P}$ which crosses only primary one-way walls.

Nonabelianization of local systems

Definition C.13 (Almost-local systems). Given a branched covering map $\pi : Z \to X$, an almost-local system L^{ab} over Z is a local system over the complement of the branch locus in Z, which has monodromy -1 around each branch point.

Definition C.14 (Nonabelianization map). Fix a path-lifting functor Lift off $\mathcal{W}$. Given an almost-local system L^{ab} over Γ, we define a local system

$$L = \mathrm{Nab}_{\mathrm{Lift}}(L^{\mathrm{ab}}) \tag{C.0.8}$$

over $C \setminus \pi(\mathcal{W})$ as follows: for an open set U, $L(U) = L^{\mathrm{ab}}(\pi^{-1}(U))$; for a path $\mathcal{P}$ from U to U', the map $L(\mathcal{P}) : L(U) \to L(U')$ is

$$L(\mathcal{P}) = L^{\mathrm{ab}}(\mathrm{Lift}(\mathcal{P}))\,. \tag{C.0.9}$$

The local system L so defined extends over C.

The case $n = 2$

The case $n = 2$ is particularly simple. In this case $\Gamma^r = \Gamma$, and the oriented foliation F_ϑ of Γ^r descends to an unoriented foliation of C. Then the WKB spectral network $\mathcal{W}(\Gamma,\vartheta)$ is the critical graph of a quadratic differential on C, as described in [21]. The relevant quadratic differential is given in terms of the sheets y_1, y_2 of Γ by

$$\varphi_2 = e^{-\mathrm{i}\vartheta}(y_1 - y_2)^2\,. \tag{C.0.10}$$

The zeroes of φ_2 are the branch points of Γ; Γ is smooth just if all these are simple. Then the critical graph consists of three trajectories emerging from each branch point, characterized by the condition that $\int \sqrt{\varphi_2}$ is real along each trajectory. Finite webs occur only when there is a trajectory which runs between branch points: such a trajectory is called a saddle connection (if the two branch points are distinct) or a closed loop (if they are the same).

[8] There is also a more canonical choice, which is a kind of geometric mean of $\mathrm{Lift}_{\mathcal{W}(\Gamma,\vartheta\pm)}$, used e.g. in [31]. That choice has better symmetry properties; in the WKB context, it is related to using median summation instead of lateral summation. However, nothing we do in this paper is sensitive to whether we take $\mathrm{Lift}_{\mathcal{W}(\Gamma,\vartheta+)}$, $\mathrm{Lift}_{\mathcal{W}(\Gamma,\vartheta-)}$ or the geometric mean; that choice only affects the $\cdots$ terms in (C.0.7).

The WKB conjecture

Now suppose given a family of flat $\mathrm{GL}(n)$-connections $\nabla(\varepsilon)$ in bundles $\mathcal{E}(\varepsilon)$ over C, such that as $\varepsilon \to 0$ the $(\mathcal{E}(\varepsilon), \varepsilon\nabla(\varepsilon))$ limit to a Higgs bundle $(\mathcal{E}, \varphi)$ over C. Let Γ be the spectral curve of $(\mathcal{E}, \varphi)$. Then the exact WKB method as employed in [22, 31] predicts:

Conjecture C.15 (Exact WKB conjecture for closed paths). There is a family $\nabla^{\mathrm{ab},\vartheta}(\varepsilon)$ of $\mathrm{GL}(1)$-connections in bundles $\mathcal{E}^{\mathrm{ab},\vartheta}(\varepsilon)$ over Γ, flat except for monodromy -1 around branch points. If there exist no finite webs on Γ of phase ϑ, then:

1. the local systems associated to connections $(\mathcal{E}(\varepsilon), \nabla(\varepsilon))$ and $(\mathcal{E}^{\mathrm{ab}}(\varepsilon), \nabla^{\mathrm{ab},\vartheta}(\varepsilon))$ are related by the nonabelianization map $\mathrm{Nab}_{\mathrm{Lift}_{\mathcal{W}(\Gamma,\vartheta)}}$.
2. For any cycle $\gamma \in H_1(\Gamma)$, the holonomy $X_\gamma^\vartheta(\varepsilon)$ of $\nabla^{\mathrm{ab},\vartheta}(\varepsilon)$ obeys $X_\gamma^\vartheta(\varepsilon) \sim \exp(Z(\gamma)/\varepsilon + \mathrm{i}\phi_\gamma)$ as $\varepsilon \to 0$ in the half-plane centered on $\arg\varepsilon = \vartheta$.

If there exist finite webs on Γ of phase ϑ, then we similarly define two different holonomies $X_\gamma^{\vartheta^\pm}(\varepsilon)$ using parallel transports of $\nabla^{\mathrm{ab},\vartheta^\pm}(\varepsilon)$, and either of them obeys $X_\gamma^{\vartheta^\pm}(\varepsilon) \sim \exp(Z(\gamma)/\varepsilon + \mathrm{i}\phi_\gamma)$.

Open paths

In this paper, we need a small extension of the above story to include open paths. This extension was not written in [22, 31] (though one special case appeared in [21]), so we formulate it here. We consider the situation where the connections $\nabla(\varepsilon)$ have an irregular singularity at a point $z^* \in \overline{C}$, such that the leading term in the expansion of φ is regular semisimple. We take the special case where the leading term is real. (This condition is satisfied in our example, where $z^* = \infty$, and the leading term is u.) As we discussed in Section 2, there are functions P_i, Q_i and $\nabla(\varepsilon)$-flat sections ψ_i in neighborhoods of anti-Stokes rays, such that $\exp(-P_i(z)/\varepsilon + Q_i(z))\psi_i(z)$ is finite as $z \to z^*$ along an anti-Stokes ray. The Stokes matrices can be understood as parallel transport matrices, relative to the bases ψ_i, along arcs which stay in a small neighborhood of z^* and run from one anti-Stokes ray to another.

In this case, the spectral curve Γ is unramified around z^*. Computing asymptotics of the Stokes data around z^* requires consideration of open paths, with endpoints among the n preimages z_i^*, and coming into z_i^* along anti-Stokes rays. To define their periods requires regularization, since ω has a pole at z_i^*. Thus suppose γ is an open path from z_i^* to $z_{i'}^*$, coming in along anti-Stokes rays. We define a regularization γ_{reg} of γ, by perturbing the endpoints z_i^*, $z_{i'}^*$ to nearby points z_i, $z'_{i'}$ on the anti-Stokes rays, and then let

$$Z(\gamma) = \int_\gamma^{\mathrm{reg}} \omega = \lim_{z_i \to z_i^*} \lim_{z'_{i'} \to z_{i'}^*} \left(-P(z'_{i'}) + P(z_i) + \int_{\gamma_{\mathrm{reg}}} \omega \right) . \tag{C.0.11}$$

Then we have an extension of Conjecture C.15, as follows:

Definition C.16 (Extended homology). Consider the real oriented blow-up $\widehat{\Gamma}$ of Γ at the n preimages of z^*. Then $\widehat{\Gamma}$ has boundary consisting of n circles. On each of these n circles, we mark points corresponding to the anti-Stokes rays; let $L(\vartheta)$ be the set of marked points. Then define

$$H(\Gamma, \vartheta) = H_1(\widehat{\Gamma}; L(\vartheta)) . \tag{C.0.12}$$

Definition C.17 (Spectral coordinates). If Γ has no finite webs of phase ϑ, the *spectral coordinates* of the connection $\nabla(\varepsilon)$ are the parallel transports $X_\gamma^\vartheta(\varepsilon) \in \mathbb{C}^\times$ of $\nabla^{\mathrm{ab},\vartheta}(\varepsilon)$ on paths $\gamma \in H(\Gamma, \vartheta)$. When γ is an open path, the parallel transport is taken relative to the basis vectors ψ_i at the two ends of the path. If Γ has finite webs of phase ϑ, then we define two different spectral coordinates $X_\gamma^{\vartheta^\pm}(\varepsilon)$ using parallel transports of $\nabla^{\mathrm{ab},\vartheta^\pm}(\varepsilon)$.

Conjecture C.18 (Exact WKB conjecture for open and closed paths). The spectral coordinates $X_\gamma^\vartheta(\varepsilon)$ obey $X_\gamma^\vartheta(\varepsilon) \sim \exp(Z(\gamma)/\varepsilon + \mathrm{i}\phi_\gamma)$ as $\varepsilon \to 0$ in the half-plane centered on $\arg\varepsilon = \vartheta$.

DT-type invariants

As we have explained, when there are finite webs with phase ϑ_0, the path-lifting functor at phase ϑ_0 is not unique: there are two canonical choices $\mathrm{Lift}_{\mathcal{W}(\Gamma,\vartheta_0^\pm)}$. These two can be understood as the limits of $\mathrm{Lift}_{\mathcal{W}(\Gamma,\vartheta)}$ as $\vartheta \to \vartheta_0^\pm$. The limits $X_\gamma^{\vartheta_0^\pm}$ of the spectral coordinates need not agree: in general they differ by some coordinate transformation. This coordinate transformation is one of the most important structural aspects of the spectral coordinates. In the generic situation, it can be written in terms of "Donaldson-Thomas-type invariants" $\Omega(\gamma)$, as follows:

Definition C.19 (Mutually local phase). We say ϑ_0 is a *mutually local* phase if, whenever γ and γ' are charges of finite webs with phase ϑ_0, we have $\langle\gamma,\gamma'\rangle = 0$.

Proposition C.20 (Transformation law for spectral coordinates). When ϑ is a mutually local phase, let B_ϑ be the set of charges of finite webs with phase ϑ; then there exists $\Omega : B_\vartheta \to \mathbb{Q}$ such that for all μ

$$X_\mu^{\vartheta+} = X_\mu^{\vartheta-} \prod_{\gamma\in B_\vartheta} (1 \pm X_\gamma)^{\langle\mu,\gamma\rangle\Omega(\gamma)} \,. \tag{C.0.13}$$

An algorithm for computing the $\Omega(\gamma)$ is given in [21, 31]. Two important special cases, which we encounter in this paper: first, if there are no finite webs with charge μ then $\Omega(\mu) = 0$; second, an isolated tree with charge μ contributes 1 to $\Omega(\mu)$.

Equivalences

Path-lifting maps admit a notion of equivalence:

Definition C.21. An *equivalence* between path-lifting maps Lift_0, Lift_1 to curves Γ_0, Γ_1 is a family of curves Γ_t and path-lifting maps Lift_t, such that for every $p \in C$ and pair $t_1, t_2 \in [0,1]$ there exists $R(p,t_1,t_2) \in \mathrm{Path}^\Gamma(C, C \setminus \pi(\mathcal{W}))$, such that for paths $\mathcal{P}$ from p to p' we have

$$\mathrm{Lift}_{t_2}(\mathcal{P}) = R(p,t_1,t_2)\,\mathrm{Lift}_{t_1}(\mathcal{P})R(p',t_1,t_2)^{-1} \,. \tag{C.0.14}$$

If Lift and Lift' are equivalent, the corresponding nonabelianization maps $\mathrm{Nab}_{\mathrm{Lift}}$ and $\mathrm{Nab}_{\mathrm{Lift}'}$ are also equivalent, in the sense that for any L^{ab}, $\mathrm{Nab}_{\mathrm{Lift}}(L^{\mathrm{ab}})$ and $\mathrm{Nab}_{\mathrm{Lift}'}(L^{\mathrm{ab}})$ are equivalent local systems.

Here is one important source of equivalences:

Proposition C.22. Fix some ϑ and consider a variation Γ_t such that there is no finite web whose phase crosses ϑ. Then the path-lifting maps Lift_t give an equivalence between Lift_0 and Lift_1.

Another way to get an equivalence is to start with the spectral network $\mathcal{W}(\Gamma,\vartheta)$ and modify it by certain topological moves, which include and generalize isotopies, as described in [21] section 10.6. After these moves, we obtain a new path-lifting map Lift' off a "topological spectral network" $\mathcal{W}'$. Lift' is equivalent to Lift but sometimes more convenient.

If no walls of the spectral network move across p or p' between t_1 and t_2, then $R(p,t_1,t_2) = R(p',t_1,t_2) = 1$, and so for paths $\mathcal{P}$ from p to p' we have just $\mathrm{Lift}(\mathcal{P}) = \mathrm{Lift}'(\mathcal{P})$. We use one such equivalence in the $n = 3$ example in the main text, where p and p' are points near infinity on the anti-Stokes lines.

References

[1] A. Alekseev and I. Davydenkova, *Inequalities from Poisson brackets*. Indag. Math. (N.S.) 25, 846–871 (2014).
[2] A. Alekseev, A. Berenstein, B. Hoffman and Y. Li, *Langlands duality and Poisson-Lie duality via cluster theory and tropicalization*, Selecta Math. (N.S.) 27 (2021), no. 4, paper no. 69.
[3] A. Alekseev, J. Lane and Y. Li, *The $U(n)$ Gelfand-Tsetlin system as a tropical limit of Ginzburg-Weinstein diffeomorphisms*, Phil. Trans. R. Soc. A 376: 20170428 (2018).

[4] A. Alekseev, M. Podkopaeva, A. Szenes, *A symplectic proof of the Horn inequalities*, Adv. Math. 318 (2017) 711-736.

[5] T. Aoki, N. Honda, T. Kawai, T. Koike, Y. Nishikawa, S. Sasaki, A. Shudo and Y. Takei, *Virtual turning points—a gift of microlocal analysis to the exact WKB analysis,* in Algebraic analysis of differential equations from microlocal analysis to exponential asymptotics, pp. 29–43. Springer, Tokyo, 2008.

[6] T. Aoki, T. Kawai, and Y. Takei, *New turning points in the exact WKB analysis for higher order ordinary differential equations*, Analyse algébrique des perturbations singulieres, I, Méthodes résurgentes, Hermann, 1994, pp. 69-84.

[7] W. Balser, *Formal power series and linear systems of meromorphic ordinary differential equations*, Springer-Verlag, New York, 2000.

[8] W. Balser, W.B. Jurkat, and D.A. Lutz, *Birkhoff invariants and Stokes' multipliers for meromorphic linear differential equations*, J. Math. Anal. Appl. 71 (1979), 48-94.

[9] H. L. Berk, W. M. Nevins and K. V. Roberts, *New Stokes' line in WKB theory*, J. Math. Phys., 23 (1982), pp. 988-1002.

[10] O. Biquard and P. Boalch, *Wild non-abelian Hodge theory on curves*, Compositio Mathematica, 140(1), 179-204 (2004).

[11] P. Boalch, *Stokes matrices, Poisson Lie groups and Frobenius manifolds*, Invent. Math. 146 (2001), 479–506. no. 3, 479-506.

[12] P. Boalch, *G-bundles, isomonodromy and quantum Weyl groups*, Int. Math. Res. Not. (2002), no. 22, 1129–1166.

[13] P. Boalch, *Topology of the Stokes phenomenon.* In Proc. Sympos. Pure Math. 103.1 (2021), American Mathematical Society, 55-100.

[14] T. Bridgeland, *Riemann-Hilbert problems from Donaldson-Thomas theory*, Invent. Math. 216 (2019), 69-124.

[15] T. Bridgeland and V. Toledano Laredo, *Stability conditions and Stokes factors*, Invent. Math. 187 (2012), 61-98.

[16] C. De Concini and C. Procesi, *Wonderful models of subspace arrangements*, Selecta Math. (N.S.) 1 (1995), no. 3, 459–494.

[17] E. Delabaere, H. Dillinger, and F. Pham, *Résurgence de Voros et périodes des courbes hyperelliptiques*, Ann. Inst. Fourier (Grenoble) 43 (1993), 163–199.

[18] B. Dubrovin, *Geometry of 2D topological field theories*, Lecture Notes in Math, 1620 (1995).

[19] H. Flaschka, T. Ratiu, *A convexity theorem for Poisson actions of compact Lie groups*, IHES, Preprint 1995. Available at http://preprints.cern.ch.

[20] D. Gaiotto, *Opers and TBA*, arXiv:1403.6137.

[21] D. Gaiotto, G. W. Moore, and A. Neitzke, *Wall-crossing, Hitchin systems, and the WKB approximation*, Adv. in Math. 234 (2013), 239–403.

[22] D. Gaiotto, G. W. Moore, and A. Neitzke, *Spectral networks*, Ann. Henri Poincaré, 14(7):1643–1731, 2013.

[23] D. Gaiotto, G. W. Moore, A. Neitzke and F. Yan, *Commuting Line Defects At* $q^N = 1$, arXiv:2307.14429.

[24] S.Galkin, V. Golyshev, H. Iritani. *Gamma classes and quantum cohomology of Fano manifolds: Gamma conjectures*, Duke Math. J. 165 (11) 2005 - 2077 (2016).

[25] O. Gamayun, N. Iorgov and O. Lisovyy. *Conformal field theory of Painlevé VI*, JHEP **10**, 038 (2012).

[26] A. Grassi, J. Gu, and M. Mari~no, *Non-perturbative approaches to the quantum Seiberg-Witten curve*, JHEP 07 (2020) 106.

[27] A. Goncharov and L. Shen. *Donaldson-Thomas transformations of moduli spaces of G-local systems*, Adv. Math. 327, 225-348 (2018).

[28] V. Guillemin and S. Sternberg, *The Gelfand-Cetlin system and quantization of the complex flag manifolds*, J. Funct. Anal 52 (1983), 106–128.

[29] V. Ginzburg and A. Weinstein, *Lie-Poisson structure on some Poisson-Lie groups*, J. Amer. Math. Soc. 5:2 (1992), 445-53.

[30] I. Halacheva, J. Kamnitzer, L. Rybnikov and A. Weekes, *Crystals and monodromy of Bethe vectors*, Duke Math. J. 169 (12) 2337-2419.

[31] L. Hollands and A. Neitzke, *Exact WKB and Abelianization for the* T_3 *Equation,* Commun. Math. Phys. volume 380, 131–186 (2020).

[32] N. Iorgov, O. Lisovyy and J. Teschner, *Isomonodromic tau-functions from Liouville conformal blocks*, Commun. Math. Phys. 336, no.2, 671-694 (2015).
[33] K. Ito, T. Kondo, K. Kuroda, and H. Shu, *WKB periods for higher order ODE and TBA equations*, arXiv:2104.13680.
[34] K. Iwaki and T. Nakanishi, *Exact WKB analysis and cluster algebras*, J. Phys. A 47, 474009 (2014).
[35] A.-K. Kashani-Poor and J. Troost, *Pure $\mathcal{N} = 2$ super Yang–Mills and exact WKB*, JHEP 08 (2015) 160.
[36] T. Kato, *Perturbation theory for linear operators*, Classics in Mathematics volume 132, Springer, 1995.
[37] M. Loday-Richaud, *Divergent series, summability and resurgence II. Simple and multiple summability*, vol. 2154 of Lecture Notes in Mathematics, Springer, 2016.
[38] J.-H. Lu and A. Weinstein, *Poisson Lie groups, dressing transformations, and Bruhat decompositions*, Journal of Differential Geometry 31 (1990), no. 2, 501-526.
[39] N. Nekrasov, *Seiberg-Witten Prepotential from Instanton Counting*, Adv. Theor. Math. Phys. 7 (5) 831-864, September 2003.
[40] N. Nekrasov, A. Rosly, and S. Shatashvili, *Darboux coordinates, Yang-Yang functional, and gauge theory*, Theor. Math. Phys. 181 (2014), no. 1, 1206–1234.
[41] H. Ooguri and C. Vafa, *Summing up D-instantons*, Phys. Rev. Lett. 77 (1996) 3296–3298.
[42] H. J. Silverstone, *JWKB connection-formula problem revisited via Borel summation*, Phys. Rev. Lett., 55(1985), 2523-2526.
[43] M. Semenov-Tian-Shansky, *Dressing transformations and Poisson group actions*, Publ. Res. Inst. Math. Sci. 21 (1985) no.6, 1237-1260.
[44] D. Speyer, *Schubert problems with respect to oscillating flags of stable rational curves*, Alg. Geom. 1 (2014), no. 1, 14–45.
[45] I. Tulli, *The Ooguri–Vafa space as a moduli space of framed wild harmonic bundles*, arXiv:1912.00261.
[46] C. Voisin, *Hodge Theory and Complex Algebraic Geometry II*, trans. Leila Schneps, Cambridge: Cambridge University Press, 2003, print, Cambridge Studies in Advanced Mathematics.
[47] A. Voros, *The return of the quartic oscillator. the complex WKB method*, Ann. Inst. Henri Poincaré 39 (1983), 211–338.
[48] W. Wasow, *Asymptotic expansions for ordinary differential equations*, Wiley Interscience, New York, 1976.
[49] X. Xu, *Regularized limits of Stokes matrices, isomonodromy deformation and crystal basis*, arXiv:1912.07196v5.
[50] X. Xu, *Representations of quantum groups arising from Stokes phenomenon*, arXiv: 2012.15673.

DEPARTMENT OF MATHEMATICS, UNIVERSITÉ DE GENEVE, 7-9 RUE DU CONSEIL GÉNÉRAL, CASE POSTALE 64, 1211 GENEVE 4, SWITZERLAND
E-mail address: anton.alekseev@unige.ch
DEPARTMENT OF MATHEMATICS, YALE UNIVERSITY, PO BOX 208283, NEW HAVEN, CT 06511, UNITED STATES OF AMERICA
E-mail address: andrew.neitzke@yale.edu
SCHOOL OF MATHEMATICAL SCIENCES & BEIJING INTERNATIONAL CENTER FOR MATHEMATICAL RESEARCH, PEKING UNIVERSITY, BEIJING 100871, CHINA
E-mail address: xxu@bicmr.pku.edu.cn
DEPARTMENT OF MATHEMATICS, NORTHEASTERN UNIVERSITY, 360 HUNTINGTON AVENUE, MA 02115, UNITED STATES OF AMERICA
E-mail address: y.zhou@northeastern.edu